ABSTRACT

Title of Dissertation: DEVELOPMENT OF AN INTEGRATED TRAFFIC SIGNAL CONTROL SYSTEM FOR ARTERIALS WITH HEAVY TRANSIT FLOWS

Hyeonmi Kim, Doctor of Philosophy, 2018

Dissertation directed by: Gang-Len Chang, Professor, Department of Civil and Environmental Engineering

Increasing ridership on transit systems has long been recognized as one of the potentially effective strategies for mitigating urban traffic congestion from the demand side. However, the complex nature of urban traffic congestion and the inevitable frictions between transit vehicles and passenger cars often negate the effectiveness of operational strategies for enhancing the service quality of a transit system. Hence, it is essential to have an effective control platform that can properly integrate available strategies in both offline and real-time operations. In need of such a platform, this study proposes an integrated operating system that consists of a traffic monitoring module, pre-timed signal optimization models, and real-time control strategies.

In the proposed system, the traffic monitoring module is to systematically convert the real-time bus GPS data into geographic-based sensors that can estimate both bus and general traffic conditions in urban networks beyond its original function

of monitoring each buses speed and locations. Taking advantage of heavy bus flows and spatial evolution over a link, the proposed pseudo detection module can provide more extensive information (such as link and movement-specific speeds) than conventional point-measurement detectors. The system can also provide the spatial and temporal variation of general traffic conditions by converting the time-varying bus speed in each sub link, viewed as a pseudo sensor.

The second part of the system constructs a bus-based signal coordination model to optimize the offsets for an urban arterial that needs to accommodate a high volume of bus flows. The corridor signal model for bus-based progression considers average bus dwell time, relatively slow bus speeds, physical constraints of bus stops, queue formation/discharging process and its relationships with the bus stop location. The enhanced model (BUSBAND) is designed to optimize the offsets at each intersection with the objective of maximizing the total effective bus bandwidth which accounts for the dwell time uncertainty.

Due to the stochastic nature of bus traveling and passenger arriving patterns, the pre-timed control may fail to contend with the fluctuation of bus arrivals at the intersection. Hence, this study has further developed a real-time signal control system which integrates an active TSP with the pre-timed BUSBAND. The integrated system dynamically adjusts the green time (i.e., early green or green extension) based on the real-time detected bus locations to facilitate the bus progression and expand bus bands. In order to best the benefits of the integrated TSP operations, the proposed system also has a module to select an intersection for deploying an active TSP, based on the pretimed signal plan.

DEVELOPMENT OF AN INTEGRATED SIGNAL CONTROL SYSTEM FOR ARTERIALS WITH HEAVY TRANSIT FLOWS

by

Hyeonmi Kim

Dissertation submitted to the Faculty of the Graduate School of the
University of Maryland, College Park, in partial fulfillment
of the requirements for the degree of
Doctor of Philosophy
2018

Advisory Committee:
Professor Gang-Len Chang, Chair
Professor Ali Haghani
Professor Lei Zhang
Professor Martin Dresner
Assistant Professor Shanjiang Zhu at the George Mason University

Dedication

To my family and all of my friends for their love and support.

Acknowledgements

First and foremost, I would like to express my gratitude to my advisor, Dr.Gang-Len Chang, for his support, guidance, encouragement, and mentorship throughout my Ph.D. study at the University of Maryland, College Park.

I am also grateful to the members of my doctoral examination committee, Dr. Ali Haghani, Dr. Lei Zhang, Dr. Martin Dresner, and Dr. Shanjiang Zhu for their constructive comments, valuable suggestions, and compliments on my research work.

I also thank my colleagues in Traffic Safety and Operations Lab.

Also, very special thanks go to my dear friends and especially housemates at Duke Street.

I would like to express my deepest appreciation to my family, Heiyoung Kim, Namhee Lee, Hyunwoo Kim, Eunjin Han, and Yeonhee Lee. Without their unlimited encouragement and support, this dissertation would not have been completed.

Finally, thank God….

Table of Contents

List of Tables

List of Figures

Chapter 1: Introduction

1.1 Research Background

Increasing the ridership of transit systems has long been recognized as one of the potentially effective strategies to mitigate urban traffic congestion from the demand side. However, a variety of factors associated with the nature of transit operations and management often prevent transit systems from increasing the market share of the daily travel demand, especially from those commuting trips. Examples of such factors causing transit systems unfavorable in comparison with the auto mode include insufficient accessibility to target destinations, unreliable operational schedules, uncertain bus dwell times at each stop, frequent stops at signalized arterials, sharing space with others, and compromised route plans to accommodate passengers of different origin and destination zones.

Conceivably, many of such factors and the resulting issues need to be addressed from the network wide perspective, based on the available resources of the transit agency and the distribution of urban traffic demands. Nonetheless, there are some control strategies that can be implemented to increase the quality and reliability of transit services under the same overall organizational and operational structures. For example, to monitor the performance of transit fleets in congested traffic conditions, one can employ on-board GPS device to track each bus's speed evaluation over roadway links, and assess its headway stability based on the predicted arrival time to each downstream bus stop. To minimize delays and stops at signalized intersections, responsible agencies can implement an arterial signal plan with a set of

bus-based offsets to facilitate the progression of bus flows over consecutive intersections. However, since most buses due to relatively low travel speeds and their dwells at a bus stop are often impeded by passenger queues at intersections, implementation of such a transit-friendly signal plan needs to take into account the impacts incurred by traffic queues.

Moreover, enhancing the bus schedule reliability or headway stability can also be done by incorporating bus dwell time variance in design of bus headways and the transit-friendly signal plan. Coping with travel time uncertainties due to traffic congestion and/or demand variance between bus stops, some real-time operational strategies, such as transit signal priority control, bus holdings and dynamic bus speed adjustment, are also applicable to ensure that transit vehicles can offer reliable service quality with less stops and stable travel time.

Note that despite the availability of aforementioned strategies for enhancing a transit system's service quality and reliability from the operations perspective, the complex nature of urban traffic congestion and the inevitable frictions between transit vehicles and passenger cars often negate their effectiveness, if implemented independently and/or only at individual level. Hence, to concurrently promote the use of transit systems and also ease traffic congestion, it is essential to have an effective control platform that can properly integrate available strategies in both off-line and real-time operations. Such a control platform shall allow the transit operational departments, working with traffic signal control agencies, to exercise both the monitoring and real-time operational functions.

The former shall include detecting the speed and location of target buses in the road network, the estimated temporal and spatial distributions of passenger-car speeds in each link and over the entire network, the accumulated and estimated delays for each bus in real time at each bus stop and intersection. All information and data produced from exercising this monitoring function can in turn be used by responsible agencies to execute real-time operational functions such as dynamically revising the signal timings at the local level, holding buses at the station, or adjusting bus speed to avoid their bunching together.

Conceivably, some unexpected problems and challenges may surface in various urban traffic scenarios, which could still degrade the performance of transit operations. However, proper integration of all such functions and operational strategies is certainly one of the essential steps toward stabilizing bus service reliability and minimizing excessive delays at signalized intersections.

1.2 Objectives and Scope of Research

The primary objective of this study is to develop an integrated traffic signal control system that can effectively assist responsible agencies in monitoring transit operations and controlling traffic signals so as to enhance the efficiency of bus operations. The first objective of this research is to develop a pseudo detection system to estimate traffic conditions using real-time bus GPS data. This is proposed in response to the need of having reliable link speed data which is one of key performance measurements for both the transit operation agency and transportation agency to monitor traffic condition and to select the proper operational strategies. A reliable

temporal and spatial distribution of such link speed data, however, cannot be measured with conventional link traffic detectors.

The second research objective is to develop an integrated traffic signal control system for improving the service reliability and quality of bus operations. Such a control system will consist of two essential modules: one for producing a bus-based signal progression offsets that can allow transit vehicles to go through multiple intersections without stop, and thus to have stable headways at each bus stop; the other is for adjusting signal timings in real time in response to unexpected traffic impedance and bus stop delay that may prevent buses from taking advantage of the specially-designed signal progression plan.

1.3 Organization

Based on the proposed objectives, this research has divided the entire scope of work into four primary tasks, each presented in one ensuing chapter. Figure 1.1 illustrates the organization of this dissertation and the interrelations between primary tasks. A brief description of the key research tasks in each chapter is presented below:

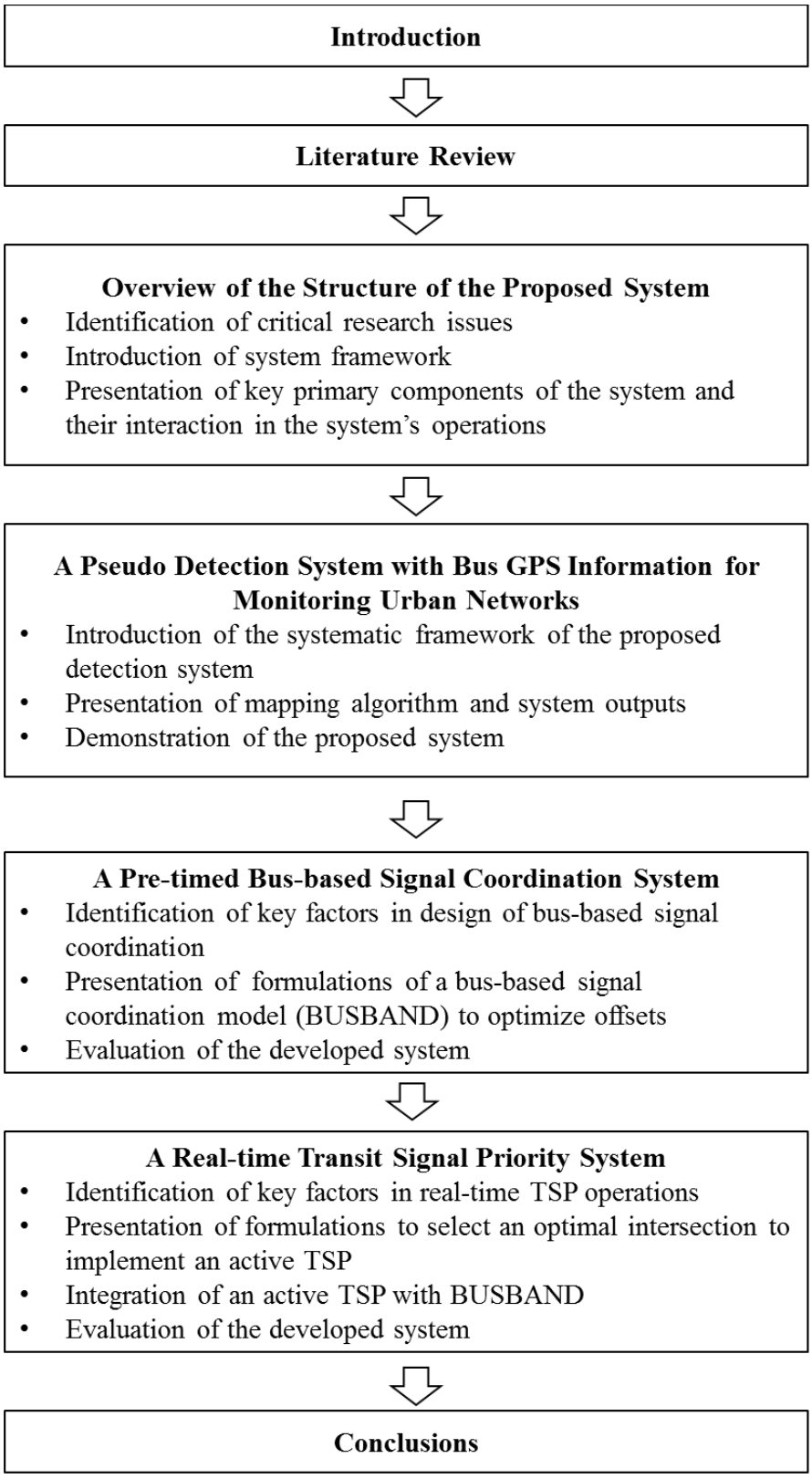

Figure 1.1 Dissertation organization

- **Chapter 2** summarizes the results of an in-depth literature review, focusing on transit management, including transit monitoring system and control strategies, including traffic signal control and transit fleet control. The review has identified the advantages of those studies and has explored additional areas for further enhancements.
- **Chapter 3** illustrates the overall structure of the proposed integrated signal control system. It has discussed all key modules and their interrelationships to provide essential system functions in a real-time operational process. A brief description of each primary component's functional requirements and its role in the system's off-line and real-time operations has also been presented in this chapter.
- **Chapter 4** presents the core logic of a pseudo traffic detection system, which is to convert the real-time transit GPS data into geographic-based sensors, and then use such a design to detect and estimate both transit and general traffic conditions along a roadway link. A detailed description of the development procedures for such a detection system is the main focus of this chapter, including its key component modules, and inputs and outputs for each module. A case study for both illustration and evaluation has also been included in this chapter.
- **Chapter 5** first discusses key factors essential for design of a pre-timed bus-based signal coordination system such as bus dwell time, the relatively slow bus speed, the physical constraints of bus stops, and traffic queues at intersections. A set of mathematical formulations, taking into account of interrelations

between these factors for producing the optimal set of progression offsets, for buses to minimize their likelihood of encountering a red phase over an arterial, constitutes the core of this chapter. For performance assessment of the proposed models and a comparative analysis with other existing models, this chapter has also reported the results of extensive simulation analyses.

- **Chapter 6** illustrates an integrated real-time transit signal priority system to deal with traffic flow fluctuations in practice. This chapter first present an integrated active TSP system with BUSBAND for real-time operations including its operating structure, and TSP activation logic at critical intersections to maximize the total bus progression bands. For performance assessment of the proposed model, this chapter has also reported the results of extensive simulation analyses. This is followed by the description of a model to select an optimal intersection to implement an active TSP so as to best utilize the pre-timed bus-based signal coordination system, which is presented in chapter 5.
- **Chapter 7** summarizes the key contributions of this dissertation and indicates the future research directions, including: development of a decision-support for the responsible agencies to decide when to activate the arterial control with one of the following progression strategies: (1) bus-based signal progression; (2) auto-based signal progression; and (3) concurrent progression for both passengers and transit vehicles. In addition, integration of traffic signal controls with transit fleet control strategies, (e.g., bus holding and speed

controls); and multi-source information available from the big data environments should also be considered in the future work.

Chapter 2: Literature Review

This chapter provides a comprehensive review of existing studies over the past decades concerning improved reliability and efficiency of transit operations including both experimental analyses and theoretical explorations. To facilitate the presentation and analysis, all such studies are divided into the following categories: (1) transit monitoring, which includes utilizing real-time bus GPS data for various levels of management, and exploring potentials for predicting bus arrival times and general traffic conditions in urban networks; (2) transit operational controls that focus on design of various strategies to improve the performance of transit services (e.g., schedule adherence and stable headways); and (3) other control strategies that are applicable for enhancing transit operations.

2.1 Transit System Monitoring

In the 1990s, transit agencies started to actively adopt GPS data to monitor their fleets in real time and improve operational efficiency. Examples of studies focusing on best use of GPS data include a data mapping algorithm to convert real-time transit location data into readily applicable information, and data applications for travel time predictions. Some key research advances on these two subjects are briefly summarized below.

Mapping: In developing detection systems with transit GPS data, it is critical to accurately match GPS data to a roadway network database. Since map matching is a pre-processing step for various applications with GPS data – such as route guidance and estimation of transit arrival time – it is necessary to employ efficient and reliable

map-matching algorithms. Note that algorithms developed for such needs vary from the use of simple search techniques to utilization of advanced methods, such as the Extended Kalman Filter, fuzzy logic, and neural networks. As pointed by Hasemi and Karimi (2014), most existing map-matching algorithms belong to one of the following three groups: simple, weighted-based, and advanced techniques.

The core logic of simple geometric algorithms based on the shape of the roadway segment is to assign each GPS point to the nearest road segment without considering continuity of vehicles' trajectories. Examples of such algorithms include point-to-point matching, point-to-curve matching, and curve-to-curve matching. For example, some researchers incorporated topological information to identify candidate matches, such as trajectory similarity, segment connectivity, direction difference, heading difference, and turn-restriction (White et al, 2000; Taylor et al., 2001; Srinivasan et al, 2003). Commonly, most such algorithms use only geometric or topological information, which can yield computing efficiency, but often does not perform as accurately as desirable.

Hence, some proposed to use the weighted-based map-matching algorithms, which assign different weights to different parameters, such as proximity of GPS point to segment, similarities between the direction of GPS points and each segment, connectivity between sequential road segments, the intersection angle between the line connecting two consecutive GPS points, etc. (Greenfeld, 2002; Quddus et al., 2003; Velaga et al., 2009; Li et al., 2013). Such weighted-based map-matching algorithms often divide their procedures and logic into different parts, depending on the encountered situations, such as if the subject vehicle's position is located ahead of

or after crossing an intersection. For example, Quddus and Washington (2015) developed a weight-based shortest path and aided map-matching algorithm with a vehicle trajectory. They derived the shortest path between two points, taking into account both link connectivity and turn restrictions at junctions. They also employed two additional weights: the distance along the shortest path and the vehicle trajectory, and the heading differences of the subject vehicle's trajectory.

Furthermore, some adopted advanced statistical, mathematical, and artificial intelligence techniques, such as the Kalman Filter (Kim et al., 2000), Belief Theory (Najjar and Bonnifait, 2003), a fuzzy logic method (Syed and Cannon, 2004; Quddus et al., 2006; Fuchs et al., 1980) or Bayesian interference (Pyo et al., 2001). It has been reported that those algorithms, grounded on advanced computing methodologies, can yield better results, but mostly demand more powerful computing functions. More detailed comparisons among different real-time map-matching algorithms are available in the review papers by Quddus et al. (2007) and Hashemi and Karimi (2014).

Travel time estimation: In an attempt to use GPS information from transit fleets for measurements of speed and travel time, Cathey and Dailey (2002, 2003) identified a wide range of critical issues associated with extracting information for monitoring freeways and arterials with transit AVL data in Seattle, Washington. They first applied Kalman Filtering methods to estimate the speed and location of each individual vehicle as a function of space and time. With such methods, researchers demonstrated the viability of using the transit-probe sensors as supplements or replacements for loop detectors (Cathey and Dailey, 2002). Later, they extended the

use of transit probe data to corridor-wide travel time estimation (Cathey and Dailey, 2003).

Along the same line, Bertini et al. (2004) investigated the bus travel time and speed information to assess traffic conditions on arterials in Portland, Oregon. They used location-based transit data, recording when vehicles approached and departed from bus stops, to explore the relationship between actual traffic and bus speeds. Note that the AVL system used by Bertini et al. (2004) reported only the position when vehicles approached and departed from bus stops, whereas Cathey and Dailey (2002, 2003) used a system that reports mainly the time points during which buses pass fixed signpost receivers.

Chakroborty and Kikuchi (2004) developed a functional form for estimating automobile travel times, based on bus travel times obtained from transit AVL data. They employed a relatively simple linear equation for conversion of travel time from buses to automobiles under different levels of congestion.

Coifman and Kim (2006) presented a data mining methodology that uses transit AVL data over some pre-specified freeway segments for monitoring the traffic conditions on freeways. Their AVL data reflect only the elapsed times, thus necessitating an essential step of parsing the data to extract travel times on the segments of interest, and to eliminate any observations that are off from the roadway networks. The extracted data were then used to measure travel time and average speed over the freeway segment, and to quantify the traffic conditions. They also validated their computed link-based and trip-based speeds with loop-detected speeds.

Pu et al. (2009) provided a framework for real-time urban travel time estimation using a Bayesian updating method – which considers the relationship between bus flows and general traffic – and identified the potential issue associated with the scenarios of having a low frequency of bus observations.

Table 2.1 Summary of selected studies using transit AVL data for measuring general traffic conditions

Authors	City, State of transit AVL data	Study (Data) scope	Applications	Method
Cathey and Dailey (2002)	Seattle, Washington	Freeways and arterials	Estimate spot speed and travel time	Kalman Filtering
Cathey and Dailey (2003)	Seattle, Washington	Freeways and arterials	Estimate corridor travel time	Kalman Filtering
Bertini et al. (2004)	Portland, Oregon	An arterial	Estimate corridor travel time	Linear Regression
Chakroborty and Kikuchi (2004)	Northern New Castle County, Delaware	Arterials	Estimate corridor travel time	Linear Regression
Coifman and Kim (2006)	Columbus, Ohio	Freeways	Estimate link speed and travel time	Heuristic Algorithm
Pu et al. (2009)	Chicago, Illinois	Arterials	Estimate speed	Bayesian Updating

2.2 Transit Control

There are two typical types of control for transit operations. The first is to set a predefined schedule for transit systems operated on service routes with long headways. The latter is mainly for services with short headways (e.g., less than 10 min). Under the scenario of high bus frequencies, travel time variability and passenger demand fluctuation often yield bus bunching on those routes having short headways. To cope with such a bus-bunching problem, researchers have conducted a large body of studies in transit operations in recent decades. According to Eberlein et al. (2001), most of such control strategies fall into one of the following two categories: 1) station control, which includes bus holing, boarding limits, and stop-skipping; and 2) interstation control, such as operating speed control, bus overtaking, and traffic signal priority.

One of the most popular strategies to allow a belated bus to catch up to the schedule or the leading vehicle is Transit Signal Priority (TSP), a method to reduce the bus delay at the traffic signal along the target arterial. On the other hand, one of the prevailing strategies to delay a bus encountering a too short headway is to exercise bus holding at a stop. A brief summary, focusing mainly on TSP and bus holding, is presented below.

Transit Signal Priority (TSP): This control strategy is used to reduce bus delays at traffic signals by allowing buses to pass a target intersection without stopping. Since it was first proposed in the late 1960s (Wilbur et al., 1968), TSP has emerged as a popular method to improve the bus schedule reliability, and a large body of such studies have been proposed over the past decades. Furth and Muller (2000) has

classified most TSP strategies into two classes: 1) passive or active control, and 2) unconditional or conditional priority.

Passive TSP control is typically operated without detectors, based mainly on offline information of transit route and ridership patterns. As a pioneering researcher, Urbanik (1977) took bus volume into account when addressing signal timing design, and proposed the following four approaches to change the signal plan to favor bus flows: adjustment of cycle length, splitting of phases, area-wide timing plans, and metering of vehicles. According to Vincent et al. (1978), passive priority is often effective under the scenarios of having high transit vehicle frequencies, predictable transit travel times, and light or moderate traffic volumes.

In contrast, execution of active TSP controls demands the placement of bus detectors at the target intersection. If one applies unconditional priority strategies under TSP control, signal priority will be granted to all detected buses to reduce bus travel time (Yagar and Han, 1994; Skabardonis, 2000; Dion and Rakha, 2005; Zhou and Gan, 2009). Through simulation experiments and pilot studies, TSP is reported to show some effectiveness in improving bus efficiency under light bus demand conditions. However, some concerns have also been raised about its potential negative impacts on side-street traffic if the bus frequency reaches a critical level.

In response to such challenges, some researchers have proposed the implementation of conditional active TSP, which only grants priority based on a set of conditions, including the maximum number of priority calls, constant cycle length, the operational condition of transit vehicles (i.e., only when a bus is behind schedule), and bus ridership. Many researchers have developed different rule-based methods for

a traffic controller to justify the need for extending the green time or to truncate the red phase (Hounsell et al., 2000; Janos and Furth, 2002; Ling and Shalaby, 2004; Satiennam et al., 2005; Ma and Yu, 2007; Altun and Furth, 2009; He et al., 2011; Hounsell and Shrestha, 2012). Such rule-based methods may not yield an optimal level of performance concurrently for both transit vehicles and passenger cars in the network.

To address the deficiencies of rule-based TSP, some researchers proposed the use of adaptive strategies, which allow controllers to consider the trade-offs between transit and traffic delays in adjusting signal timings. Such methods are designed to optimize the performance of buses and all other vehicles by quantitatively evaluating the costs and benefits resulting from a priority decision. Their objectives can be to minimize total bus delay as well as total person delay (Dion and Hellinga. 2002; Zhou et al., 2007; Muthuswamy et al., 2007 ; Stevanovic et al., 2008; Furth et al., 2010; Ma et al., 2010; Christofa and Skabardonis, 2011; Mesbah et al., 2011; Lin et al., 2013a; Lin et al., 2013b; Lin et al., 2013c; Hu et al., 2015; Christofa et al., 2016; Xu et al., 2016; Hu et al., 2016; and Ye and Xu, 2017; Yu et al., 2017). For example, Christofa et al. (2016) presented a real-time signal control system accounting for minimizing person delay on an arterial. At the same time of maintaining auto vehicle progression, their method recognizes the schedule adherence of buses and can provide priority to transit vehicles even when they travel on conflicting routes. Yu et al. (2017) combined adaptive TSP strategies and person-based signal timing with consideration of uncertain bus arrival times when determining green extensions. Xu et al. (2016),

Hu et al.(2016) and Ye and Xu (2017) further conducted research to accommodate conflicting TSP requests on different routes using optimization formulations.

Holding: Holding strategies are often considered a means to mitigate bus bunching, which may increase passenger waiting times at bus stop and in-vehicle time for onboard passengers. Hence, many such studies aim at reducing passenger waiting time or/and travel time by computing the optimal holding times for target buses at selected control stops under various scenarios, including availability of real-time information, and constraints of vehicle capacity, stochastic attributes, and multiple control stops.

The core logic of most such studies in the early research stage is to execute the holding action if the target bus headway falls below a given threshold. For example, Barnett (1974) developed a simple holding model at a given control station, aiming to minimize the sum of waiting times and the extra delays of onboard passengers. Turnquist and Blume (1980) further identified some conditions under which holding strategies can be beneficial to the entire operation.

With the advance in information and communication technologies (e.g., Automatic Vehicle Location (AVL), Automatic Vehicle Identification (AVI), and Automatic Passenger Counting (APC) systems), it becomes possible to obtain reliable bus arrival times at the stops and the numbers of in-vehicle and at-stop passengers. Researchers can thus use such information to develop more sophisticated models that can determine the optimal holding time for each arriving vehicle so as to minimize either the total waiting time at stops or the sum of the waiting times and in-vehicle delays for passengers.

Along the same line, Eberlein et al. (2001) formulated the holing problem as a deterministic quadratic program with the object function of minimizing the headway variation, to achieve minimization of average passenger waiting time at stops. Unlike the threshold-based control, the researchers employed a rolling-horizon scheme, which is capable of reducing the impacts of the stochastic nature of the system on the resulting effectiveness. The researchers' formulations were designed mainly for a rail transit system, and thus are not directly transferable for bus operations, which are heavily impacted by other traffic and signal controls.

Focusing on bus operations, Hickman (2001) presented a stochastic holding model at control stops along a transit route, which considers the stochastic attributes of vehicle running times and passenger boarding as well as alighting processes. Fu and Yang (2002) formulated a model for threshold-based control, which considers headways between the preceding and following vehicles to minimize average waiting times at bus stops. The results of extensive simulation experiments show that the effectiveness of such holding controls varies with location and the number of stops under control, as well as the selected holding parameters.

For the same purpose, Zhao et al. (2003) proposed a distributed holding control approach. In the researchers' negotiation-based framework, buses and stops act as agents and negotiate based on their marginal costs by harnessing real-time information. Their simulation results indicated that the negotiation algorithm is robust and flexible for a variety of operating conditions.

Zolfaghari et al. (2004) first took into account vehicle capacity in formulating the holding problem by focusing on minimizing the waiting times for users arriving at

a stop and those who have to wait for the next bus due to the capacity constraint. Yet authors did not consider the extra waiting time endured by passengers held at a stop. Sun and Hickman (2008) approached the same problem by holding multiple buses at a predefined set of control stations. They showed that by properly exercising the holding strategy at multiple stations, one can better stabilize bus headways and achieve a higher cost reduction than those with single station holding.

Yu and Yang (2007) presented a dynamic holding strategy, which considers the on-time performance of the leading bus operation at the next stop, and optimizes holding times for the subject bus at the target stop to minimize total user costs, i.e., waiting times and in-vehicle times. They also developed a model to forecast the departure times of buses dispatched ahead of the target bus from their next stop, based on the support vector machine (SVM) method.

Sáez et al. (2011) developed a hybrid predictive control (HPC) model where holding and stop-skipping control actions were taken to minimize user cost, based on total in-vehicle and waiting times. Their proposed HPC strategy was formulated under a discrete event simulation environment and solved with Genetic Algorithm tools. The results of numerical analyses show that their proposed model outperforms a benchmark algorithm (Expert System Control).

Delgado et al. (2009) formulated a real-time mathematical programming model for buses operated in a transit corridor that aims to minimize the total passenger travel times, including at-stop waiting times and in-vehicle times. Considering vehicle-capacity constraints, the researchers incorporated boarding limits in design of the holding strategies. Case study results also show that the strategy

considering both holding and boarding limits can outperform the holding-only control. Delgado et al. (2012) further improved their previous models by considering the flexibility of boarding limit activation, heterogeneous fleets of vehicles with different physical capacities, and station-specific dwell times. They formulated the entire issue into a deterministic mathematical programming model that can be simulated with a rolling horizon scheme. The numerical results of their study show that combining holding strategies with proper boarding limits can yield performance superior to those under no-control, threshold-based holding, and holding-only strategies under various measurements of effectiveness, such as average and variance of waiting times, bus-loading levels, cycle time distribution for operational speeds, waiting time distribution, and frequency of holdings. Delgado et al. (2015) further expanded their work by integrating their holding/boarding limit strategy with TSP control to shorten a bus's running time between stations.

Table 2.2 summarizes the primary features of some key studies on holding strategies, including the control points (at single control point or at several points along a corridor), vehicle capacity, real-time operations, the stochastic operational properties, objective functions, and the combination of holding with other control strategies (e.g., boarding limit, stop-skipping, and transit signal priority).

Table 2.2 Summary of studies regarding holding strategies

Author	Real time	Mode	Vehicle Capa.	Stochasticity	Routes	Holding Stop	Objective Function	Combined strategies
Barnett (1974)	No	Bus	No	No	Single	Single	Wtime + Win-veh	-
Eberlein et al. (2001)	Yes	Rail	No	No	Single	Single	Wtime +Win-veh	-
Hickman (2001)	Yes	Bus	No	Yes	Single	Multi	Wtime +Win-veh	-
Fu and Yang (2002)	Yes	Bus	No	No	Multiple	Multiple	Var h	-
Zhao et al. (2003)	Yes	Bus	No	No	Multiple	Multiple	Wtime +Win-veh	-
Zolfaghari et al. (2004)	Yes	Rail	Yes	No	Single	Multiple	Wtime +Wextra	-
Yu and Yang (2007)	Yes	Bus	No	No	Single	Multiple	Wtime +Win-veh	
Sáez et al.(2011)	Yes	Bus	Yes	No	Single	Multiple	Wtime +Win-veh	Stop skipping
Delgado et al. (2009)	Yes	Bus	Yes	No	Single	Multiple	Wtime+Win-veh+Wextra	Boarding limits
Delgado et al. (2012)	Yes	Bus	Yes	No	Single	Multiple	Wtime+Win-veh+Wextra	Boarding limits
Delgado et al. (2015)	Yes	Bus	Yes	No	Single	Multiple	Wtime+Win-veh+Wextra +Wlight	Boarding limits, Signal priority

* Wtime: waiting time at bus stop, Win-veh: extra in-veh time due to holding, Wextra: extra waiting time at bus stop due to boarding limie

2.3 Signal Progression

In review of the literature on arterial traffic signal controls, one may classify existing studies into two categories: maximizing progression and minimizing total vehicular delay. As the former strategies may offer the basis for design of bus progression control, this section briefly reviews some key studies on this subject. The core logic of such studies is to synchronize signals on an arterial with the optimized offsets and common cycle length to facilitate the movements of vehicles over consecutive intersections. As pioneering researchers on this subject, Morgan and Little (1964) first presented a model to maximize the total two-way progression bandwidth on an arterial. Little (1966) later further proposed an advanced model to concurrently optimize the common cycle length, progression speeds, and offsets with mixed-integer programming.

Along the same line, Little et al., (1981) presented a model called MAXBAND, an enhanced version of their earlier work that can concurrently optimize the offsets, the prevailing speed at each link, and the left-turn phases. The objective function of MAXBAND is to maximize the weighted sum of the two-way bandwidths. Grounded on the core logic of MAXBAND, Gartner et al. (1991) formulated the progression model with various bandwidths, called MULTIBAND, for links with different volumes. As another series of bandwidth-based models, PASSER II was developed independently by the Texas Transportation Institute (Chaudhary et al., 2002.) To ensure the effectiveness of the optimized progression control, Tian and Urbanik (2007) developed a partition technique to facilitate the progression on the

direction of higher volume, and to keep a sufficient green-band within the subsets of intersections.

Aside from those studies on the arterial signals, some researchers extended progression logic to various applications, ranging from grid networks to unconventional intersections. For example, Chang et al. (1988) implemented the MAXBAND model to a multi-arterial closed network and developed an optimization program, named MAXBAND-86. Stamatiadis and Gartner (1996) developed another network version of their multiband work, named MULTIBAND-96. In view of the fact that such extensions often significantly increase modeling complexity due to the expanded size of the integer variable set, Gartner and Stamatiadis (2002, 2004) proposed a two-step solution procedure to improve the computing efficiency of existing progression models. Their focus was to provide green bands to traffic movements along those key routes, rather than solely along the arterial. Yang et al. (2015) proposed a multi-path progression model for synchronization of arterial signals for traffic flows along the critical path/routes. Based on the same notion, Yang et al. (2014) further developed a progression model which can concurrently provide green bands to the off-ramp flows and local through traffic at the diverging diamond interchanges (DDI).

2.4 GLOSA

Green Light Optimized Speed Advisory (GLOSA) system is designed to produce advisory speeds for vehicles approaching an intersection so that they can arrive at the intersection during the green phase and also take less stops to go through traffic signals. This system needs timely and accurate information such as traffic signal

timings and approaching vehicles locations to traffic signals to compute an advisory speed.

With the emergence of connected vehicles, a large body of studies concerning GLOSA has been conducted for improving mobility, safety, and fuel efficiency at both the intersection and arterial levels. For example, Katsaros et al. (2011) proposed a GLOSA-like application and evaluated its performance using an integrated cooperative ITS simulation platform. Their evaluation results show that GLOSA systems could reduce both fuel consumption and traffic congestion.

Asadi and Vahidi (2011) proposed a predictive vehicle cruise control, based on optimized vehicular trajectories through several downstream traffic signals to reduce idle times and fuel consumption. Their simulations results, based on the proposed model, show that signal-to-vehicle communication technologies can contribute to the reduction in fuel consumption, greenhouse gas emissions, and trip time. For the same purposes, Alsabaan et al. (2013) developed a comprehensive optimization model that involves V2V and V2I communications to minimize fuel consumption and emissions.

Seredynski et al. (2013) introduced a multi-segment GLOSA for an arterial with multiple lights in sequence on a vehicle's route. The experimental results show that the multi-segment GLOSA under free-flow conditions can be much more effective than with a single-segment approach.

Stevanovic (2013) evaluated a GLOSA implementation for two types of traffic signals: predictable fixed-time signal timing and unpredictable actuated–coordinated signal timing. A two-intersection traffic network was modeled in

VISSIM and an emission model was used to estimate the resulting emissions. Their results for extensive simulation experiments indicate that GLOSA has a significantly positive effect on all performance measures under fixed-time signal-control where the phase durations are predictable, but not under actuated–coordinated signal operations.

Xu at al. (2015) developed the branch and bound (B&B) algorithm for applying the GLOSA system to a series of intersections, and reported to achieve a reduction in stop times and fuel consumption without affecting operational efficiency (i.e., travel time) under free-flow conditions. Drawing from their previous work (Bodenheimer et al., 2014), Bodenheimer et al. (2015) presented an approach to forecast the phase duration under adaptive traffic control by using graph transformation, and reportedly achieved the expected level of performance.

2.5 Closure

In summary, this chapter has provided a comprehensive review of research efforts on the subject of transit monitoring system and transit controls in urban networks. Those studies, using transit GPS data to monitor transit fleets, focused mainly on exploring the viability of using transit fleets as probe vehicles for detecting general traffic conditions. However, research on extending the use of bus GPS data to replace existing traffic network detectors and to detect traffic conditions at movement levels has not been addressed yet.

In addition, a variety of TSP models have been proposed in the literature, and reported to achieve promising results with respect to enhancing bus schedule reliability and reducing average personal delays. However, those developed models cannot be used on arterials with heavy bus volume due to negative impacts on the

non-priority traffic and the subject intersection's downstream arriving patterns. Certainly, embedded TSP under a full-scale adaptive signal control may minimize the negative impact raised in the state of practices. But the cost associated with deployment, operations, and maintenance of an effective and reliable adaptive network signal control systems is practically beyond the bearable level for most responsible traffic agencies, as evidenced by the fact that adaptive network signal control systems up to date are mostly deployed at the demonstration, but not the day-to-day operation level.

Under such circumstances, a passive traffic signal control strategy – which considers the bus volume directly in design of signal offsets – can be a viable option for facilitating bus flows, providing reliable bus travel times along an arterial, and increasing bus ridership. Most existing studies on this subject, however, are for general traffic, and thus are unlikely to be applicable for transit systems.

Furthermore, it is expected that an integrated transit signal priority control system which first employs an off-line module to yield the optimal offsets for bus progression, and then activates an active TSP at critical intersections in real-time operations, can yield the benefits for the entire arterial, not an individual intersection; and the negative impact of real-time TSP activations and cost of the TSP system can be minimized.

With respect to bus operations, a rich body of studies regarding bus holding control has been conducted over the past decades and reported to be promising in enhancing bus reliability and reducing travel times. In practice, however, executing those holding controls is subjected to some operational constraints, such as capacity

of bus stops and travel time variability due to traffic signals. The impacts of such constraints on the design of bus-holding strategies remain to be further investigated.

Lastly, despite the progress of existing studies on traffic control, some critical issues associated with facilitating bus progress on arterials under congested conditions have not been studied. Examples of such issues include:

- How to design signal plans (i.e., offset) at intersections along an arterial having heavy transit flows;
- How to deal with the conflicts between general traffic flows and bus flows, and to facilitate both types of traffic flows;
- How to deal with the uncertainty of bus arrivals at intersections due to variable passenger demands at bus stops and fluctuation of traffic conditions to facilitate bus flows with less stop and delay;
- How to optimize transit control strategies considering transit reliability, fuel consumption, and passenger comfort;
- How to design real-time integrated control strategies for traffic signals and the transit management systems when bus-bunches have been detected.

Chapter 3: The Structure of the Integrated Traffic Signal Control System

3.1 Introduction

Consider the scenario where a major commuting arterial comprises a series of signalized intersections, multiple transit routes, and bus stops on each of its congested roadway links. Conceivably, to best accommodate the daily transit demands from the perspective of transit operators, it is imperative to ensure service reliability along such an arterial so as to sustain or increase ridership. However, it is very challenging to maintain the service reliability of a transit system on congested arterials because any of the following frequently encountered conditions may derail a transit vehicle from its operational schedule:

- Frequent encountering of the red-phase and the resulting wait time at signalized intersections;
- Traffic queues by passenger cars at signalized intersections, which often prevent transit vehicles from moving within the signal progress bands;
- Dwell time variance at each bus stop due to the unpredictable distribution of arriving passengers; and
- The stochastic nature of bus travel speeds along a congested arterial link, which may differ significantly from the speed distribution of passenger-car flows under congested conditions, and also cannot be detected at the desirable level of accuracy with conventional point-based traffic sensors.

To minimize the potential impacts of all aforementioned factors on transit system service reliability, a responsible operational agency needs to design craft strategies that can take proactive or reactive control actions in a timely manner so as to circumvent various scenarios that may cause service schedule delays. Examples of such actions include: real-time monitoring of each target transit vehicle's speed and location, predicting the temporal and spatial distributions of both bus and passenger-car speeds, designing signal progression plans to facilitate transit vehicles' unique stop-and-go (i.e., service at bus stops) pattern in each link, and performing signal adaptive control in real time to accommodate the delay caused by unexpected intersection traffic queues.

In review of related literature, it is evident that the above challenges and effective responsive strategies to ensure transit service reliability have not been adequately addressed yet. This chapter presents an integrated traffic signal control system that is designed in response to the aforementioned needs from the operations perspective. The proposed system features its following unique functions:

- Monitoring the time-varying speed and location of each target transit vehicle over an arterial link so as to provide the essential information for the control models to update key parameters and to execute the proper control strategies;
- Executing a pre-timed, but bus-based signal coordination model to facilitate transit vehicles to move over an arterial under different traffic demand levels and different dwell time variances;

- Estimating intersection queues and their relationship with the bus stop location so as to prevent traffic queues from interrupting the precomputed bus progression bands;
- Estimating bus arrivals by considering the uncertainty of dwell times at the upstream bus stops so as to sustain more buses throughout the bus progression band along the arterial;
- Selecting an optimal intersection to implement an active TSP so as to best utilize the pre-timed bus-based signal coordination system;
- Integrating an active TSP with a pre-timed bus based progression signal plan; and
- Estimating traffic conditions of an active TSP intersection and bus arrivals at its downstream intersections so as to better implement transit signal priority control in real-time operations.

The structure of the entire system to provide the above functions is presented in the next section.

3.2 System Structure

Figure 3.1 depicts the structure of the proposed integrated transit signal priority control system, which includes traffic detection, pre-timed signal control, and real-time signal operations.

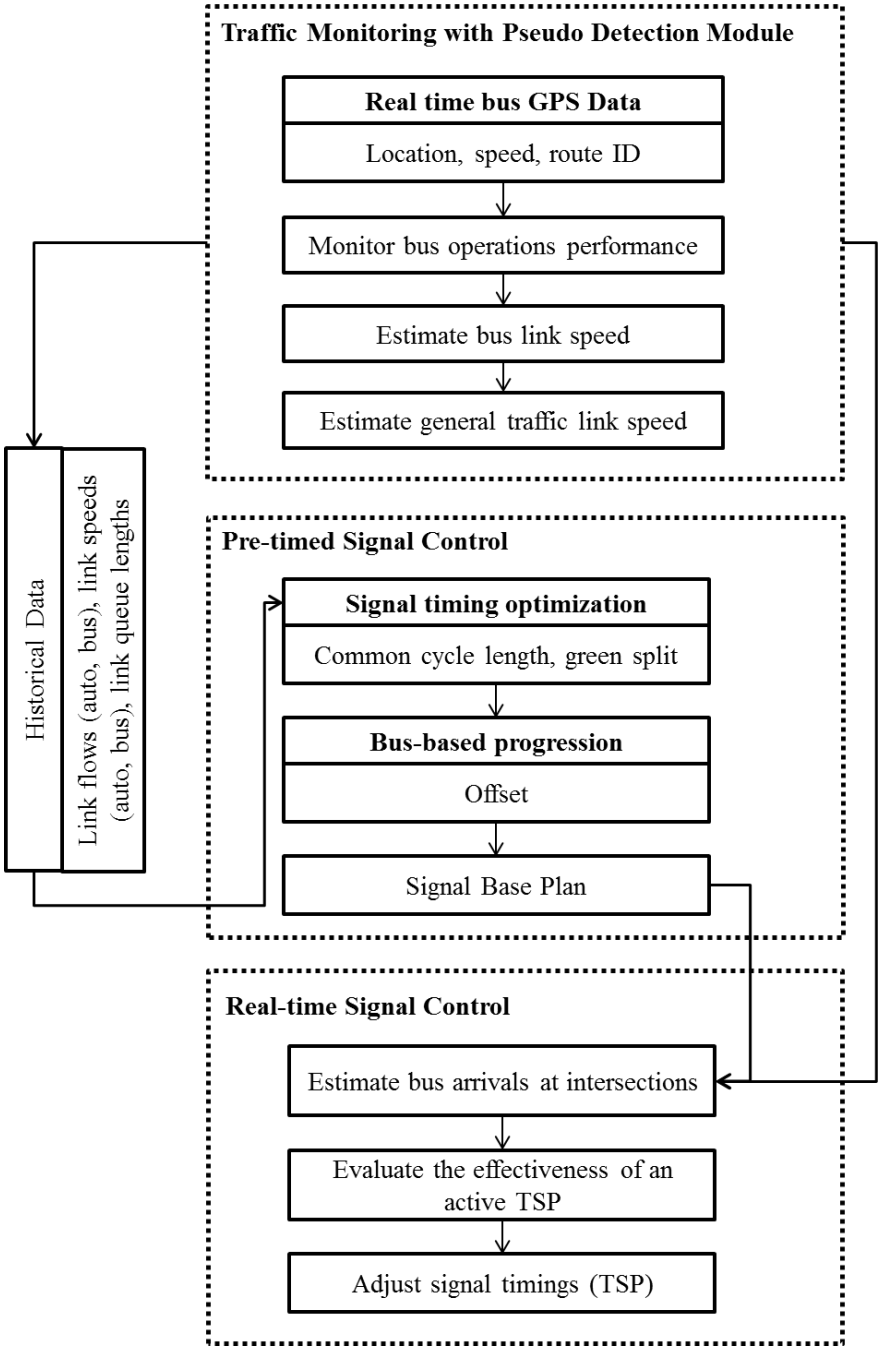

Figure 3.1 Structure of the integrated traffic signal control system

A brief description of each primary component and its role in the system's operations is presented below:

- **Bus-GPS-based pseudo detection module:** The core logic of a pseudo detection system is to convert the real-time bus GPS data into geographic-based sensors that can estimate both bus and general traffic conditions in urban networks beyond its original function of monitoring each buses speed and locations. The proposed detection module is to decompose the network into sub-links and view each as one pseudo detector, in which a bus in a sub-link is to function as a moving pseudo sensor so as to provide time-varying speed data (Figure 3.2).

  Taking advantage of heavy bus flows and spatial evolution over a link, the proposed pseudo detection module can provide more extensive information (such as link and movement-specific speeds) than conventional point-measurement detectors. The system can also provide the spatial and temporal variation of general traffic conditions by converting the time-varying bus speed in each sub link, viewed as a pseudo sensor. With such a cost-benefit pseudo detection module, responsible agencies can use sufficient information to determine key parameters in the control models and to activate the responsive strategies adopted in the optimal real-time control process. Chapter 4 will discuss all embedded formulations and modeling concepts in detail, including a GPS data-map-matching algorithm, missing data imputation, and data output analysis. A case study to demonstrate such a pseudo system's application will also be reported in Chapter 4.

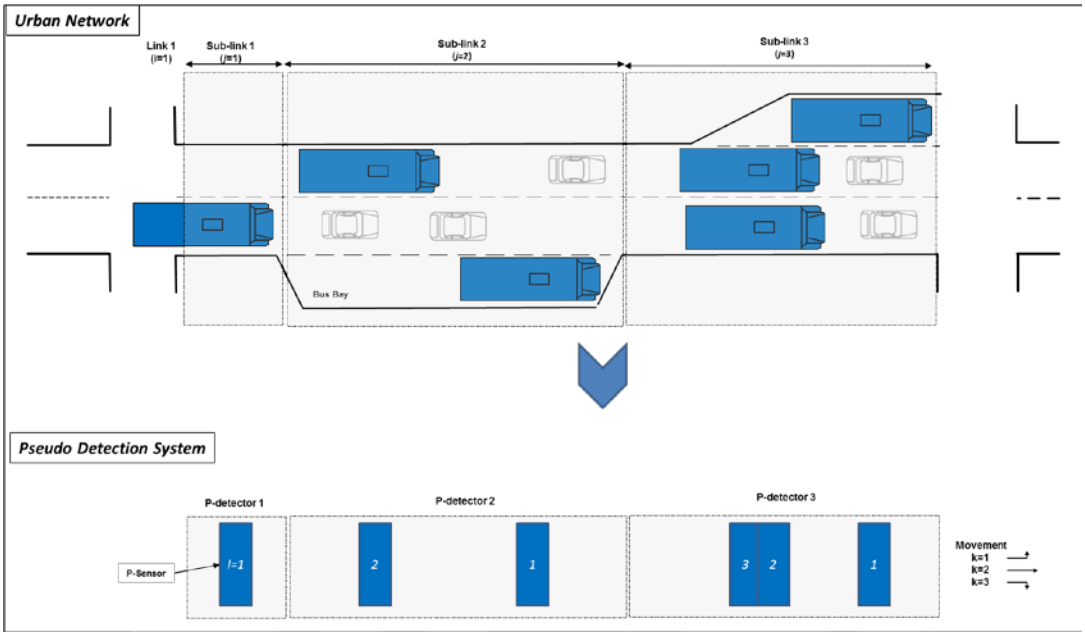

(a) A conceptual illustration of the pseudo detection system

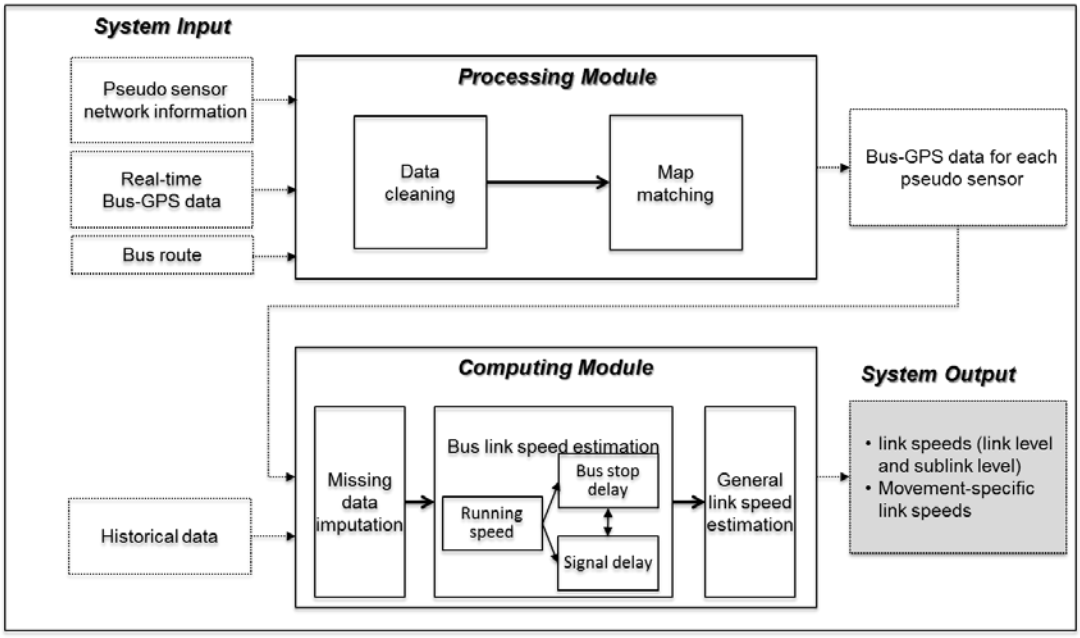

(b) A systematic framework of the pseudo detection system

Figure 3.2 Bus-GPS-based pseudo detection system

- **Bus-based signal coordination:** This module aims to design the signal plans to successively progress buses over intersections with minimal intersection delays. The off-line model first optimizes the offset at each intersection with the objective of maximizing bus bandwidths. It takes into account both bus operational characteristics and surrounding traffic conditions, including the impacts of bus dwell times on their travel times between intersections, bus stop capacity constraints to cause the spillover of arriving buses, and intersection traffic queues, and their relations with bus stop locations in the design of bus progression bands. The enhanced model (BUSBAND) is designed to optimize the offsets at each intersection with the objective of maximizing the total effective bus bandwidth which further accounts for the dwell time uncertainty. Chapter 5 will discuss the details of critical research issues associated with formulations of the proposed optimization model. It will also evaluate their performance with the extensive simulation experiments.

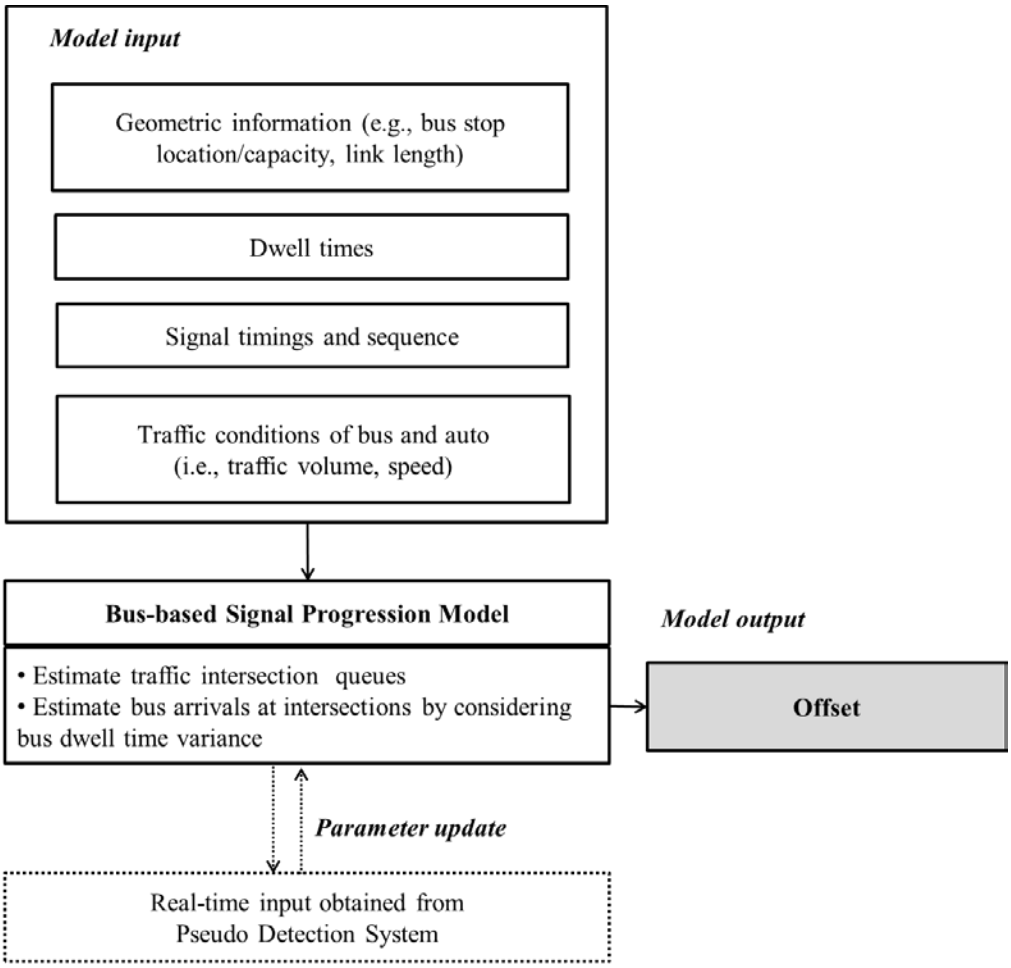

Figure 3.3 Input and output of the bus-based signal progression model (Passive TSP)

- **TSP Selection module:** The TSP selection module is proposed to determine an intersection for deploying an active TSP, based on the passive TSP design to best the benefits of the integrated TSP operations. Effective operations of an active TSP at a candidate intersection can be conditioned on the following issues: busband widths, the location of busbands within green times, its effectiveness at the downstream intersections, and its impacts on non-priority traffic movements at the TSP intersections.
- **Integrated real-time transit signal priority controls:** This module is to integrate an active TSP with a pre-timed BUSBAND for real-time operations. The integrated system is mainly to mitigate the impacts of bottleneck intersections on the bus progression band by offering a more flexible function for their signal controls to facilitate the bus progression and bus band expansion. More specifically, its main function is to dynamically adjust the green time (i.e., early green or green extension) based on the real-time detected bus locations to reduce bus delays and stops at intersections. Chapter 6 will describe such an integrated real-time TSP system, including its operating structure, TSP activation logic at critical intersections to maximize the total bus progression bands, and systematical procedures to select such intersections. Evaluations of their effectiveness will also be conducted with experimental analyses using various simulation scenarios.

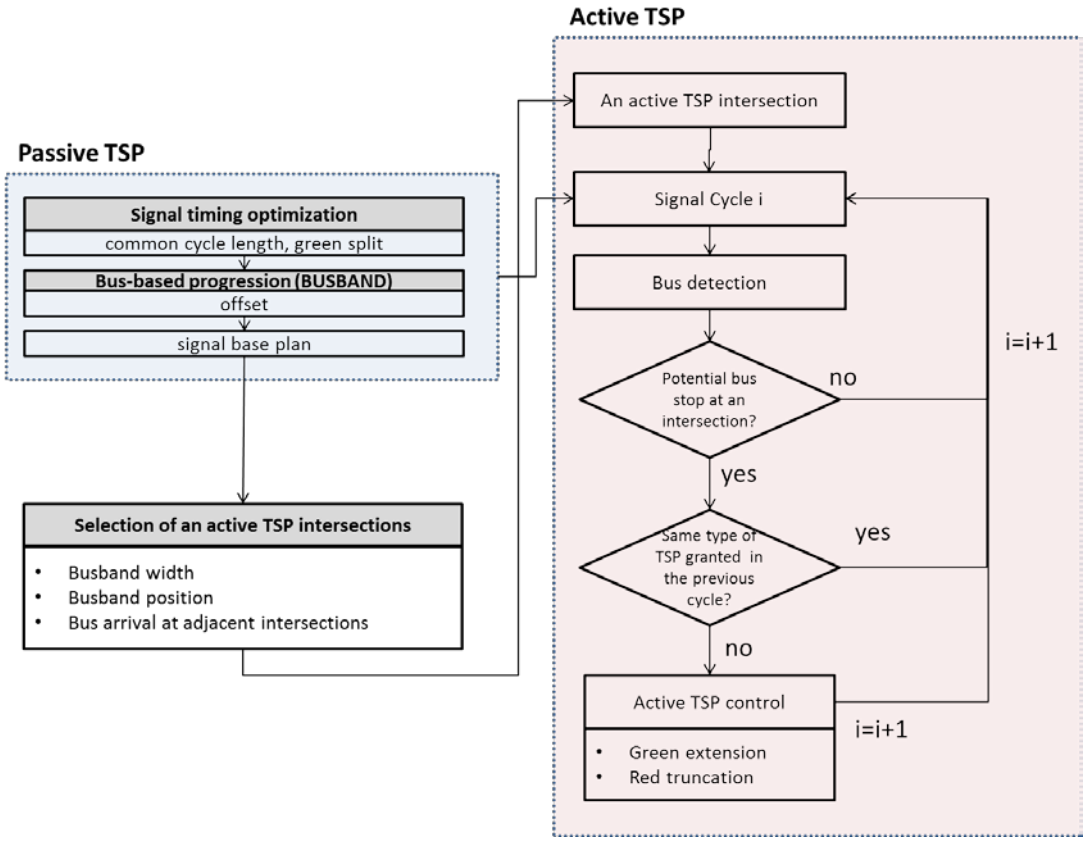

Figure 3.4 Flowchart of the integrated TSP control system

Chapter 4: A Pseudo Traffic Detection System with Bus GPS Information for Monitoring Urban Networks

4.1 Introduction

The time-varying network link speed is one of the most critical measurements for monitoring urban traffic conditions. Obtaining such information has commonly relied on either extensive deployment of link sensors or a fleet of probe vehicles. Unfortunately, such methods are quite costly from both deployment and maintenance perspectives. Furthermore, link detectors provide only point-measurement of traffic conditions, but do not assess congestion patterns over the entire link. Despite the recent advent of traffic data suppliers such as INRIX and Google for collecting traffic information, such information remains costly to most traffic agencies, and thus has not been fully utilized in contending with urban congestions.

Over the past decades, an increasing number of transit agencies adopted the GPS technologies to monitor fleets and to improve service quality. In many urban areas, a large number of buses equipped with a GPS receiver constantly traverse various parts of urban networks, transmitting their current locations and speeds to the operational center at each preset small interval. With the vast amount of bus GPS data, transit agencies can actually track bus locations, predict bus arrival times, monitor bus schedule adherence, and provide transit information to on-board passengers or those waiting at bus stops.

In review of the literature, it is noticeable that a large body of studies has been conducted on such applications, including estimating bus travel time, computing

aggregate link speeds for transit operational needs (Cathey and Dailey, 2002; Cathey and Dailey, 2003), and sharing traffic information with the general public (Bertini et al., 2004; Chakroborty and Kikuchi, 2004; Coifman and Kim, 2006; Pu et al., 2009). Furthermore, some metropolitan areas with large fleets of transit vehicles, such as Portland and Chicago, have demonstrated the potential of using transit vehicles as probing sensors (Washington State Transportation Center, 2005), but often suffered from insufficient data density for the temporal and spatial coverage. By incorporating historic data, those agencies have shown that transit vehicles could be a viable option to supplement the existing loop surveillance systems. Moreover, with the expanded spatial coverage and frequency of such advanced transit systems, the bus GPS data offer the potential for use in monitoring traffic congestion.

Existing studies on this regard are quite limited, mostly focusing on using GPS data for estimating bus travel time and traffic conditions, but not with a systematic structure to efficiently convert extensive bus GPS data into a pseudo-sensor network. Moreover, transit GPS data in a link with proper processing and clustering can yield much more information than those by point-measurement traffic detectors. For instance, one can categorize the GPS data by bus movement on a link, such as right-turn, through, and left-turn. These available movement-specific speeds in each link provide valuable information for transit managers and traffic operators to further estimate the speed differences between through and turning traffic flows in addition to the average time-varying link speed.

Thus, to best use such real-time bus GPS data this study proposes a design that can systematically convert such real-time bus GPS data into pseudo detectors

which can provide reliable link and movement-specific speeds for monitoring traffic conditions. The development procedures for such a system are also presented in detail with associated algorithms for use in tackling critical design and operational issues. An example to demonstrate the applicability of the proposed methodology is also illustrated in this chapter.

The remaining sections are organized as follows. Section 4.2 presents the structure of the pseudo detection system, including its primary technical modules and key computing issues. Section 4.3 then illustrates an experimental study with a real-world application. The last section summarizes the main contributions and comments.

4.2 Structure of a Pseudo Detection System

The core logic of a pseudo detection system is to convert real-time transit GPS data in each link into multiple interconnected pseudo sensors in detecting traffic conditions in urban networks beyond its original monitoring function for transit vehicles. As shown in Figure 4.1 (a), the proposed system is first to decompose a spatial link in the network into several sub-links based on the geometric features (e.g., the existence of bus bays and intersections) and view each of them as a pseudo detector. A bus in the network will then function as a moving sensor of each pseudo detector. Such pseudo sensors will transmit data over time to the computing function of each pseudo detector, including sensor ID (bus ID), route ID, recording time, recording location, and speed. The number of moving sensors in each pseudo detector varies with the number of buses located within the spatial boundaries of each detector at each time interval.

Figure 4.1 (b) shows the movement of pseudo sensors over time and their speed measurements as fed to the pseudo detectors. Since GPS data for recording/transmitting interval is relatively short (e.g., 10 sec), the detector may receive no data for a certain time interval. For instance, pseudo detector-1 has speed measurements at time intervals of t=1 and t=2, but does not information at time of t=3. Over a properly-defined data aggregation interval (e.g., 30 sec, 1min, and 5min), it is most likely that each pseudo detector shall have sufficient measurements for estimating the time-varying link speeds. Moreover, since each speed measurement has a turning movement flag for left, through, and right at the upcoming intersection from bus route information, the pseudo detectors can sort such information and produce movement-specific speed measurements for a target intersection.

Taking advantage of heavy transit flows, a pseudo detection system can provide the temporal and spatial variations of link speeds and movement-specific speeds, which cannot be achieved using the existing loop detector-based system (Figure 4.1. (c)). Depending on the signal phase at the intersection or the downstream traffic condition for a specific movement, its speed can be different. For instance, among vehicles approaching an intersection, through and right-turning vehicles may proceed to the downstream link, but left-turning vehicles may have to stop at the intersection and form queues. Thus, such movement-specific information is essential for monitoring traffic conditions in each link and to estimate the travel times by route in a network.

Figure 4.1(d) shows the network-wide view of the pseudo detection system. Compared to the conventional detector system for link point-measurement, the

pseudo detection system with bus GPS data can provide both the temporal and spatial distribution of traffic speeds over a link, and also the movement-specific speed estimates at the exit of each roadway link.

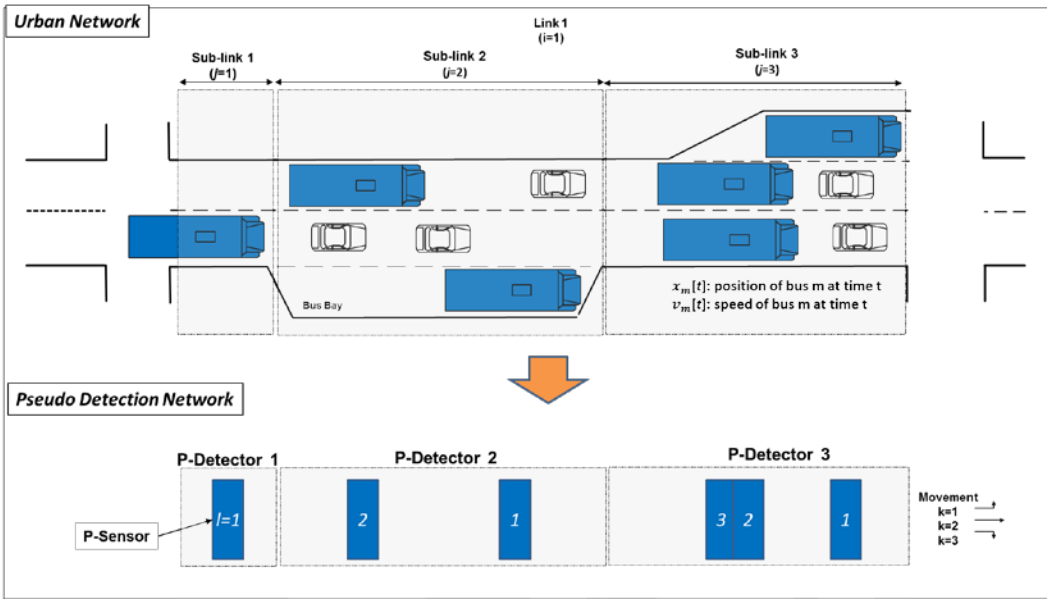

(a) Pseudo detectors and pseudo sensors

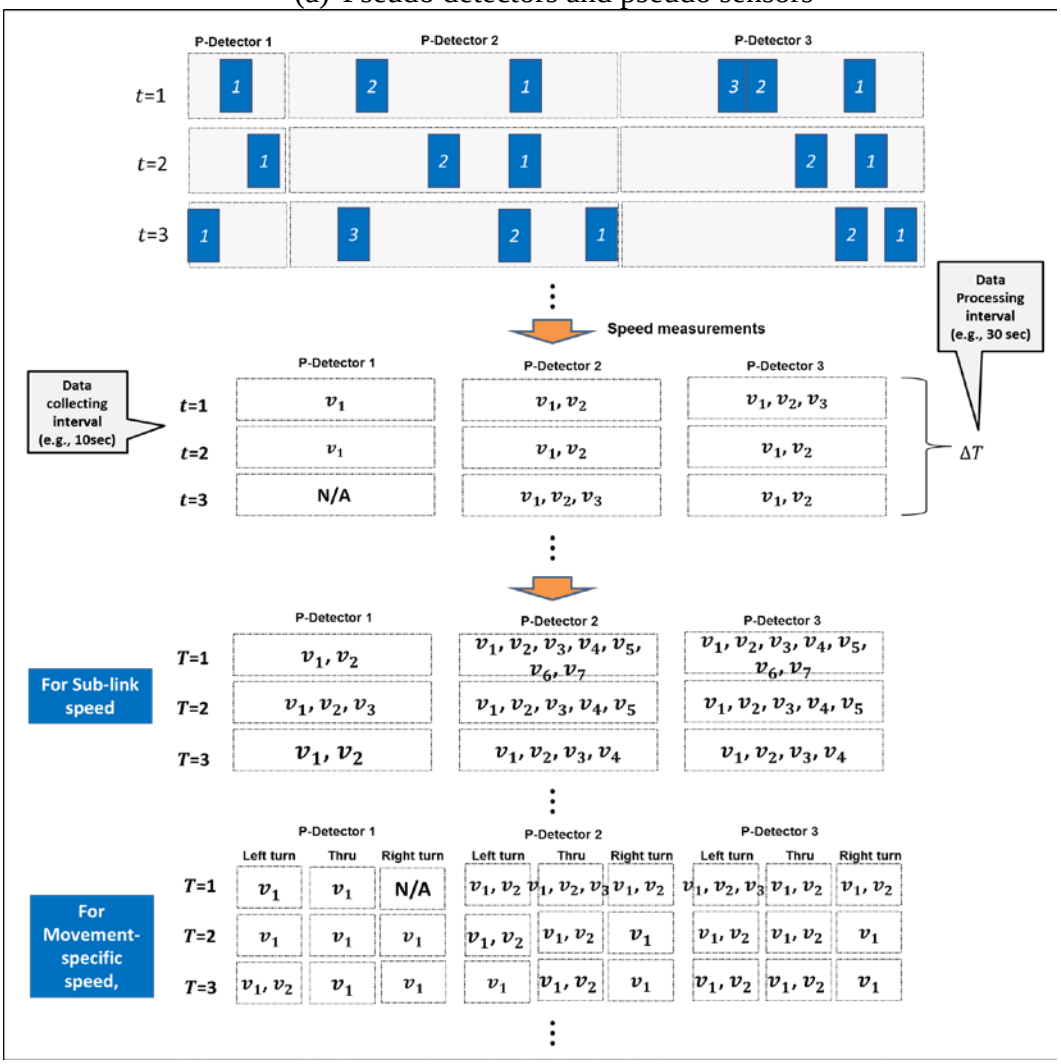

(b) Speed measurements with pseudo sensors

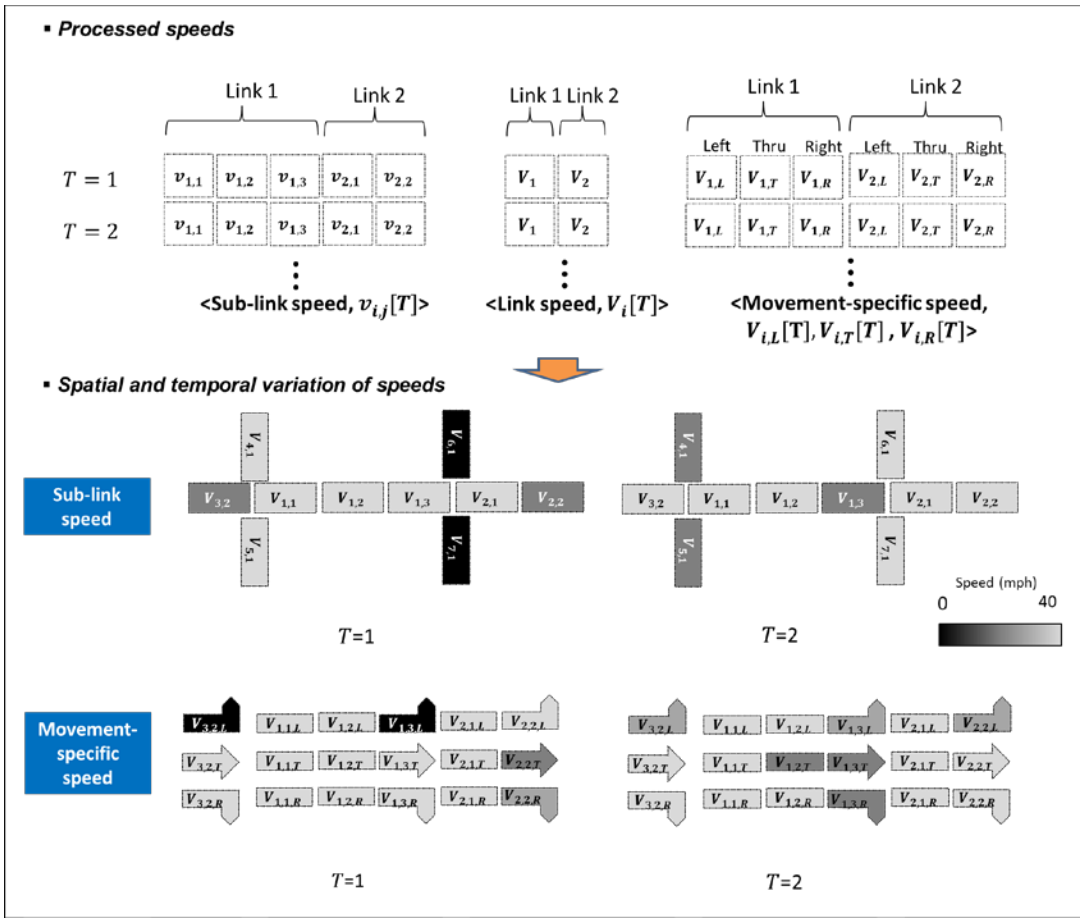

(c) Output of the pseudo detection system

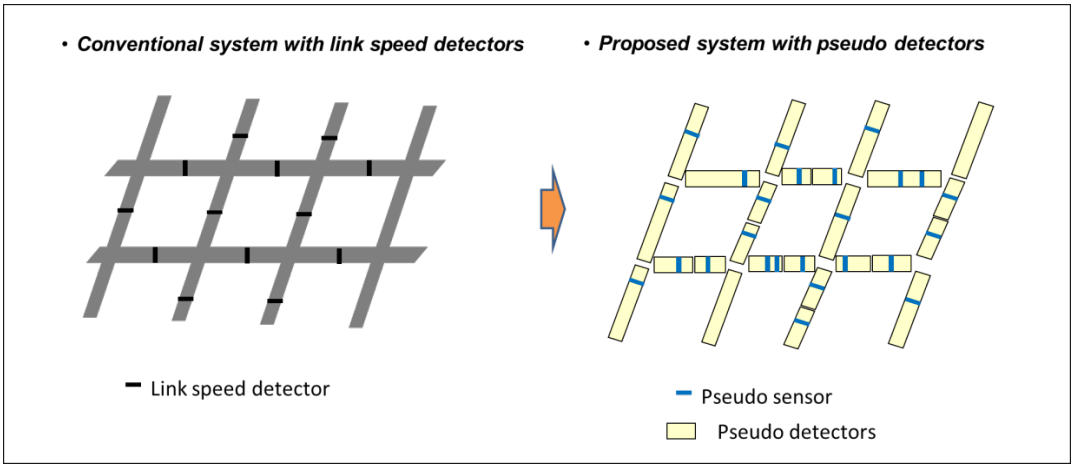

(d) Network-wide view of Pseudo Detection System

Figure 4.1 Conceptual illustration of the proposed pseudo detection system

In developing the proposed pseudo detection system, one needs to tackle several critical issues. First, it is necessary to map the collected GPS data to the traffic network. Since the GPS data location information is provided in the format of latitude and longitude coordinates, one needs to determine on which link each target bus is traveling. Due to the errors inherent in the GPS data and the dense nature of urban streets, it is challenging to assign the collected GPS data to the road network at the required level of accuracy. Secondly, there may be missing observations in each roadway link over some short intervals, despite having a large number of buses equipped with GPS receivers – especially when movement-specific speeds are of interest. Depending on the traffic conditions or bus schedules, some links could have only a few data points or none at all over a certain time period. Thirdly, instantaneous speed data computed from individual buses over short intervals are subjected to inevitable fluctuations. Thus, data imputation and smoothing are necessary to ensure the data quality and usability for target applications. Lastly, since the observed speed data of each bus in a roadway link often with factors such as the presence of a bus stop, passenger requests, and responses to traffic signals, one needs to calibrate the relationship between buses and general traffic so that traffic conditions based on bus GPS measurements can be converted properly to those experienced by passenger cars.

As shown in Figure 4.2, the proposed pseudo detection system consists of several modules to support potential users to best utilize bus GPS data for measuring a network's general traffic conditions. The development procedures and logic underlying the proposed detection system for estimating link speed with the real-time bus GPS data are presented below.

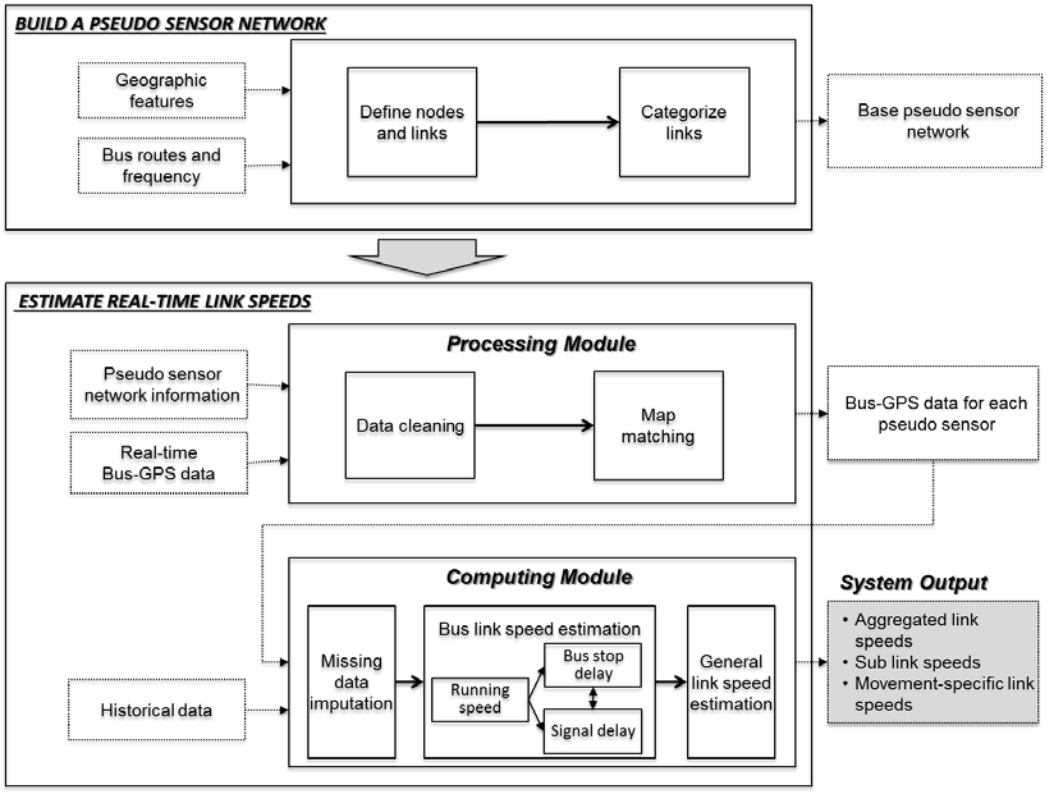

Figure 4.2 Operational flows of the proposed pseudo detection system

System Development Procedures

Step 1. Identify the location of each pseudo sensor in a link based on geographic features

The behaviors of buses often differ significantly from those of automobiles on roadway segments having bus stops, bus-exclusive lanes, or traffic signals. Thus, to obtain performance measurements for general traffic with bus GPS data, it is necessary to take into account the differences between those two types of vehicles. Given geographic features and bus route information, one can first decompose the roadway network into nodes and links, where a node can be an intersection, a point of geometric change, or for merging or diverging maneuvers. A link in the pseudo detection system functions as a pseudo detector. If the distance between nodes is too

long, one can add one or more to decompose a link into multiple sub-links. Links are determined by the identified nodes and can be generally categorized by considering the following factors:

- The existence of a traffic signal, or a bus stop along the link
- The existence of bus exclusive lanes or high occupancy vehicle (HOV) operations
- The location of bus stops (e.g., far-side, near-side, and mid-block)
- The configuration of bus stop (e.g., bus bay and bus turnout), etc.

Step 2. Process bus GPS data in real time with an efficient computing module

The main focus of this step is to convert real-time GPS data into a pseudo detector network. Note that each bus company can have its own data-recording interval, ranging from 10s to 60s, and most such bus GPS data are transmitted to the transportation center in real time. Each set of the GPS data contains the route number, bus ID, recorded date and time, recorded location, heading of a bus, and spot speed. These raw data may contain unreliable records such as duplicated, incomplete and mis-recorded data. Thus, the data must be preprocessed prior to undergoing any analysis.

For the location information given in the format of longitude and latitude, the GPS records after the preprocessing process need to be matched with the predefined links. Hence, such a system needs to have map-matching algorithms to address the issue of correctly assigning location measurements from a GPS device to the corresponding network. Note that the complexity of this task is compounded by the

often low sampling rate in some network links and the measurements noises. As such, an efficient and robust algorithm to do so will be essential.

Grounded on the related study by Li et al. (2013), this study develops a robust and efficient map-matching algorithm for real-time applications using an optimization-based approach with the shortest path concept. The proposed algorithm intends to minimize the stitching cost, the distance between two successively matched links, by adopting the shortest path concept. Furthermore, bus route information can offer the basis for the algorithm to exercise a more efficient selection of candidate links. The mathematical formulations of the algorithm can be expressed as follows:

$$\text{Minimize } \sum_{t \in T} \gamma_t \tag{4.1}$$

Subject to

$$\sum_{j \in C_t} x_{t,j} = 1 \qquad \forall\, t \in T \tag{4.2}$$

$$\sum_{j \notin C_t} x_{t,j} = 0 \qquad \forall\, t \in T \tag{4.3}$$

$$\sum_{j \notin C_t} \gamma_t \geq (x_{t,i} + x_{t+1,j} - 1) \cdot sp_{i,j} \qquad \forall\, t \in T \backslash \|T\|, i \in C_t, j \in C_{t+1} \tag{4.4}$$

$$\gamma_{\|T\|} = 0 \tag{4.5}$$

$$x_{t,j} = [0,1] \qquad \forall\, t \in T, \text{j} \tag{4.6}$$

where T is the set of GPS observations; γ_t is the stitching cost from the t^{th} assigned sublink to the $t+1^{st}$ assigned sublink; C_t is the set of the candidates of record t; and $sp_{i,j}$ is the shortest path from sublink i to sublink j.

Constraint (4.2) represents that record *t* is assigned to the one among all candidate links. Constraint (4.3) denotes that if sublink j is not in the candidate set of record t, the record t will not be assigned. Constraint (4.4) shows that if two consecutive records (t and $t+1^{st}$) are on different unit links, then the directed shortest

path from the end of the current sublink to the start of the next sublink will be calculated. By taking the directed shortest path, hopping from one side of the road to the other is discouraged since this would make the shortest path distance excessively long. At an intersection, these two ways will meet and their shortest path cost will be zero since they can directly link up. Thus, a penalty (e.g., 50 feet) for switching to a different way is introduced so that this can prevent the trajectory from momentarily hopping to a different road.

Constraint (4.5) is to ensure that if all candidates are along the same sublink, the stitching cost is zero, which discourages them from departing away the current sublink. Through Constraints (4.4) and (4.5), one can ensure the direction and connectivity of the roadway network. Constraint (4.6) presents that variable $x_{t,j}$ is equal to 1 if point t is matched to sublink j, and 0 otherwise. Table 4.1 shows the key steps of the proposed map matching algorithm.

Table 4.1 A modified single-track map matching algorithm

Step 1. Form all k-segments in the graph.
Step 2. Create a square region around each sublink for obtaining candidates
Step 3. Calculate the shortest paths between any pair of their candidates for any pair of records t and t+1
Step 4. Assign an id number to all records based on their timestamps
Step 5. Assign an id number to all sub links that have been identified as candidates of any record
Step 6. Run the integer programing

Step 3. Estimate the link speeds with the computing module

Data Imputation: The main focus of this step is to obtain the reliable link speed information using pseudo sensor data. Despite the increasing availability of bus GPS data, there may be some periods during which no buses are on a particular link.

For instance, some links during recurrent or non-recurrent congestion periods can experience random missing data over certain time intervals or during consecutive time periods. Due to a preset bus schedule, some links without any bus service during some periods (e.g. non-operational hours) will also have inherent missing data. Furthermore, since GPS data are from individual buses in motion, instantaneous speed data computed over short intervals are subjected to inevitable fluctuations. Thus, data imputation for missing and smoothing is necessary to ensure the data quality and usability for target applications.

To contend with those issues, researchers have developed numerous data imputation algorithms, including replacement and interpolation to Expectation Maximization (EM), Autoregressive integrated moving average (ARIMA), Bayesian Inference, Kalman filtering, and artificial neural networks (Smith et al., 2002; Chen et al., 2003; Smith et al., 2003; Zhong et al., 2004; Ni, 2005; Chiou et al., 2014). Depending on the data collecting/processing frequency and availability, one may employ different algorithms for the target level of accuracy.

Link and Movement-Specific Speed Measurements*:* The speed for each pseudo detector can be estimated by aggregating the processed speed measurements from pseudo sensors within each pseudo detector. Since a link comprises several pseudo detectors, the spatial and temporal variations of speeds over the link will be available for traffic management. Moreover, the speeds of traffic flows often vary by their movements at the end of the link such as at a traffic signal but such discrepancies cannot be captured with conventional detection systems. Since bus routes are fixed, the pseudo detection system can thus use such information to

estimate movement-specific speed by aggregating speed measurements by movement at a downstream diverging point. The availability and reliability of such spatial and temporal variations of movement specific speeds over the link certainly depend on the density of transit vehicles in real time along the link.

Converting to General Traffic Speed: The estimated speeds on sub-links using bus GPS data can be converted into speeds for general traffic by taking into account the unique features of bus behaviors, such as their tendency to use the right lanes, lower speeds than automobiles, and the impact of delays due to bus stops and traffic signals. The differences between the bus and general traffic speeds can be estimated by employing existing models. For instance, regression models built on a relationship between automobile and bus speeds can be used for converting bus speeds to general traffic information (Bertini et al., 2004; Chakroborty and Kikuchi, 2004). Depending on the link characteristics and associated factors, one may employ different algorithms to convert the available data from the pseudo sensors to approximate the general traffic speeds.

4.3 Illustration of the System Development

Study Site

To illustrate the procedures for developing the proposed pseudo detection system, this study uses bus GPS data from a corridor connected to Yu'ao Bridge in the city of Chongqing, China. The bridge is one of the busiest corridors, and is about a half mile long and one-way southbound. The GPS data came from five bus companies of 35 routes with about 1,000 buses traversing over the Yu'ao Bridge on April 11, 2012. The logging intervals of GPS data vary across routes and buses, ranging from 10 – 30

seconds. The GPS data contained bus company ID, route number, bus ID, date and time, longitude, latitude, speed, and angle (i.e., heading of a bus). Figure 4.3 shows the design of pseudo sensors in the study area. Based on geographic features, bus stop existence, and bus routes, the network is decomposed into five links with the nodes merging to the bridge and diverging from the bridge. Furthermore, based on the bus stop existence, its location and link length, links are decomposed into several sub-links.

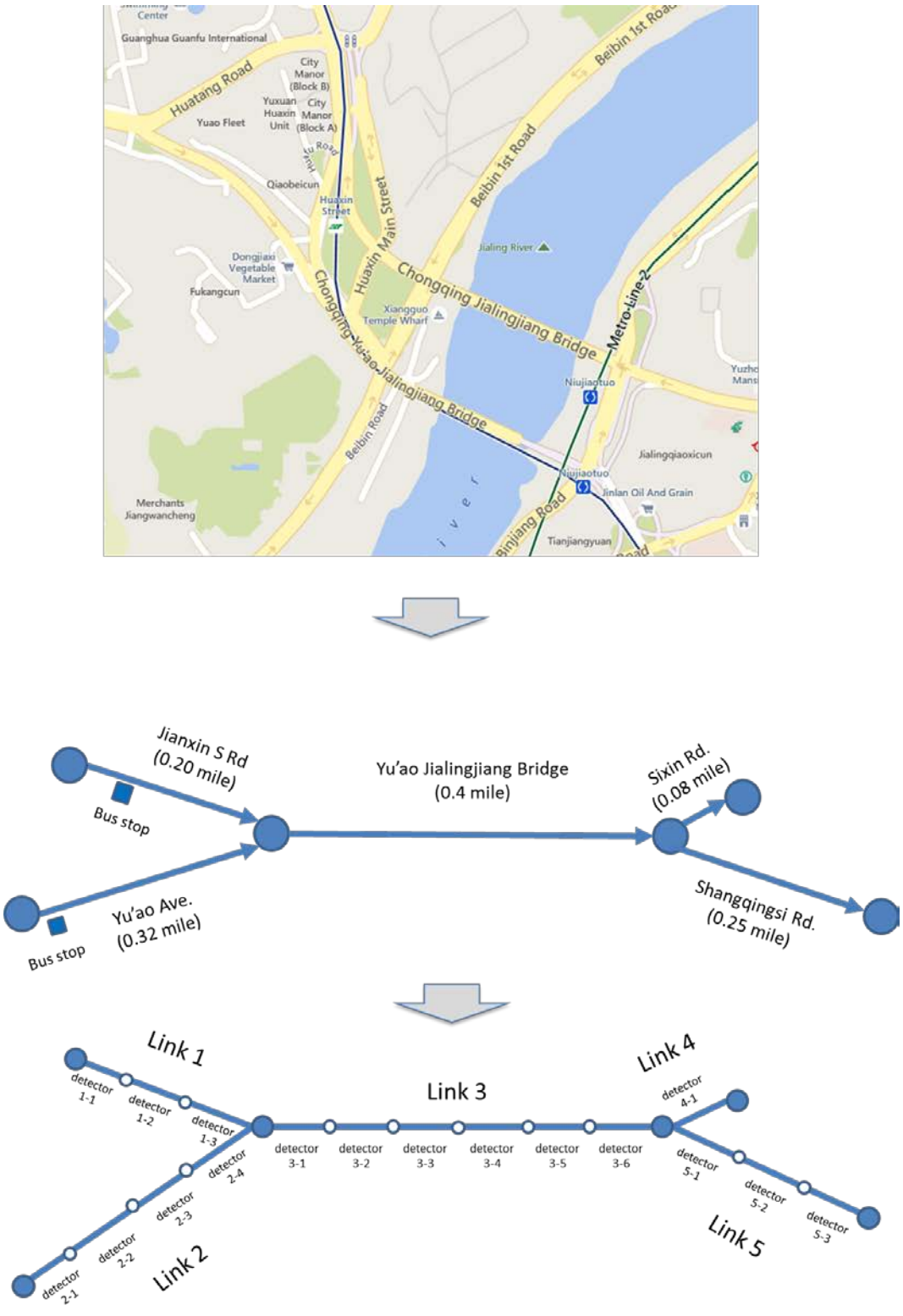

Figure 4.3 The target link for computing time-varying link speed and movement-based speed with bus GPS data

Executing the Map-matching algorithm

To ensure computing efficiency, the next step is to process the blocks of 500 records at one time using the map-matching algorithm proposed in the previous section, and to achieve the optimality gap of 2 percent. Note that this task of matching can be done under either the online or offline conditions.

Computing the data

Using the well-matched bus GPS data, the next step is to estimate sub-link speeds. This study employs the Bayesian updating procedure. If bus GPS data are available for the current time interval, the data from the previous five-minute period will be used to obtain the prior distribution, and the updated mean speed with the current one minute data will be used to execute the computation. If no bus GPS data is available, the mean of the previous five-minute speeds will be selected for the need. A detailed description of such an updating algorithm is available elsewhere (http://www.mhnederlof.nl/bayesnormalupdate.html).

The aggregate link speed of several pseudo detectors can be calculated with Equation 4.7.

$$v_i(t) = \frac{1}{l_i}\sum_{j=1}^{N} l_{i,j} * v_{i,j}(t) \qquad (4.7)$$

where, $v_i(t)$ denotes speed of link i at time t; $v_{i,j}(t)$ denotes speed of sublink j of link i at time t; l_i denotes length of link i; $l_{i,j}$denotes length of sublink j of link i; and N is the number of sublinks of link i.

System output I: Spatial distribution of link speeds

Note that one link can have several sub-links that function as pseudo detectors, and thus can be used to obtain the spatial distribution of link speeds. Figure 4.4 shows the temporal variation of aggregated link speeds and spatial distribution of link speeds in the study area on April 11, 2012 (Wednesday) during PM peak hours. The Yu'ao Bridge (Link 3) has six pseudo detectors (i.e., P 3-1, P 3-2…, and P 3-6), and the speed data from each detector shows the speed transition pattern on the bridge over time. As shown in Figure 4.4 (a), the aggregate link speed during PM peak hours gradually decreases over time from 4:30 p.m. and bottoms out around 5:30 p.m. More specifically, as shown in Figure 4.4 (b), the speed drop on the bridge starts from the most downstream segment of the bridge (S 3-6) around 4:40 p.m., and the congestion evolves later to the furthest upstream segment of the bridge. Finally, the entire bridge experiences traffic congestion from 5:30 p.m. The sub-link speeds from the pseudo detection system can provide more detailed information on the temporal and spatial distribution of congestion patterns (Figure 4.4. (c)).

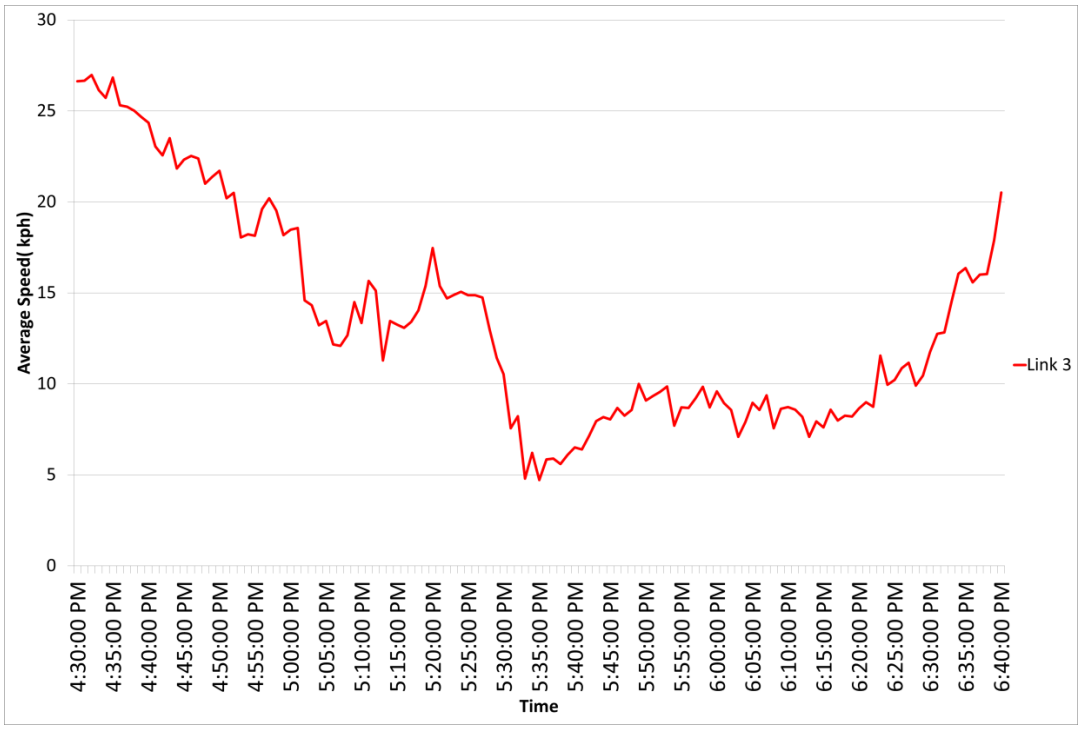

(a) Temporal link speed

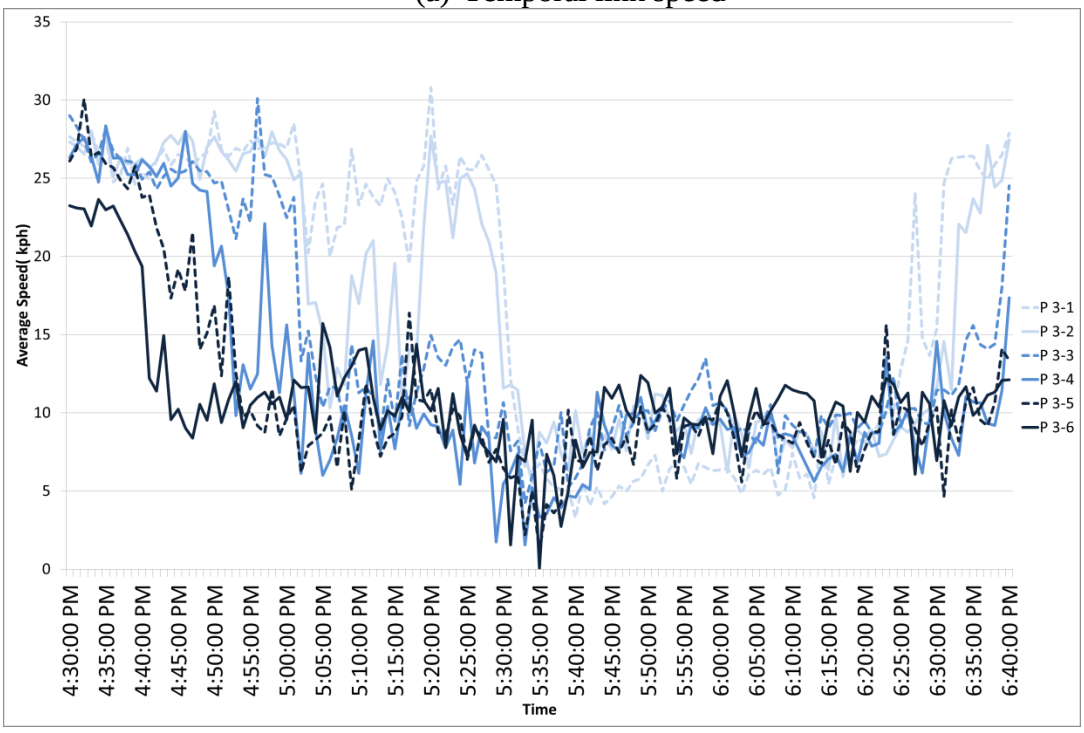

(b) Temporal sublink speed

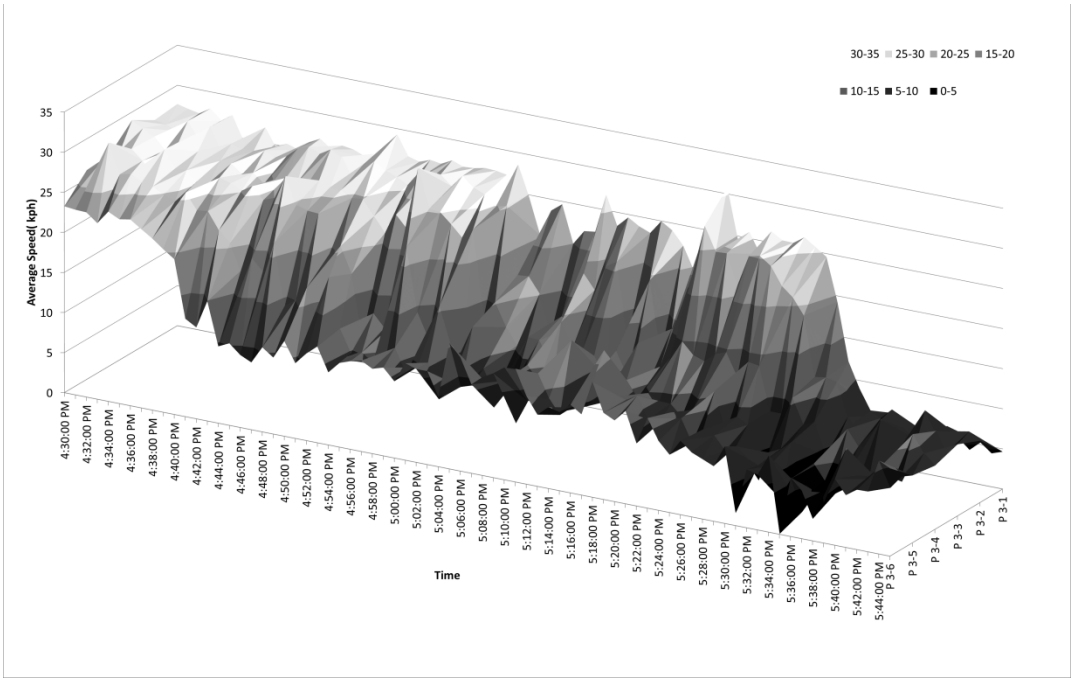

(c) Spatial and temporal speed

Figure 4.4 Estimated link speed of the Yu'ao Bridge (Link 3) at the interval of one min

System output II: Movement-specific link speeds

Since bus GPS data contain route number information, the received GPS data for a given link can be categorized by its entry and exit on a roadway segment. For example, the Yu'ao Bridge is connected with two entry roads (Jianxin S Rd. and Yu'ao Ave.) and two exit roads (Shangqingsi Rd. and Sixin Rd.), and the movement-specific link speeds for the bridge are shown in Figure 4.5. Overall, four different disaggregated speeds on the bridge exhibit a similar pattern over time, where the average speed for the off-peak period is around 25 km/hr, and the speed decreases to around 10 km/hr during peak hours. However, vehicles with different movements clearly experience different levels of traffic congestion during peak periods. For instance, vehicles heading to the more congested link, Sixin Rd. (Link 4), experienced a lower travel speed than other movements heading to Shangqingsi Rd. (Link 5).

Furthermore, among the two movements with the most severe congestion, the movement from Yu'ao Ave, a weaving maneuver, shows a lower speed. Such movement-specific link speeds and spatial speed variation over a link are the most valuable information that can be uniquely provided with the proposed pseudo detector system.

With the proposed system, one can obtain spatial link speeds and movement-specific link speeds for the transit agencies to predict travel times and arrival times to a bus stop. By converting bus speed to general traffic speed, traffic operators can also utilize this speed information as an input to identifying bottlenecks within a link, and for design of traffic control strategies.

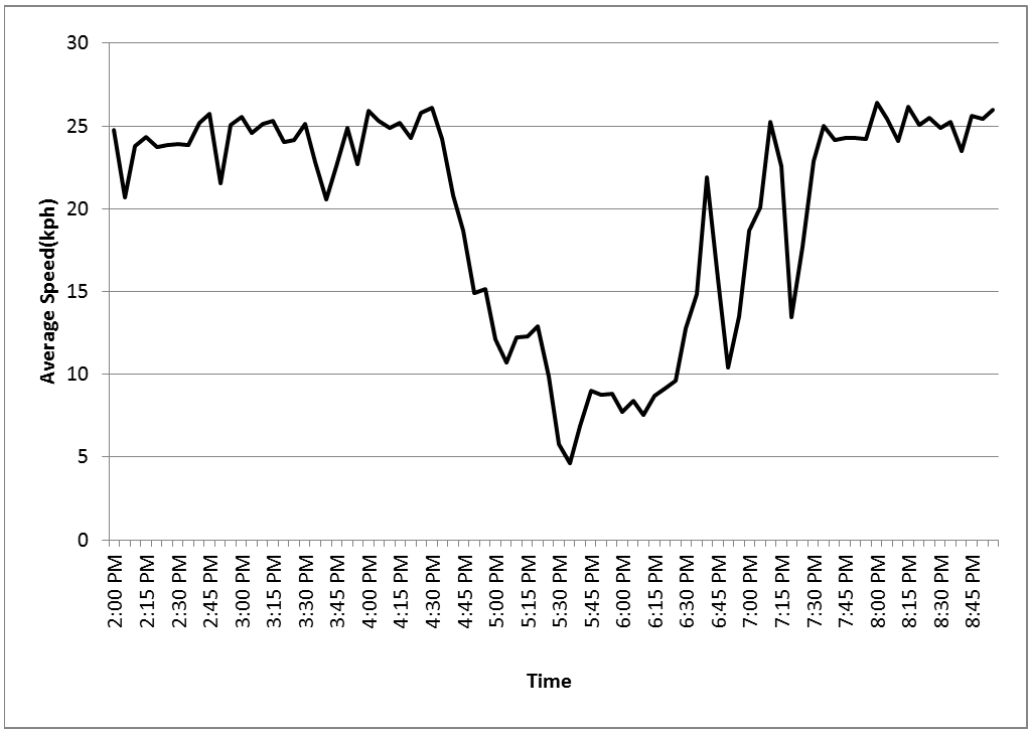

(a) Link speed

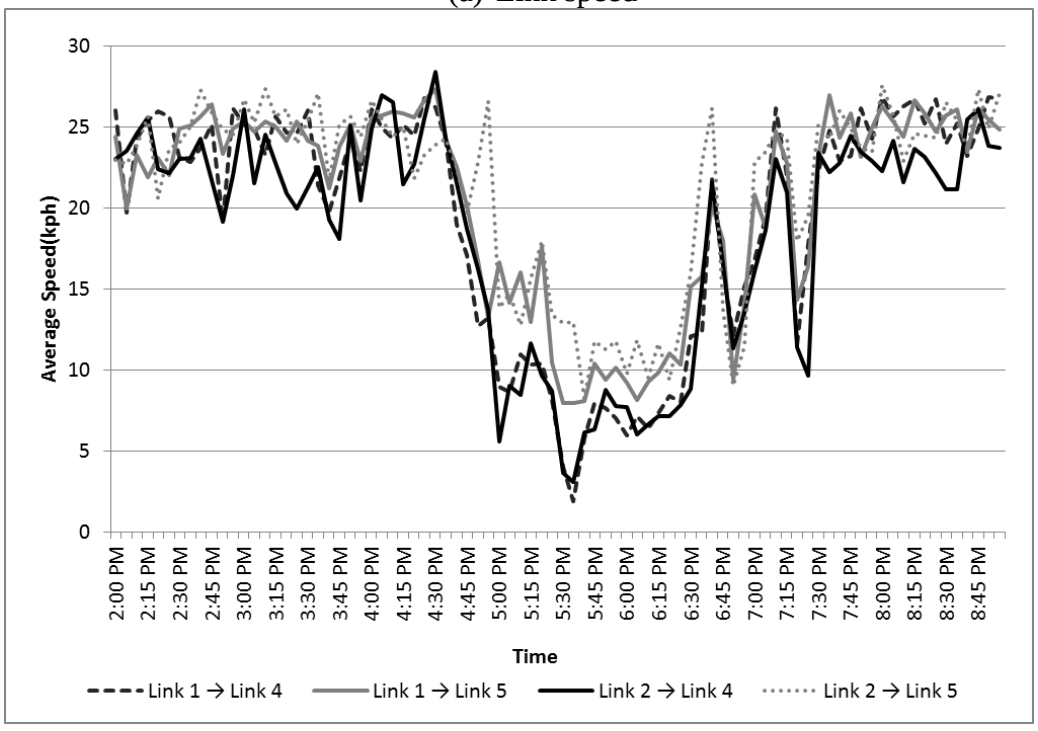

(b) Movement specific speed

Figure 4.5 Movement-specific link speeds on the Yu'ao Bridge(Link 3) during PM peak in 5 min intervals

4.4 Closure

This chapter has presented a pseudo detection system and the development procedures using real-time bus GPS data. A case study for illustration has also been conducted with bus GPS data from a corridor in the city of Chongqing, China. The numerical results clearly demonstrate the unique strengths of the proposed system, which features an ability to offer an estimated link speed by movement, and the temporal and spatial variation of speeds within a link. Since the infrastructure for receiving bus GPS data is available in most urban transit systems, traffic agencies can conveniently take advantage of such data at insignificant cost to develop our proposed pseudo sensor system for network traffic monitoring. Furthermore, the resulting movement-based link speed information can be used in traffic signal design or transit fleet controls.

Chapter 5: A Pre-timed Arterial Coordination System for Bus-based Progression

5.1 Introduction

As is well recognized, signal plans are coordinated mainly for general traffic, and thus buses often suffer from frequent stops at signals caused by a variety of factors associated with buses operations (e.g., dwell times at bus stops and their uncertainty, lower travel speeds than general traffic, and location and storage capacity of bus stops). In an attempt to enhance service quality of bus operations, over the past decades a rich body of research has proposed various Transit Signal Priority (TSP) strategies which allow a bus to pass an intersection without experiencing stop delays. However, despite the significant contributions of those studies, implementing TSP in urban networks remains quite limited in practice. Among various issues causing limited usage of the TSP, its negative impacts on the side-street traffic and potential disruption of coordinated traffic signals deserve the most attention.

Hence, to concurrently minimize such negative impacts and bus delays at signalized intersection, a passive control strategy that employs the bus flow patterns in design of signal offsets emerges as one viable cost-benefit option. Such a strategy can facilitate bus progression operations without investing on on-line surveillance and control devices. Certainly, it can also serve as the basis for computing the number of arterial intersections to be deployed with real-time TSP control for further upgrading the quality of bus progression operations.

This chapter presents such a model to yield the optimal offsets for a pre-timed arterial signal control for bus progression. Section 5.2 highlights some key issues in design of a bus progression. Section 5.3 presents the mathematical formulations for the signal progression model designed to address those critical issues. Section 5.4 reports the results of extensive evaluations with simulation experiments with respect to the selected measures of effectiveness along with a summary of the main contributions in the last section.

5.2 Modeling Methodology

In design of a signal plan to progress buses over consecutive intersections, the proposed model, grounded on the pioneering work of MAXBAND (Little et al. 1981), especially takes into account the following critical issues: dwell times at bus stops and their variance, bus stop storage capacity, and traffic queues at intersections and their relationship with bus stop location.

Bus Dwell Time at a Bus stop

As shown in Figure 5.1(a), if a bus dwells at a stop, it is likely to deviate away from the progression band designed mainly for passenger cars and thus encounter a red phase at the downstream intersection. To ensure the signal progression for buses, it is essential to take into account the impacts of bus dwell times on their travel times between intersections. Furthermore, it is noticeable that bus dwell time of buses varying with transit demands at each stop is stochastic in nature. Figure 5.1 (b) depicts an example of such impacts on the bus progression, where Bus-1 receives a green phase at the downstream intersection but not for Bus-2 since it has a longer

dwell time. Hence, dwell time variance is one of the critical factors to be considered in design of an effective bus signal progression system.

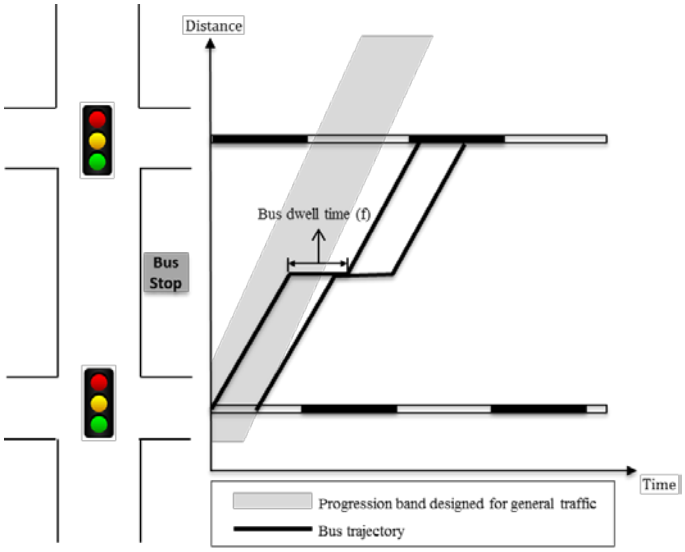

(a) Impacts of bus dwelling at a bus stop on the progression

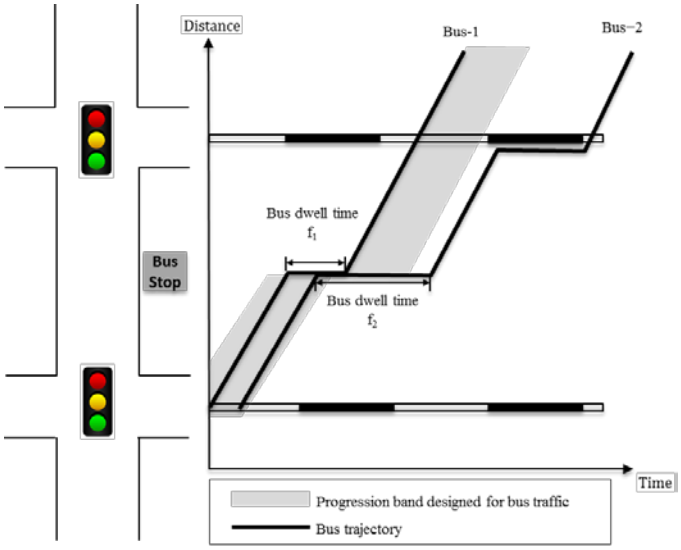

(b) Stochastic nature of bus dwell times and its impact on progression.

Figure 5.1 Bus progression with bus dwell time uncertainty

One alternative to address this issue is to introduce a variable-band scheme that allows the bandwidth to vary along an arterial, as shown in Figure 5.2. Unlike the typical signal progression for passenger cars which takes each intersection as a

control point, the proposed bus progression model views each bus stop as a control point. The change in bandwidths will take place at a bus stop, and the transition between two consecutive bands (i.e., bands that are arriving at and departing from a bus stop) may determine the effectiveness of the entire system's performance.

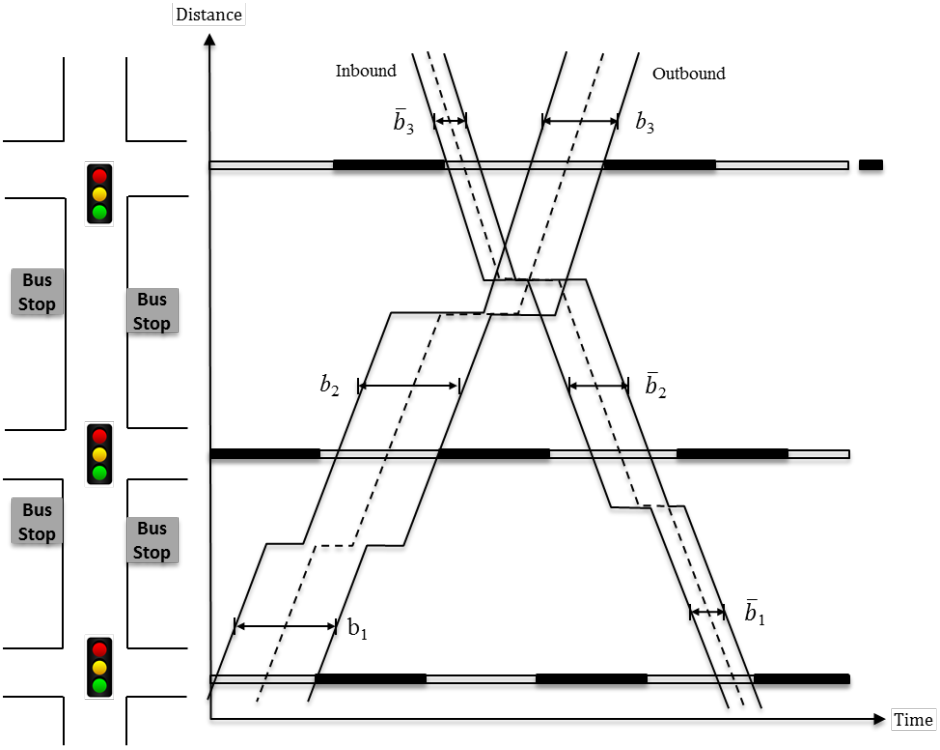

Figure 5.2 Variable bus progression bands

Note that although different progression plans may yield the identical total bandwidth, their resulting performance for bus flows can be quite different. For example, a wider arriving band in Figure 5.3 (a) can certainly receive more buses, but only a few of those are likely to stay in the departing band toward the downstream intersection due to the inevitable dwell time variation. In contrast, a narrower arriving band as shown in Figure 5.3 (b) may receive fewer buses from the upstream link, but most of those can leave the bus stop within the departing band. Noticeably, these two

progression plans yield the identical total bandwidth, but the resulting bus delays are quite different. In fact, the effectiveness of a bus progression plan depends on not only the total progression bandwidth, but also the relationship between the arriving and departing bands at each bus stop. Hence, to estimate whether or not a bus can pass through consecutive intersections without encountering a red phase, one should first estimate if the bus can stay in the departing band or not after leaving the bus stop.

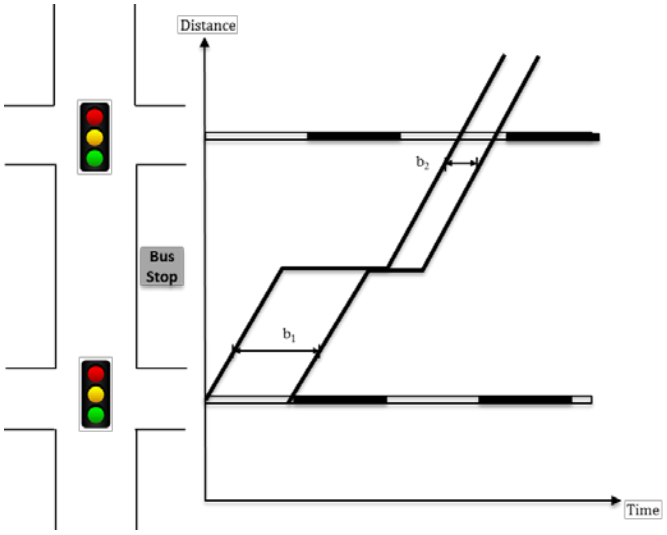

(a) A wide arriving band versus a narrow departing band

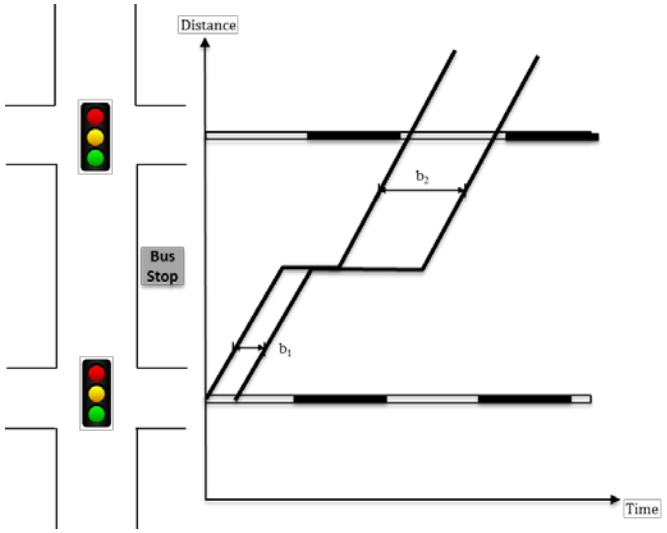

(b) A narrow arriving band versus a wide departing band

Figure 5.3 Relationship between neighboring bands at a bus stop

Storage Capacity of Bus Stops

Another critical issue to be addressed in design of a bus progression system is the storage capacity of bus stops. If the number of arriving buses exceeds the storage capacity of the bus stop, the queuing buses may spill back to the nearby intersection and block the incoming traffic flows. Such spillovers yield the following undesirable consequences: 1) causing potential safety concerns at the upstream intersection near the bus stop, 2) increasing the delay of vehicles approaching the intersection, 3) increasing the total delay for buses arriving at the bus stop, and 4) contributing to the bus dwell time uncertainty. Hence, in design of a bus-based progression, one shall preset an upper bound for the bus bandwidth so that the number of buses arriving at a bus stop in a short period will not exceed the available storage.

Note that whether a bus bandwidth may or may not cause spillover at the bus stops depends on not only the bus stop's capacity but also the distribution of bus dwell durations. Taking Figure 5.4 as an example, if most buses dwell at a bus stop for a short time (Figure 5.4(a)), the arriving buses can enter bus stop storage without extra waiting time near the bus stop. Otherwise (see Figure 5.4(b)), some arriving buses may need to wait after the departure of those dwelling buses, thus often causing spillover and queues. Hence, in setting an upper bound for the bus bandwidth, one shall consider both the available storage as well as the dwell time duration.

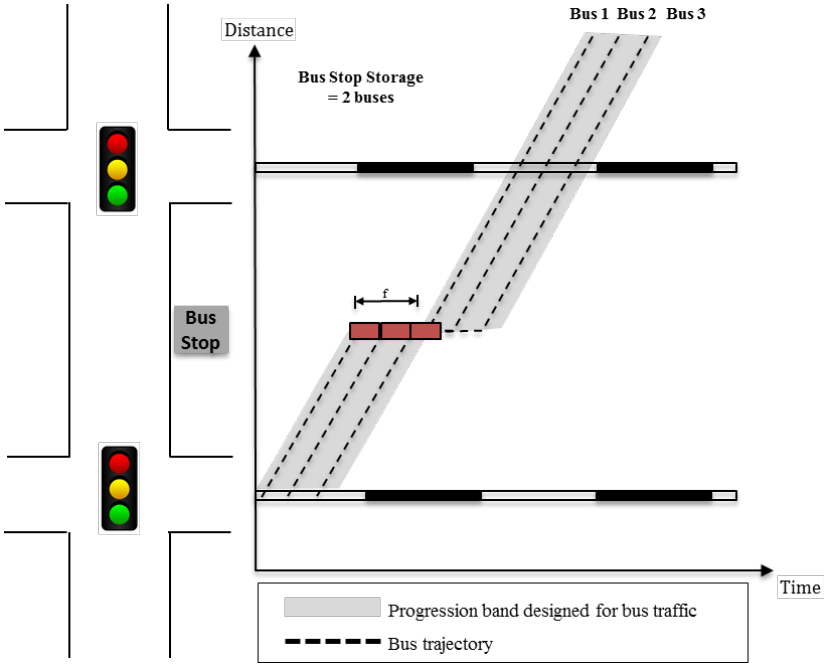

(a) Short dwell times at bus stop

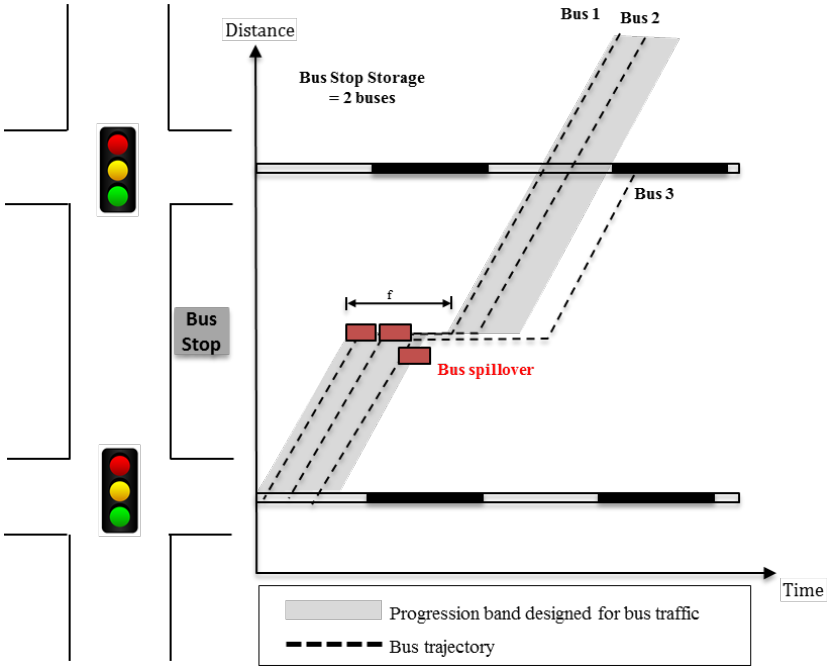

(b) Long dwell times at bus stop

Figure 5.4 Impacts of bus stop storage and bus dwell time on bus progression

Intersection Traffic Queue and Bus Stop Location

In a bus progression system, passenger cars not within a bus band may encounter a red phase at traffic signals, and thus form the initial queue during the red phase. The location of the bus stop can be a key factor to affect whether or not the bus bands are blocked by traffic queues. For example, Figure 5.5 (a) shows the time space relations between the queue discharging pattern and arriving buses on an arterial segment, where one bus first arrives at the far-side stop near the upstream intersection for passengers, and then departs to approach the intersection. Note that if the bus stop is located near the downstream intersection as shown in Figure 5.5 (b), the resulting bus bandwidth may be reduced significantly, even if all other factors remain identical. Thus, in developing the bus progression model, one shall account for all interfering factors, including intersection queues, bus stop location and bus dwell times so as to ensure that the anticipated bus band would not be interrupted.

To estimate the initial queue length and the clearance time for the given offsets between two neighboring intersections, one shall note that the queue formation and discharging at intersections depend on not only the offsets, but also the arriving traffic pattern and their distribution between through and turning flows from the upstream intersection over a cycle. Thus, the optimal offsets for bus progression between consecutive intersections shall be designed not only to maximize the total bus bandwidth, but also to concurrently minimize the uncoordinated passenger car flows. Note that intersection traffic queues actually vary with arrival flow patterns during a red phase and discharging period, the traffic conditions, the distance between neighboring intersections, and the implemented signal plan. Consider two 2-phase

intersections (Figure 5.6), where the turning-vehicles from intersection i-1, ($q_{2,i}$), arriving at intersection i during a red

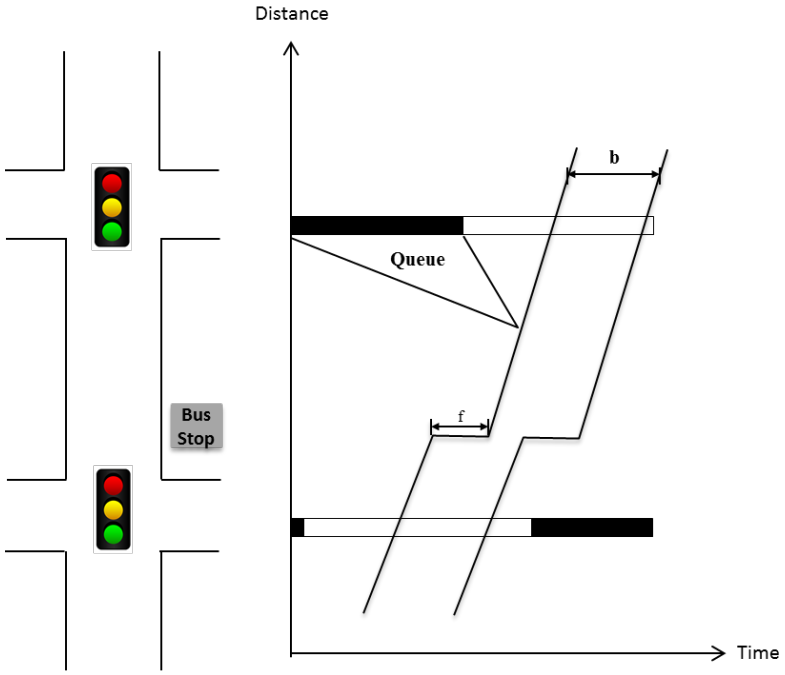

(a) A far-side bus stop

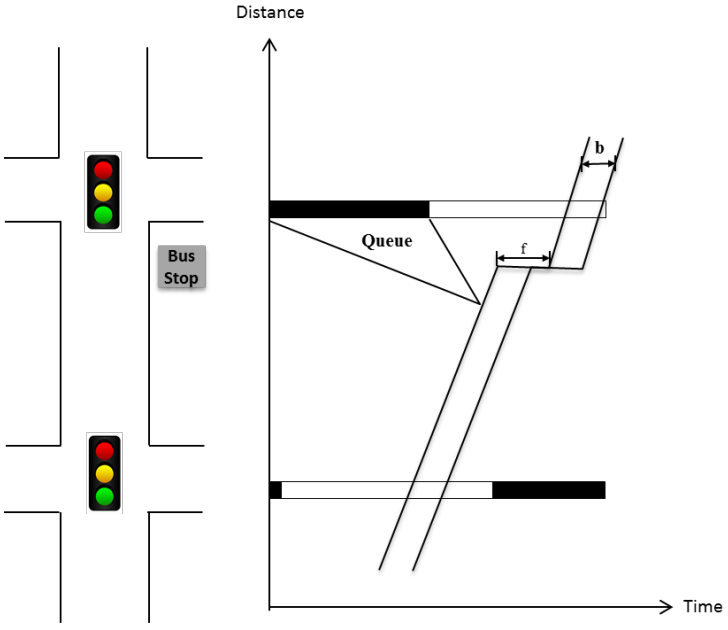

(b) A near-side bus stop

Figure 5.5 Illustration of the bus progression operations under a far-side bus stop and a near-side bus stop

phase, have formed queues, and are served at the rate of *s*. The through-vehicles from intersection i-1, ($q_{1,i}$),discharged based on the offsets and travel time, $t_{c,i-1}$, arrive at intersection i during the synchronized green interval, g_i. Depending on the arriving flow patterns during the green interval, it may result in the following two scenarios: Scenario 1) some leading through-vehicles from the upstream intersection join the discharging queues, and Scenario II) all through-vehicles from the upstream intersection may smoothly pass the intersection without stop.

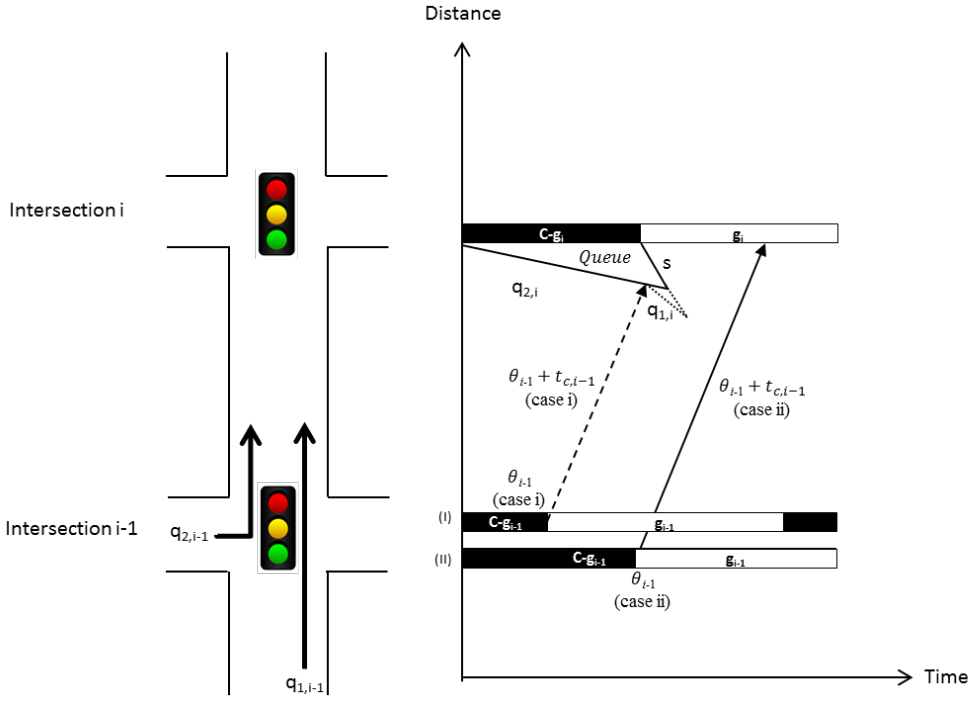

Figure 5.6 Impacts of signal timings on queue formation and discharging

Given the traffic volumes, travel times of passenger cars between intersections, and signal timings, one can categorize different vehicle arrival patterns into the following six types of queue formation and discharging patterns, as shown in Figure 5.7.

- Type 1: All through vehicles from the upstream intersection encounter a green phase at the downstream intersection (Figure 5.7 (a)).
- Type 2: Through vehicles from the upstream intersection encounter the green-red-green phases over consecutive cycles at the downstream intersection (Figure 5.7 (b)).
- Type 3: Through vehicles from the upstream intersection encounter the red-green phases at the downstream intersection (Figure 5.7 (c)).
- Type 4: Through vehicles from the upstream intersection encounter the green-red phases at the downstream intersection (Figure 5.7 (d)).
- Type 5: All through vehicles from the upstream intersection encounter a red phase at the downstream intersection (Figure 5.7 (e)).
- Type 6: Through vehicles from the upstream intersection encounter the red-green-red phases at the downstream intersection (Figure 5.7 (f)).

Furthermore, those vehicles classified in Type 1 to Type 4, arriving at the intersection during its queue discharging period can come from two incoming flow sources, depending on the offsets between intersections and the green interval of an upstream intersection (see transition between T3 and T4 in Figure 5.8). Hence, in design of a bus-based progression, one should account for the intersection traffic queues mostly from passenger-car flows, and the queue clearance time under the given offsets and upstream traffic flow patterns.

In brief, to formulate an effective bus progression model, one need to explicitly account for all critical factors that may interrupt the bus progression

operations, including the average and variance of dwell times, intersection residual queue and constraints at physical bus stops.

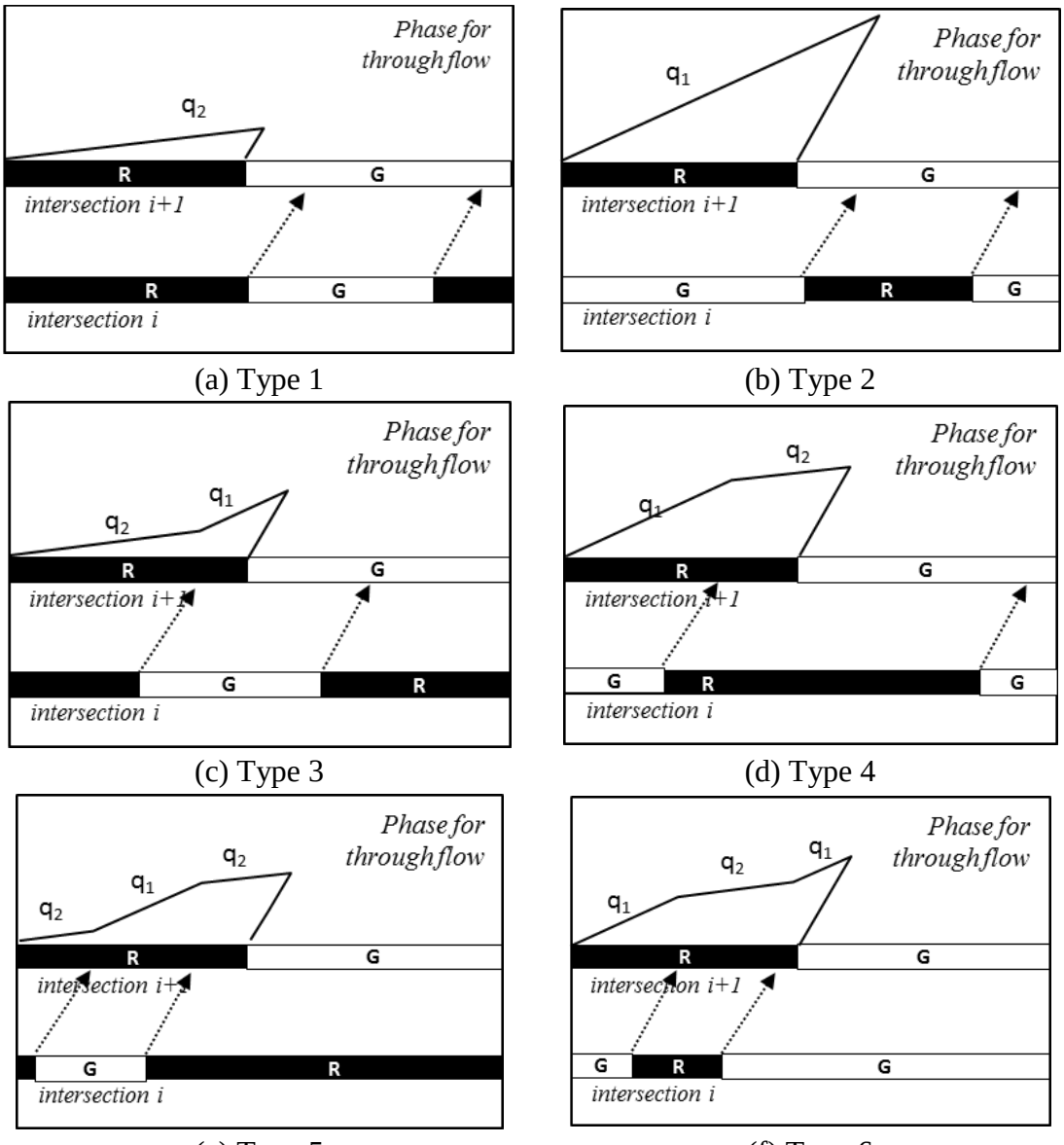

Figure 5.7 Six vehicle arrival pattern types and resulting intersection queue formation and discharging

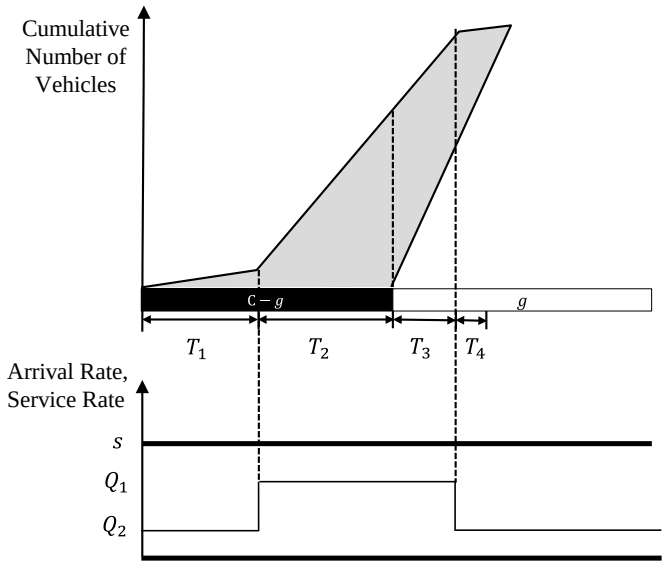

Figure 5.8 Time intervals during queue formation and discharging

5.3 Model Formulations

This section presents a set of formulations for the bus progression design. The entire formulations are divided into two stages, where Stage-I is to extend the MAXBAND to account for the average bus dwell time at a bus stop, capacity of a bus stop, and traffic queues at signals and their relationship with bus stop location. Stage-2 further takes into account the stochastic nature of bus dwell times. Key notations used in the proposed model are shown in Table 5.1 and Figure 5.9.

Table 5.1 Key notations

Notation	Description
Parameters	
$\Omega(\bar{\Omega})$	The set of intersections in outbound (inbound)
$g_i(\bar{g}_i)$	The outbound(inbound) green interval at intersection i (sec)
N	Total number of intersections
r_i	Time difference between the start of the outbound green and the end of the inbound green at intersection i (sec)
$t_{c,i}$ ($\bar{t}_{c,i}$)	Average outbound (inbound) travel time for passenger cars from intersection i (i+1) to intersection i+1 (i) (sec)
$t_{b,i}$ ($\bar{t}_{b,i}$)	Average outbound (inbound) travel time for buses from intersection i (i+1) to intersection i+1 (i), which is sum of bus running time and bus dwell time (sec)
$t_{b,1,i}$ ($\bar{t}_{b,1,i}$)	Average bus running time from intersection i (i+1) to a bus stop i (sec)
$t_{b,2,i}$ ($\bar{t}_{b,2,i}$)	Average bus running time from a bus stop i to intersection i+1 (i)
d_i	Distance from intersection i (i+1) to intersection i+1 (i) (ft)
l_i	Distance from intersection *i* (i+1) to a bus stop between intersections *i* (*i*+1) and *i*+1 (*i*) (feet)
v_i ($\bar{v}_i$)	Average bus running speed from intersection i (i+1) to intersection i+1 (i) (ft/sec)
$f_i(\bar{f}_i)$	Average dwell time at the outbound(inbound) bus stop after (before) intersection i (i+1) (sec)
$\sigma_i(\bar{\sigma}_i)$	Standard deviation of dwell times for the outbound (inbound) buses at the stop ahead of intersection i (i+1)
$m_i(\bar{m}_i)$	The expected number of outbound (inbound) buses passing intersection i during the synchronized phase in one hour
C	Cycle length (sec)
$k_{b,i}$, $\varphi_i(\bar{\varphi}_i)$	Weighting factors
s	Saturation flow rates (veh/hr)
$q_{1,i}(\bar{q}_{1,i})$	Average discharging rate of thru movement of intersection i (i+1) to intersection i+1(i) (veh/hr)
$q_{2,i}(\bar{q}_{2,i})$	Average discharging rate of turning movement of intersection i (i+1) to intersection i+1(i) (veh/hr)
$N_i\left(\bar{N}_i\right)$	Number of lanes for outbound (inbound) through movement at intersection i
$C_{s,i}(\bar{C}_{s,i})$	Bus stop capacity (vehs)
$\lambda_i(\bar{\lambda}_i)$	Bus arrival rate at outbound (inbound) intersection i during a cycle
p_i ($\bar{p}_i$)	Reliability of the bus queue spill back at outbound (inbound) intersection i
b_i^j ($\bar{b}_i^j$)	Candidate maximal bandwidth not to exceed the capacity of bus stop i at the user defined probability for j=1,2
b_i^{max}($\bar{b}_i^{max}$)	Maximal bandwidth not to exceed the capacity of bus stop i at the user defined probability
l	Vehicle length (ft)
M	Large number

Variables	
b_i ($\bar{b}_i$)	Bus outbound (inbound) bandwidth at intersection i (sec)
b_i^e ($\bar{b}_i^e$)	Effective outbound (inbound) bandwidth at intersection i for buses (sec)
w_i ($\bar{w}_i$)	Time period between the start (end) of a green phase and the center of the bus band at intersection i for the outbound (inbound) direction (sec)
θ_i	Offset at intersection i
$T_{1.i}$ ($\bar{T}_{1,i}$)	Time interval used for queue to accumulate before there is a change in arrival flows at intersection i (sec)
$T_{2.i}$ ($\bar{T}_{2,i}$)	Time interval used for queue to accumulate after there is a change in arrival flows at intersection i (sec)
$T_{3.i}$ ($\bar{T}_{3,i}$)	Time interval used for queue to discharge before there is a change in arrival flows at intersection i (sec)
$T_{4.i}$ ($\bar{T}_{4,i}$)	Time interval used for queue to discharge after there is a change in arrival flows at intersection i (sec)
$\gamma_{1.i}$ ($\bar{\gamma}_{1,i}$)	Time difference between onset of green and arrival of first possible thru leading vehicle from the upstream intersection at intersection i (sec)
$\gamma_{2.i}$ ($\bar{\gamma}_{2,i}$)	Time difference between onset of green and arrival of first possible turning leading vehicle from the upstream intersection at intersection i (sec)
τ_i ($\bar{\tau}_i$)	Queue clearance time for outbound (inbound) at the intersection i (sec)
$x_{1.i}$ ($\bar{x}_{1,i}$)	Binary variable indicating the phase that the first vehicle of outbound (inbound) traffic flows from the main streets at the intersection i encountered
$x_{2.i}$ ($\bar{x}_{2,i}$)	Binary variable indicating the phase that the last vehicle of outbound (inbound) traffic flows from the main streets outbound (inbound) at the intersection i encountered
$x_{3.i}$ ($\bar{x}_{3,i}$)	Binary variable indicating if there is a change in the phases that outbound (inbound) through or turning vehicles from upstream intersection i-1 (i+1)
n_i ($\bar{n}_i$)	Integer variable to represent the number of signal cycles for progression constrains
$c_{i,j}$ ($\bar{c}_{i,j}$)	Integer variable to represent the number of signal cycles for traffic queue constrains
s_i ($\bar{s}_i$)	Binary variable ensuring the upper bound of bus bandwidth
$c_{i,j}$($\bar{c}_{i,j}$)	Loop integer variable for passenger car for intersection i
ς_i($\bar{\varsigma}_i$),	Maximum queue length at intersection I (ft)
$y_{i,j}$ ($\bar{y}_{i,j}$)	Binary decision variable which indicates the arrival flow rate at intersection j
$a_i(\bar{a}_i)$, $a_{i,j}(\bar{a}_{i,j})$	The time when the queue vanish at intersection i
$S_i(\bar{S}_i)$	The distance from intersections i-1(i+1) to the end of maximum queue at intersection i

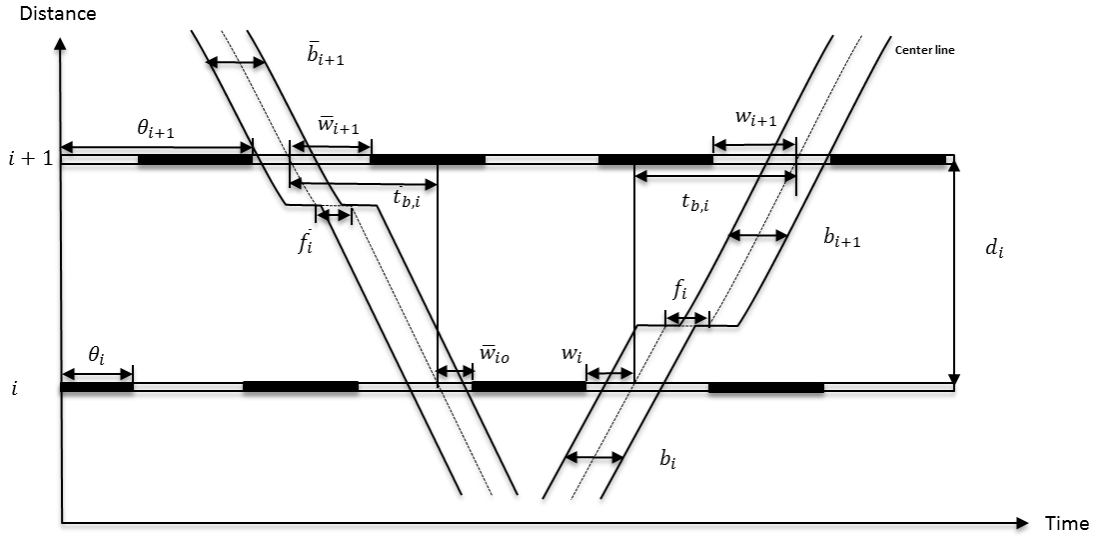

Figure 5.9 Graphical illustrations of key variables and parameters in the model

5.3.1 Stage-1: Design a Set of Bus-based Progression Bands along an Arterial

As discussed previously with the given phase plans, traffic flow patterns, bus schedule, and bus dwell times, one can directly extend MAXBAND, but use each bus stop as a control point under the following objective function to produce the offsets for bus progression:

$$\text{Max} \sum \mathrm{b}_i + \mathrm{k}_{\mathrm{b,i}}\bar{\mathrm{b}}_i \qquad (5.1)$$

$$(1 - \mathrm{k}_{\mathrm{b,i}})\bar{\mathrm{b}}_i \geq (1 - \mathrm{k}_{\mathrm{i,b}})\mathrm{k}_{\mathrm{b,i}}\mathrm{b}_i \qquad (5.2)$$

where $\mathrm{k}_{\mathrm{b,i}}$ is a weighting factor of the bus bandwidth for each direction. Eq. (5.2) will ensure that the bandwidth for the less favored direction would remain within a reasonable range. The key to ensure the progression for buses, however, depends on the specification of the following constraints.

Interference constraints

The first for directional interference constraints is to ensure that the bus progression bands use only the available green time at intersection i. Such constraints can be specified as follows:

$$0.5b_i \le w_i \le g_i - 0.5b_i \qquad \forall i \in \Omega \qquad (5.3a)$$

$$0.5\bar{b}_i \le \bar{w}_i \le \bar{g}_i - 0.5\bar{b}_i \qquad \forall i \in \bar{\Omega} \qquad (5.3b)$$

As shown in Figure 5.9, Eq. (5.3a) indicates that the start of green bands should not be within the queue clearance time, whereas Eq. (5.3b) forces the bands to end within a green phase.

Progression constraints

The second is a set of loop integer constraints specified to ensure that the intersection signals do not stop the bus flows from moving during the bands. Each constraint functions to limit the differences between the centers of the inbound or outbound bands for each pair between neighboring intersections. For a pair of neighboring intersections, i and i+1, one can express the progression constraints as follows:

$$\theta_i + w_i + t_{b,i} + C(n_i) = \theta_{i+1} + w_{i+1} + C(n_{i+1}) \qquad \forall i \in \Omega \qquad (5.4a)$$

$$-\theta_i - r_i + \bar{w}_i + \bar{t}_{b,i} + C(\bar{n}_i) = -\theta_{i+1} - r_{i+1} + \bar{w}_{i+1} + C(\bar{n}_{i+1}) \qquad \forall i \in \bar{\Omega} \qquad (5.4b)$$

The bus travel times, $t_{b,i}(\bar{t}_{b,i})$, between intersections i (i+1) and i+1 (i) specified in the progression constraints are the sum of bus running time and dwell time at a bus stop, as shown in (5.5), where $f_i(\bar{f}_i)$ denotes the average dwell time; and

$t_{b,o,i}$ ($\bar{t}_{b,o,i}$) represents the bus running time. For those links without a bus stop, the average dwell time and running time after a bus stop are set as zero.

$$t_{b,i} = t_{b,0,i} + f_i \qquad \forall i \in \Omega \qquad (5.5a)$$

$$\bar{t}_{b,i} = \bar{t}_{b,0,i} + \bar{f}_i \qquad \forall i \in \bar{\Omega} \qquad (5.5b)$$

Bus stop storage capacity constraints

The bus stop capacity constraint is to ensure that the number of buses arriving at a bus stop in any time interval does not exceed its available storage capacity. This can be fulfilled by setting the upper bound on the bus bandwidth. Assuming that the bus arriving frequency at each stop follows a Poisson distribution, the probability for k buses (less than the physical capacity of bus stop i) in the outbound green band can be expressed as follows:

$$f(k) = \frac{(\lambda_i b)^k \times e^{-\lambda_i b}}{k!} \qquad (5.6)$$

where λ_i denotes the bus discharging rate from the upstream intersection i-1 during the green phase, which is also the bus arrival rate during a cycle. Then, the upper bound of a bus bandwidth can be computed as follows:

$$b_i^1 = arc\max_{b_i}\left\{1 - \sum_{k=0}^{C_{s,i}} \frac{(\lambda_i b_i)^k \times e^{-\lambda_i b_i}}{k!} \le p_i\right\} \qquad \forall i \in \Omega$$

(5.7a)

$$\bar{b}_i^1 = arc\max_{\bar{b}_i}\left\{1 - \sum_{k=0}^{\bar{C}_{s,i}} \frac{(\bar{\lambda}_i \bar{b}_i)^k \times e^{-\bar{\lambda}_i \bar{b}_i}}{k!} \le \bar{p}_i\right\} \qquad \forall i \in \bar{\Omega} \qquad (5.7b)$$

where $C_{s,i}$ ($\bar{C}_{s,i}$) denotes the capacity of bus stop i, and p_i ($\bar{p}_i$) is a parameter to indicate the probability of having bus queue spillback at intersection i. In Eq. (5.7),

b_i^1 ($\bar{b}_i^1$) can be the maximal bandwidth that will not exceed the capacity of a bus stop between intersections *i* and i +1 at the user defined probability. Furthermore, if the average dwell time is shorter than the estimated maximum bandwidth, the bus stop can serve more buses than the estimated capacity, and thus the maximum bandwidth associated with the storage capacity can be extended as shown in Eq. (5.8).

$$b_i^2 = arc\max_{b_i}\left\{1-\sum_{k=0}^{C_{s,i}}\frac{\left(\lambda_i(f_i+b_i)\right)^k\times e^{-\lambda_i(f_i+b_i)}}{k!}\le p_i\right\} \quad \forall i \in \Omega$$

(5.8a)

$$\bar{b}_i^2 = arc\max_{\bar{b}_i}\left\{1-\sum_{k=0}^{\bar{C}_{s,i}}\frac{\left(\bar{\lambda}_i(\bar{f}_i+\bar{b}_i)\right)^k\times e^{-\bar{\lambda}_i(\bar{f}_i+\bar{b}_i)}}{k!}\le \bar{p}_i\right\} \quad \forall i \in \bar{\Omega} \qquad (5.8b)$$

where f_i ($\bar{f}_i$) represents the average dwell time of a bus stop between intersection i and i+1; and b_i^2 ($\bar{b}_i^2$) is the maximal bandwidth not to exceed the capacity of bus stop i at the user defined probability. Then, the maximum bandwidth can be determined from the average dwell time as shown in Eqs. (5.9).

$$b_i^{\max} = \begin{cases} b_i^1 & if \quad b_i^1 < f_i \\ f_i + b_i^2 & if \quad b_i^1 \ge f_i \end{cases} \qquad \forall i \in \Omega \qquad (5.9a)$$

$$\bar{b}_i^{\max} = \begin{cases} \bar{b}_i^1 & if \quad \bar{b}_i^1 < \bar{f}_i \\ \bar{f}_i + \bar{b}_i^2 & if \quad \bar{b}_i^1 \ge \bar{f}_i \end{cases} \qquad \forall i \in \bar{\Omega} \qquad (5.9b)$$

However, due to the inequality of interference constraints shown in Eq. (5.3), directly adding an upper bound $b_i^{\max}$($\bar{b}_ı^{\max}$) for b_i($\bar{b}_ı$) may force the solution algorithm to simply reduce the value of b_i($\bar{b}_ı$) without searching for the other feasible values for the control variables (i.e., offsets). As such, the resulting value of b_i($\bar{b}_ı$) can be smaller than the maximum feasible bandwidth under the offset setting. Therefore, to ensure that the upper bound constraint for the green bandwidth can

function effectively, one shall set the following constraints with a set of new binary variables, $s_i(\bar{s}_{i+1})$, as shown in Eqs. (5.10)

$$w_i - 0.5 \times b_i^{\max} \le M \times s_i \qquad \forall i \in \Omega \text{ (5.10a)}$$

$$w_i + 0.5 \times b_i^{\max} \ge g_i - M \times (1 - s_i) \qquad \forall i \in \Omega \text{ (5.10b)}$$

$$\bar{w}_{i+1} - 0.5 \times \bar{b}_i^{\max} \le M \times \bar{s}_{i+1} \qquad \forall i \in \bar{\Omega} \text{ (5.10c)}$$

$$\bar{w}_{i+1} + 0.5 \times \bar{b}_i^{\max} \ge g_{i+1} - M \times (1 - \bar{s}_{i+1}) \qquad \forall i \in \bar{\Omega} \text{ (5.10d)}$$

where M is a large positive number that dominates all decision variables and parameters. Taking Eqs. (5.10a) and (5.10b) as an example, if s_i equals 1, it ensures that the time interval from the center of bus band to the end of a green phase is less than a half of the bandwidth's upper bound. Similarly, if s_i equals 0, it ensures that the time interval from the start of a green phase to the center of a bus band does not exceed a half of its upper bound.

Traffic Queue Constraints

Another important constraint is to account for intersection traffic queues which rely highly on the total arriving traffic flows over a cycle. Given the traffic volumes, the travel times of passenger cars between intersections, and signal timings, one can approximate the queue length and queue clearance time for each type in Figure 5.7 in the previous section. To identify the type of arriving traffic pattern, this study has further introduced the following three sets of auxiliary binary variables:

$$x_{1,i} = 1, if\ \theta_i + C \times c_{1,i} \le \theta_{i-1} + t_{c,i-1} \le \theta_i + g_i + C \times c_{1,i};\ 0, otherwise \qquad \text{(5.11a)}$$

$$\bar{x}_{1,i} = 1, if\ \theta_i + C \times \bar{c}_{1,i} \le \theta_{i+1} + \bar{t}_{c,i} \le \theta_i + \bar{g}_i + C \times \bar{c}_{1,i};\ 0, otherwise \qquad \text{(5.11b)}$$

$$x_{2,i} = 1, if\ \theta_i + C \times c_{2,i} \leq \theta_{i-1} + g_{i-1} + t_{c,i-1} \leq \theta_i + g_i + C \times c_{2,i};\ 0, otherwise$$

(5.12a)

$$\bar{x}_{2,i} = 1, if\ \theta_i + C \times \bar{c}_{2,i} \leq \theta_{i+1} + \bar{g}_{i+1} + \bar{t}_{c,i} \leq \theta_i + \bar{g}_i + C \times \bar{c}_{2,i};\ 0, otherwise$$

(5.12b)

$$x_{3,i} = 1, if\ x_{1,i} \neq$$

$$x_{2,i}\ or \begin{pmatrix} x_{1,i} = x_{2,i}\ and\ \theta_{i-1} + g_{i-1} + t_{c,i-1} = \\ \left(\theta_i + C \times c_{1,i} + x_{1,i} \times g_i + \left(1 - x_{1,i}\right) \times (C - g_i)\right) \end{pmatrix};\ 0, otherwise$$

(5.13a)

$$\bar{x}_{3,i} = 1, if\ \bar{x}_{1,i} \neq$$

$$\bar{x}_{2,i}\ or \begin{pmatrix} \bar{x}_{1,i} = \bar{x}_{2,i}\ and\ \theta_{i+1} + \bar{g}_{i+1} + \bar{t}_{c,i} = \\ \left(\theta_i + C \times \bar{c}_{1,i} + \bar{x}_{1,i} \times \bar{g}_i + \left(1 - \bar{x}_{1,i}\right) \times (C - \bar{g}_i)\right) \end{pmatrix}; 0, otherwise$$

(5.13b)

where $x_{1,i}$ ($\bar{x}_{1,i}$) is set to be 1 if the first possible leading through vehicle from the upstream outbound (inbound) intersection i-1 (i+1) encounters the green at the intersection i, otherwise 0; $x_{2,i}$ ($\bar{x}_{2,i}$) is set to 1 if the last passible lagging through vehicle from the outbound (inbound) upstream intersection i-1 (i+1) experiences the green phase at the intersection i, otherwise 0; and $x_{3,i}$ ($\bar{x}_{3,i}$) is set to 1 if through vehicles from the outbound (inbound) upstream intersection i-1 (i+1) experience phase changes at the intersection i(i), otherwise 0. All such variables are formulated and presented in Table 5.2.

For example, when $x_{1,i}$=1, Eqs. (5.14a) and (5.14c) are open with variables (i.e., θ_{i-1}, θ_i, and $c_{1,i}$) due to the large number M in the right-side of inequalities, and Eqs. (5.14b) and (5.14d) are bounded, resulting in $\theta_i + C\left(c_{1,i}\right) \leq \theta_{i-1} + t_{c,i-1} \leq \theta_i +$

$C(c_{1,i}) + g_i$, and indicating that the leading vehicle of the synchronized through traffic from the upstream outbound intersection i-1 encounters the green at the intersection i. On the other hand, when $x_{1,i}$=0, Eqs. (5.14b) and (5.14d) leave variables (i.e., θ_{i-1}, θ_i, and $c_{1,i}$) open due to the large number M in the right-side of inequalities, and Eqs. (5.14a) and (5.14c) are bounded, resulting in $\theta_i + C(c_{1,i}) \geq \theta_{i-1} + t_{c,i-1}$ and $\theta_{i-1} + t_{c,i-1} \geq (\theta_i + C(c_{1,i}) + g_i) - C$, which indicate that the leading vehicle of the synchronized through traffic from the upstream outbound intersection i-1 encounters the red phase at intersection *i*. Eqs. (5.15)-(5-17) follows the same logic.

Regarding variable, $x_{3,i}(\bar{x}_{3,i})$, there exist the following two conditions, based on its definition for through vehicles from the upstream intersection i-1 to experience phase changes at the downstream intersection i (i.e., $x_{3,i}$=1);

Case 1) the leading and lagging vehicles in the through flows from the upstream intersection i-1 face different phases ($x_{1,i} \neq x_{2,i}$); and

Case 2) the leading and lagging vehicles in the through flows face the same phases ($x_{1,i} = x_{2,i}$), but the green time of the upstream intersection i-1 is longer than the duration of the encountered phase at downstream intersection *i*.

When $x_{1,i} \neq x_{2,i}$ (i.e., Case 1), regardless of which equals 1, either of two variables ($x_{5,i}$ and $x_{6,i}$) should be set to 1 in Eq. (5.18e) and in turn $x_{3,i}$ and $x_{4,i}$ are set to 1 in Eqs (5.18c) and (5.18d). Also, Eqs. (5.18a) and (5.18b) are open due to the specification of a large number (M) in the right side.

On the other hand, when $x_{1,i} = x_{2,i}$, then $x_{4,i} = x_{5,i} = x_{6,i} = 0$ in Eqs. (5.18d) and (5.18e), and $x_{3,i}$ leaves open in Eq. (5.18c). Hence, based on the value of $x_{1,i}$, the interval of the phase where the leading vehicles in the through traffic encounter at the downstream intersection i will be compared to the green interval at upstream intersection i-1 for the value of $x_{3,i}$. When $x_{1,i} = 1$, one can employ (5.18a) and (5.18b) to compare the green time intervals for the through movement traffic at two intersections as follows:

$$\left(\theta_i + g_i + t_{c,i}\right) - \left(\theta_{i+1} + C\left(c_{1,i+1}\right) + \left(g_{i+1}\right)\right) \geq -M\left(1 - x_{3,i+1}\right) \quad (5.20a)$$

$$\left(\theta_i + g_i + t_{c,i}\right) - \left(\theta_{i+1} + C\left(c_{1,i+1}\right) + \left(g_{i+1}\right)\right) \leq M x_{3,i+1} \quad (5.20b)$$

when $g_i \geq g_{i+1}$, $x_{3,i+1}$ is set to 1, Eq. (5.20b) is open, due to the large number M in the right side, and Eq. (5.20a) is bounded; otherwise $x_{3,i+1}$ is set to 0. On the other hand, when $x_{1,i} = 0$, one can simplify (5.18a) and (5.18b) as follows for comparing the intervals between the red at the downstream intersection *i* and the green at the upstream intersection i-1:

$$\left(\theta_i + g_i + t_{c,i}\right) - \left(\theta_{i+1} + C\left(c_{1,i+1}\right) + \left(C - g_{i+1}\right)\right) \geq -M\left(1 - x_{3,i+1}\right) \quad (5.20c)$$

$$\left(\theta_i + g_i + t_{c,i}\right) - \left(\theta_{i+1} + C\left(c_{1,i+1}\right) + \left(C - g_{i+1}\right)\right) \leq M x_{3,i+1} \quad (5.20d)$$

when $g_i \geq C - g_{i+1}$, $x_{3,i+1}$ is set to 1, Eq. (5.20b) is open, due to the large number M in the right side, and Eq. (5.20a) is bounded; otherwise $x_{3,i+1}$ is set to 0. For (5.13b), the same logic with Eq. (5.19) is applicable.

Table 5.2 Mathematical equations of variables, $x_{1,i}(\bar{x}_{1,i})$, $x_{2,i}(\bar{x}_{2,i})$, $x_{3,i}(\bar{x}_{3,i})$

Variable $x_{1,i}(\bar{x}_{1,i})$	Variable $x_{2,i}(\bar{x}_{2,i})$	Variable $x_{3,i}(\bar{x}_{3,i})$
For $\forall i \in \Omega$	**For $\forall i \in \Omega$**	For $\forall i \in \Omega$
$\theta_{i+1} + C(c_{1,i+1}) - (\theta_i + t_{c,i}) \geq -Mx_{1,i+1}$ (5.14a)	$\theta_{i+1} + C(c_{2,i+1}) - (\theta_i + g_i + t_{c,i}) \geq -Mx_{2,i+1}$ (5.16a)	$(\theta_i + g_i + t_{c,i}) - \begin{pmatrix} \theta_{i+1} + C(c_{1,i+1}) + x_{1,i+1}(g_{i+1}) + \\ (1 - x_{1,i+1})(C - g_{i+1}) \end{pmatrix} \geq -M(1 - x_{3,i+1}) - Mx_{4,i+1}$ (5.18a)
$\theta_{i+1} + C(c_{1,i+1}) - (\theta_i + t_{c,i}) \leq M(1 - x_{1,i+1})$ (5.14b)	$\theta_{i+1} + C(c_{2,i+1}) - (\theta_i + g_i + t_{c,i}) \leq M(1 - x_{2,i+1})$ (5.16b)	$(\theta_i + g_i + t_{c,i}) - (\theta_{i+1} + C(c_{1,i+1}) + x_{1,i+1}(g_{i+1}) + (1 - x_{1,i+1})(C - g_{i+1})) \leq Mx_{3,i+1} + Mx_{4,i+1}$ (5.18b)
$\theta_i + t_{c,i} - (\theta_{i+1} + C(c_{1,i+1}) + g_{i+1}) \geq -Mx_{1,i+1} + C(x_{1,i+1} - 1)$ (5.14c)	$\theta_i + g_i + t_{c,i} - (\theta_{i+1} + C(c_{2,i+1}) + g_{i+1}) \geq -Mx_{2,i+1} + C(x_{2,i+1} - 1)$ (5.16c)	$x_{3,i+1} \geq x_{4,i+1}$ (5.18c)
$\theta_i + t_{c,i} - (\theta_{i+1} + C(c_{1,i+1}) + g_{i+1}) \leq M(1 - x_{1,i+1}) + C(x_{1,i+1} - 1)$ (5.14d)	$\theta_i + g_i + t_{c,i} - (\theta_{i+1} + C(c_{2,i+1}) + g_{i+1}) \leq M(1 - x_{2,i+1}) + C(x_{2,i+1} - 1)$ (5.16d)	$x_{4,i+1} = x_{5,i+1} + x_{6,i+1}$ (5.18d)
		$x_{1,i+1} - x_{2,i+1} = x_{5,i+1} - x_{6,i+1}$ (5.18e)

For $\forall \mathbf{i} \in \bar{\Omega}$

$\theta_i + C(\bar{c}_{1,i}) - (\theta_{i+1} + \bar{t}_{c,i}) \geq -M\bar{x}_{1,i}$

(5.15a)

$\theta_i + C(\bar{c}_{1,i}) - (\theta_{i+1} + \bar{t}_{c,i}) \leq M(1 - \bar{x}_{1,i})$

(5.15b)

$\theta_{i+1} + \bar{t}_{c,i} - (\theta_i + C(\bar{c}_{1,i}) + \bar{g}_i)$

$\geq -M\bar{x}_{1,i} + C(\bar{x}_{1,i} - 1)$

(5.15c)

$\theta_{i+1} + \bar{t}_{c,i} - (\theta_i + C(\bar{c}_{1,i}) + \bar{g}_i)$

$\leq M(1 - \bar{x}_{1,i}) + C(\bar{x}_{1,i} - 1)$

(5.15d)

For $\forall \mathbf{i} \in \bar{\Omega}$

$\theta_i + C(\bar{c}_{2,i}) - (\theta_{i+1} + \bar{g}_{i+1} + \bar{t}_{c,i}) \geq$

$-M\bar{x}_{2,i}$ (5.17a)

$\theta_i + C(\bar{c}_{2,i}) - (\theta_{i+1} + \bar{g}_{i+1} + \bar{t}_{c,i}) \leq$

$M(1 - \bar{x}_{2,i})$

(5.17b)

$\theta_{i+1} + \bar{g}_{i+1} + \bar{t}_{c,i} - (\theta_i + C(\bar{c}_{2,i}) + \bar{g}_i)$

$\geq -M\bar{x}_{2,i} + C(\bar{x}_{2,i} - 1)$

(5.17c)

$\theta_{i+1} + \bar{g}_{i+1} + \bar{t}_{c,i} - (\theta_i + C(\bar{c}_{2,i}) + \bar{g}_i)$

$\leq M(1 - \bar{x}_{2,i}) + C(\bar{x}_{2,i} - 1)$

(5.17d)

For $\forall \mathbf{i} \in \bar{\Omega}$

$(\theta_{i+1} + \bar{g}_{i+1} + \bar{t}_{c,i})$

$- (\theta_i + C(\bar{c}_{1,i}) + \bar{x}_{1,i}(\bar{g}_i) + (1 - \bar{x}_{1,i})(C - \bar{g}_i))$

$\geq -M(1 - \bar{x}_{3,i}) - M\bar{x}_{4,i}$

(5.19a)

$(\theta_{i+1} + \bar{g}_{i+1} + \bar{t}_{c,i}) - (\theta_i + C(\bar{c}_{1,i}) +$

$\bar{x}_{1,i}(\bar{g}_i) + (1 - \bar{x}_{1,i})(C - \bar{g}_i)) \leq$

$M(1 - \bar{x}_{3,i}) + M\bar{x}_{4,i}$ (5.19b)

$\bar{x}_{3,i} \geq \bar{x}_{4,i}$

(5.19c)

$\bar{x}_{4,i} = \bar{x}_{5,i} + \bar{x}_{6,i}$

(5.19d)

$\bar{x}_{1,i} - \bar{x}_{2,i} = \bar{x}_{5,i} - \bar{x}_{6,i}$

(5.19e)

For the arriving traffic pattern, one can distinguish traffic flows during the queuing and discharging periods with the three variables, $x_{j,i}(\bar{x}_{j,i})$ for j=1, 2, 3. For instance, one can identify the traffic flows, approaching intersection *i* at the onset of a green phase, as the through movement from the upstream intersection i-1, under either of the following scenarios

Case 1) the leading vehicle of the through movement faces a red phase at intersection *i* ($x_{1,i} = 0$) and the last vehicle of the movement encounters a green at intersection i ($x_{2,i} = 1$); or

Case 2) both the leading and lagging vehicles in the through traffic arrive during a green phase ($x_{1,i} = x_{2,i} = 1$), and the through traffic flows experience the phase changes ($x_{3,i} = 1$).

To facilitate the model formations, this study has further introduced a set of auxiliary binary variables to identify the approaching traffic flows. More specifically, let

$$y_{1,i} = 1, \text{if } \left(x_{1,i} = x_{2,i} \text{ and } x_{3,i} = 1\right) \text{ or } \left(\left(x_{1,i} \neq x_{2,i}\right) \text{ and } x_{1,i} = 0\right);\ 0, \text{otherwise} \tag{5.21a}$$

$$\bar{y}_{1,i} = 1, \text{if } \left(\bar{x}_{1,i} = \bar{x}_{2,i} \text{ and } \bar{x}_{3,i} = 1\right) \text{ or } \left(\left(\bar{x}_{1,i} \neq \bar{x}_{2,i}\right) \text{ and } \bar{x}_{1,i} = 0\right);\ 0, \text{otherwise} \tag{5.21b}$$

where $y_{1,i}(\bar{y}_{1,i})$ is set to be 1 if approaching vehicles to intersection *i* at the onset of a green phase are the through flows from upstream intersection *i*-1; otherwise 0. Based on the definition, one can specify the following relations:

$$y_{1,i+1} = x_{3,i+1} - x_{4,i+1} \times x_{x,i+1} \tag{5.22}$$

where $x_{4,i+1}$ is set to 1, if $x_{1,i} \neq x_{2,i}$; otherwise 0 in Eq. (5.18d). However, Eq. (5.22) is a nonlinear functional form due to the second term in the right side. Thus, by introducing a binary variable, $y_{2,i}$, Eqs. (5.23) is the linearized from of Eq. (5.22). Eqs. (5.24) can be derived with the same logic for the inbound traffic flows.

Those variables can be formulated as shown in Table 5.3.

Table 5.3 Mathematical equations of variables, $y_{1,i}(\bar{y}_{1,i})$

Variable $y_{1,i}$	**Variable $\bar{y}_{1,i}$**
For $\forall i \in \Omega$,	**For $\forall i \in \bar{\Omega}$,**
$y_{1,i} = x_{3,i} - y_{2,i}$	$\bar{y}_{1,i} = \bar{x}_{3,i} - \bar{y}_{2,i}$
(5.23a)	(5.24a)
$-y_{2,i} + x_{4,i} + x_{1,i} \leq 1$	$-\bar{y}_{2,i} + \bar{x}_{4,i} + \bar{x}_{1,i} \leq 1$
(5.23b)	(5.24b)
$2y_{2,i} - x_{4,i} - x_{1,i} \leq 0$	$2\bar{y}_{2,i} - \bar{x}_{4,i} - \bar{x}_{1,i} \leq 0$
(5.23c)	(5.24c)

In summary, one can differentiate the arrival flow rates with the associated variables for each case shown in Table 5.4, where $Q_{1,i}$ and $Q_{2,i}$ are the arrival traffic flows at intersection i during queue formation and discharging periods.

Table 5.4 Arrival traffic flow patterns for outbound

Pattern	$x_{1,i}$	$x_{2,i}$	$x_{3,i}$	$y_{1,i}$	$Q_{1,i}$	$Q_{2,i}$
1	1	1	0	0	$q_{1,i}$	$q_{2,i}$
2	1	1	1	1	$q_{2,i}$	$q_{1,i}$
3	0	1	1	1	$q_{2,i}$	$q_{1,i}$
4	1	0	1	0	$q_{1,i}$	$q_{2,i}$
5	0	0	0	0	$q_{1,i}$	$q_{2,i}$
6	0	0	0	1	$q_{2,i}$	$q_{1,i}$

Using those arrival traffic flows along with travel times between intersections and signal timings (i.e., cycle length and green intervals), one can then compute the resulting

queue clearance time and maximum queue length, $\tau_i(\bar{\tau}_i)$ and $\varsigma_i(\bar{\varsigma}_i)$, with the equations shown here after.

First, the discretized time intervals, $T_{1,i},\ldots, T_{4,i}$ in Figure 5.8 are constrained by the signal phase.

$$T_{1,i} + T_{2,i} = C - g_i \qquad \forall i \in \Omega \qquad (5.25a)$$

$$\overline{T}_{1,i} + \overline{T}_{2,i} = C - \bar{g}_i \qquad \forall i \in \overline{\Omega} \qquad (5.25b)$$

$$T_{3,i} + T_{4,i} \leq g_i \qquad \forall i \in \Omega \qquad (5.26a)$$

$$\overline{T}_{3,i} + \overline{T}_{4,i} \leq \bar{g}_i \qquad \forall i \in \overline{\Omega} \qquad (5.26b)$$

Eqs. (5.25) indicate that the sum of $T_{1,i}$ and $T_{2,i}$, the queue accumulating period, equals the red interval, and Eqs. (5.26) represents that the sum of $T_{3,i}$ and $T_{4,i}$, the queue discharging period, is less than or equal to the green interval. Furthermore, the queue clearance time and maximum queue length at intersection i, $\tau_i(\bar{\tau}_i)$ and $\varsigma_i(\bar{\varsigma}_i)$, can be determined as follows:

$$\tau_i = T_{3,i} + T_{4,i} \qquad \forall i \in \Omega \qquad (5.27a)$$

$$\bar{\tau}_i = \overline{T}_{3,i} + \overline{T}_{4,i} \qquad \forall i \in \overline{\Omega} \qquad (5.27b)$$

$$\varsigma_i = (Q_{1,i} \times (T_{1,i} + T_{4,i}) + Q_{2,i} \times (T_{2,i} + T_{3,i}))/N_i \times l \qquad \forall i \in \Omega \qquad (5.28a)$$

$$\bar{\varsigma}_i = (\overline{Q}_{1,i} \times (\overline{T}_{1,i} + \overline{T}_{4,i}) + \overline{Q}_{2,i} \times (\overline{T}_{2,i} + \overline{T}_{3,i}))/\overline{N}_i \times l \qquad \forall i \in \overline{\Omega} \qquad (5.28b)$$

where $N_i(\overline{N}_i)$ is the number of lanes at intersection I, and l is the length of vehicles. According to the identified queue formation and discharging types under each offset, one can estimate each sub-time-interval, $T_{1,i}\ldots,T_{4,i}$, with the formulations shown in the Table 5.5.

Table 5.5 Sub-time-intervals by types of intersection queue formation and discharging patterns.

Type	$T_{1,i}\left(\overline{T}_{1,i}\right)$	$T_{2,i}\left(\overline{T}_{2,i}\right)$	$T_{3,i}\left(\overline{T}_{3,i}\right)$	$T_{4,i}\left(\overline{T}_{4,i}\right)$
1	0	$C-g_i$ $\left(C-\overline{g}_i\right)$	$Min\left[\left(q_{2,i-1}\times(C-g_i)\right)/\left(s\times L_i-q_{2,i-1}\right),-\gamma_{1,i}\right]$ $\left(Min\left[\left(\overline{q}_{2,i+1}\times(C-g_i)\right)/\left(s\times\overline{L}_i-\overline{q}_{2,i+1}\right),-\overline{\gamma}_{1,i}\right]\right)$	$\left(q_{2,i-1}\times(C-g_i)-\left(q_{2,i-1}-s\times L_i\right)\times T_{3,i}\right)/\left(s\times L_i-q_{1,i-1}\right)$ $\left(\left(\overline{q}_{2,i+1}\times\left(C-\overline{g}_i\right)-\left(\overline{q}_{2,i+1}-s\times\overline{L}_i\right)\times\overline{T}_{3,i}\right)/\left(s\times\overline{L}_i-\overline{q}_{1,i+1}\right)\right)$
2	0	$C-g_i$ $\left(C-\overline{g}_i\right)$	$Min\left[\left(q_{1,i-1}\times(C-g_i)\right)/\left(s\times L_i-q_{1,i-1}\right),-\gamma_{2,i}\right]$ $\left(Min\left[\left(\overline{q}_{1,i+1}\times(C-\overline{g}_i)\right)/\left(s\times\overline{L}_i-\overline{q}_{1,i+1}\right),-\overline{\gamma}_{2,i}\right]\right)$	$\left(q_{1,i-1}\times(C-g_i)-\left(q_{1,i-1}-s\times L_i\right)\times T_{3,i}\right)/\left(s\times L_i-q_{2,i-1}\right)$ $\left(\left(\overline{q}_{1,i+1}\times\left(C-\overline{g}_i\right)-\left(\overline{q}_{1,i+1}-s\times\overline{L}_i\right)\times\overline{T}_{3,i}\right)/\left(s\times\overline{L}_i-\overline{q}_{2,i+1}\right)\right)$
3	$C-g_i-T_{2,i}$ $\left(C-\overline{g}_i-\overline{T}_{2,i}\right)$	$\gamma_{1,i}$ $\left(\overline{\gamma}_{1,i}\right)$	$Min\left[g_{i-1}-\gamma_{1,i},\left(q_{2,i-1}\times\left(C-g_i-\gamma_{1,i}\right)+q_{1,i-1}\times\gamma_{1,i}\right)/\left(s\times L_i-q_{1,i-1}\right)\right]$ $\left(Min\left[\overline{g}_{i+1}-\overline{\gamma}_{1,i},\left(\overline{q}_{2,i+1}\times\left(C-\overline{g}_i-\overline{\gamma}_{1,i}\right)+\overline{q}_{1,i+1}\times\overline{\gamma}_{1,i}\right)/\left(s\times\overline{L}_i-\overline{q}_{1,i+1}\right)\right]\right)$	$\left(q_{2,i-1}\times\left(C-g_i-\gamma_{1,i}\right)+q_{1,i-1}\times\gamma_{1,i}-\left(q_{1,i-1}-s\times L_i\right)\times T_{3,i}\right)/\left(s\times L_i-q_{2,i-1}\right)$ $\left(\left(\overline{q}_{2,i+1}\times\left(C-\overline{g}_i-\overline{\gamma}_{1,i}\right)+\overline{q}_{1,i+1}\times\overline{\gamma}_{1,i}-\left(\overline{q}_{1,i+1}-s\times\overline{L}_i\right)\times\overline{T}_{3,i}\right)/\left(s\times\overline{L}_i-\overline{q}_{2,i+1}\right)\right)$
4	$C-g_i-T_{2,i}$ $\left(C-\overline{g}_i-\overline{T}_{2,i}\right)$	$\gamma_{2,i}$ $\left(\overline{\gamma}_{2,i}\right)$	$Min\left[C-g_{i-1}-\gamma_{2,i},\left(q_{1,i-1}\times\left(C-g_i-\gamma_{2,i}\right)+q_{2,i-1}\times\gamma_{2,i}\right)/\left(s\times L_i-q_{2,i-1}\right)\right]$ $\left(Min\left[C-\overline{g}_{i+1}-\overline{\gamma}_{2,i},\left(\overline{q}_{1,i+1}\times\left(C-g_i-\overline{\gamma}_{2,i}\right)+\overline{q}_{2,i+1}\times\overline{\gamma}_{2,i}\right)/\left(s\times\overline{L}_i-\overline{q}_{2,i+1}\right)\right]\right)$	$\left(q_{1,i-1}\times\left(C-g_i-\gamma_{2,i}\right)+q_{2,i-1}\times\gamma_{2,i}-\left(q_{2,i-1}-s\times L_i\right)\times T_{3,i}\right)/\left(s\times L_i-q_{1,i-1}\right)$ $\left(\left(\overline{q}_{1,i+1}\times\left(C-\overline{g}_i-\overline{\gamma}_{2,i}\right)+\overline{q}_{2,i+1}\times\overline{\gamma}_{2,i}-\left(\overline{q}_{2,i+1}-s\times\overline{L}_i\right)\times\overline{T}_{3,i}\right)/\left(s\times\overline{L}_i-\overline{q}_{1,i+1}\right)\right)$
5	g_{i-1} $\left(\overline{g}_{i+1}\right)$	$C-g_i-g_{i-1}$ $\left(C-\overline{g}_i-\overline{g}_{i+1}\right)$	$\left(q_{1,i-1}\times g_{i-1}+q_{2,i-1}\times\left(C-g_i-g_{i-1}\right)\right)/\left(s\times L_i-q_{2,i-1}\right)$ $\left(\left(\overline{q}_{1,i+1}\times\overline{g}_{i+1}+\overline{q}_{2,i+1}\times(C-\overline{g}_i-\overline{g}_{i+1})\right)/\left(s\times\overline{L}_i-\overline{q}_{2,i+1}\right)\right)$	0
6	$C-g_{i-1}$ $\left(C-\overline{g}_{i+1}\right)$	$g_{i-1}-g_i$ $\left(\overline{g}_{i+1}-\overline{g}_i\right)$	$\left(q_{2,i-1}\times\left(C-g_{i-1}\right)+q_{1,i-1}\times\left(g_{i-1}-g_i\right)\right)/\left(s\times L_i-q_{1,i-1}\right)$ $\left(\left(\overline{q}_{2,i+1}\times\left(C-\overline{g}_{i+1}\right)+\overline{q}_{1,i+1}\times(\overline{g}_{i+1}-\overline{g}_i)\right)/\left(s\times\overline{L}_i-\overline{q}_{1,i+1}\right)\right)$	0

where, $\gamma_{1,i}=\theta_i+C\times c_{1,i}-\left(\theta_{i-1}+t_{c,i-1}\right)$, $\overline{\gamma}_{1,i}=\theta_i+C\times c_{1,i}-\left(\theta_{i+1}+\overline{t}_{c,i}\right)$, $\gamma_{2,i}=\theta_i+C\times c_{2,i}-\left(\theta_{i-1}+g_{i-1}+t_{c,i}\right)$, $\overline{\gamma}_{2,i}=\theta_i+C\times c_{2,i}-\left(\theta_{i+1}+\overline{g}_{i+1}+\overline{t}_{c,i}\right)$

By referring to the onset of a green phase at the outbound (inbound) upstream intersection i-1 (i+1), one can define the point where queues vanish in Figure 5.9, (a_i, S_i) $((\bar{a}_i, \bar{S}_i))$, as follows:

$$a_{i+1} = (w_i - w_{i+1}) + t_i + f_i + \tau_{i+1} \qquad \forall i \in \Omega \qquad (5.29a)$$

$$S_{i+1} = d_i - \varsigma_{i+1} \qquad \forall i \in \Omega \qquad (5.29b)$$

$$\bar{a}_i = \left((1 - r_{i+1}) - \bar{w}_{i+1}\right) + \bar{t}_i + \bar{f}_i - \left((1 - r_i) - \bar{w}_i\right) + \bar{\tau}_i \quad \forall i \in \bar{\Omega} \quad (5.30a)$$

$$\bar{S}_i = \bar{d}_i - \bar{\varsigma}_i \qquad \forall i \in \bar{\Omega} \qquad (5.30b)$$

Eq (5.29 a) indicates that the time when the queues vanish at the downstream intersection *i*+1, a_{i+1}, is the sum of the offsets from intersection *i* to intersection *i*+1, $(w_i - w_{i+1}) + t_i + f_i$, and the queue clearance time at intersection *i*+1, τ_{i+1}. Eq (5.29 b) represents the available storage space of the segment (S_{i+1}) at that time (a_{i+1}), which is the length of link between intersections *i* and *i*+1, d_i, subtracted by the maximum queue length, ς_{i+1}. By the same token, one can set the constraints for the inbound direction as shown in Eqs (5.30 a) and (5.30 b) (see Figure 5.9 (b)).

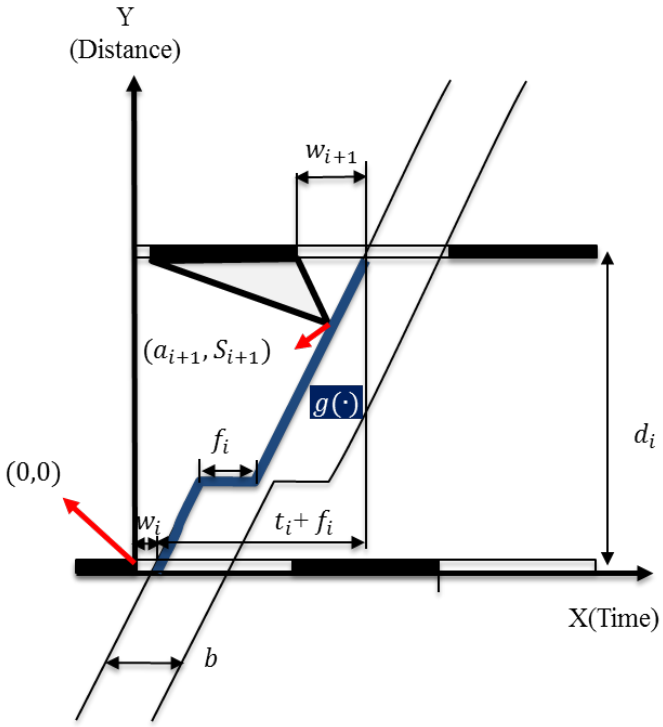

(a) outbound

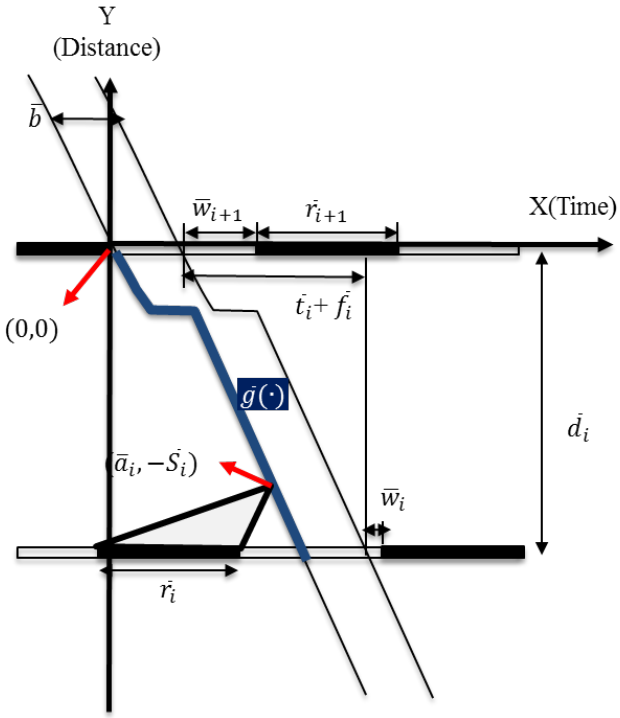

(b) inbound

Figure 5.9 An illustration of a relationship of traffic queue and bus progression band.

The left boundary of the bus progression band is determined by the bus stop location and bus travel time (running and dwell times) between the intersections. The entire band can be divided into three time intervals: 1) before the bus stop, 2) at the bus stop, and 3) after the bus stop. As shown in Figure 5.9 where the origin is the onset of a green phase at the outbound (inbound) upstream intersection *i* (*i*+1), one can formulate the left boundary of the bus band in a time-space diagram, as follows:

$$g(z_{i+1}) = \begin{cases} v_i \times (z_{i+1} - (w_i)), & w_i \le z_{i+1} \le w_i + t_i \times l_i/d_i \\ v_i \times t_i \times l_i/d_i, & w_i + t_i \times l_i/d_i \le z_{i+1} \le w_i + t_i \times l_i/d_i + f_i \\ v_i \times (z_{i+1} - (w_{i1} + f_i)), & w_i + t_i \times l_i/d_i + f_i \le z_{i+1} \end{cases}$$

$$\forall i \in \Omega \qquad (5.31\ a)$$

$$\bar{g}(z_i) = \begin{cases} -\bar{v}_i \times (z_i - (1 - \bar{r}_{i+1} - \bar{w}_{i+1})), & 1 - \bar{r}_{i+1} - \bar{w}_{i+1} \le z_i \le 1 - \bar{r}_{i+1} - \bar{w}_{i+1} + \bar{t}_i \times \bar{l}_i/\bar{d}_i \\ -\bar{v}_i \times \bar{t}_i \times \bar{l}_i/\bar{d}_i, & 1 - \bar{r}_{i+1} - \bar{w}_{i+1} + \bar{t}_i \times \bar{l}_i/\bar{d}_i \le z_i \le 1 - \bar{r}_{i+1} - \bar{w}_{i+1} + \bar{t}_i \times \bar{l}_i/\bar{d}_i + \bar{f}_i \\ -\bar{v}_i \times \left(z_i - \left(1 - \bar{r}_{i+1} - \bar{w}_{i+1} + \bar{f}_i\right)\right), & 1 - \bar{r}_{i+1} - \bar{w}_{i+1} + \bar{t}_i \times \bar{l}_i/\bar{d}_i + \bar{f}_i \le z_i \end{cases}$$

$$\forall i \in \bar{\Omega} \qquad (5.31\ b)$$

where v_i ($\bar{v}_i$) denotes the average bus running speed between intersections *i* (*i*+1) and *i*+1 (*i*); and l_i ($\bar{l}_i$) denotes the distance from the upstream intersection to a bus stop between intersections *i* (*i*+1) and *i*+1 (*i*). In Eq (5.31), an array of functions represents the left boundary of a bus band for the corresponding time interval.

Note that the available storage, $S_{i+1}(\bar{S}_i)$, needs to be sufficiently long to prevent the intersection traffic queues from breaking the left boundary of the bus band due to the on-going discharging process of queues, $g(a_{i+1})\left(\bar{g}(\bar{a}_i)\right)$. Hence, it is specified as follows:

$$g(a_{i+1}) \le S_{i+1} \qquad \forall i \in \Omega \qquad (5.32\ a)$$

$$-\bar{g}(\bar{a}_i) \le \bar{S}_i \qquad \forall i \in \bar{\Omega} \qquad (5.32\ b)$$

Eq. (5.32) shows that the available storage is long enough to prevent the intersection traffic queues from breaking the left boundary of a bus band prior to the queue vanishing time, a_i.

In brief, the base model proposed in Stage-1 for computing the bus progression bands can be summarized as follows:

M-1: Max $\sum b_i + k_{b,i}\bar{b}_i$

s.t. Eqs (5.2)-(5.5), (5.10), (5.14)-(5.19), (5.23)-(5.32)

$b_i, \bar{b}_i, w_i, \bar{w}_i, \tau_i, \bar{\tau}_i, \varsigma_i, \bar{\varsigma}_i, a_i, \bar{a}_i, S_i, \bar{S}_i \geq 0$ for i=1,..,N

n_i, $\bar{n}_i$, $c_{1,i}$, $\bar{c}_{1,i}$, $c_{2,i}$, $\bar{c}_{2,i}$ are integer variables for i=1,…,N

s_i, $\bar{s}_i$ are binary variables, for i=1,…,N

$x_{j,i}$, $\bar{x}_{j,i}$, are binary variables, for j=1,2,3 and i=1,…,N

$y_{j,i}$, $\bar{y}_{j,i}$, are binary variables, for j=1,2 and i=1,…,N.

$T_{j,i}, \bar{T}_{j,i} \geq 0$ for j=1,…,4 and i=1,…,N

5.3.3 Stage-2: An Enhanced Bus Progression Model to Account for Dwell Time Uncertainty

The enhanced model (BUSBAND), proposed to further account for dwell time uncertainty with variable bus bands along the segment has the following revised objective function:

$$Max \sum_i \varphi_i b_i^e + \sum_i \bar{\varphi}_i \bar{b}_i^e \quad (5.33)$$

where $\varphi_i(\bar{\varphi}_i)$ is a weighting factor of intersection i for the outbound (inbound) direction; and $b_i^e(\bar{b}_i^e)$ is the effective bandwidth for buses at intersection i. The weighting factor, $\varphi_i(\bar{\varphi}_i)$, can be specified with the expected number of outbound

(inbound) buses per hour passing intersection i during the synchronized phase, $m_i(\bar{m}_i)$, as follows:

$$\varphi_i = \frac{m_i}{\sum m_i + \sum \bar{m}_i} \qquad \forall i \in \Omega \tag{5.34 a}$$

$$\bar{\varphi}_i = \frac{\bar{m}_i}{\sum m_i + \sum \bar{m}_i} \qquad \forall i \in \bar{\Omega} \tag{5.34 b}$$

The effective bandwidth, $b_i^e(\bar{b}_i^e)$, affecting the number of buses staying within the band at intersection i and its downstream intersection, can be defined as follows:

1) Scenario 1: No bus stop on a link

If no bus stop is located between two consecutive intersections i and i+1, all buses in the progression band are expected to stay within the band, and the effective bandwidth shall be identical to the bandwidth for intersection i(i+1), that is,

$$b_i^e = b_i \tag{5.35 a}$$

$$\bar{b}_{i+1}^e = \bar{b}_{i+1} \tag{5.35 b}$$

2) Scenario 2: Incorporating the dwell time variance in the formulations

If a bus stop is located between two consecutive intersections i and i+1, one can compute the effective bandwidth for intersection *i*, based on the probability that a bus from the arriving band can stay within the departing band after leaving the bus stop. Figure 5.10 shows an example of bus bands at two consecutive intersections, where the dashed line indicates the center of green bands, and the solid line represents the trajectory of one bus moving in the outbound direction; e_i denotes the bus arrival time at intersection i, which is measured by its deviation from the center of the band. Then, the expected arrival time of the bus at intersection i+1, e_{i+1}, shall equal e_i,

because the travel time plus the expected dwell time is the horizontal difference between the centers of these two bands.

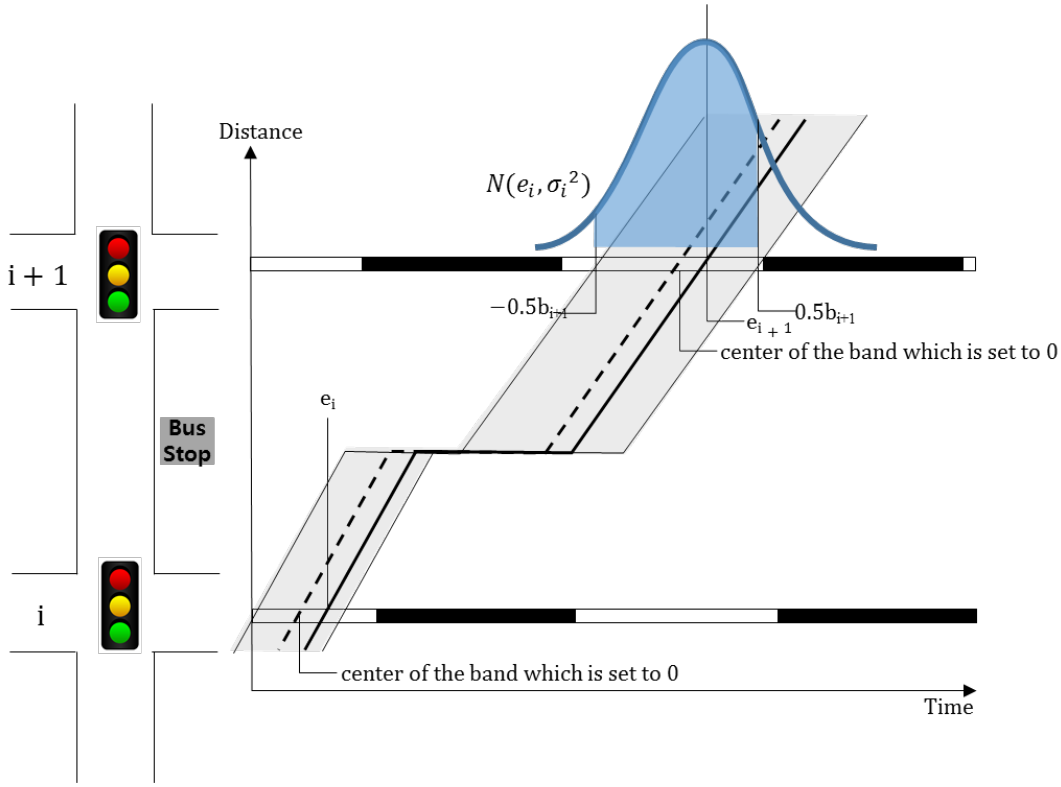

Figure 5.10 Illustration of dwelling time variance between two adjacent intersections

Assuming that all buses travel at the same speed within one cycle and their dwell times follow a normal distribution with a mean of μ_i and a standard deviation, σ_i, the arrival times to the downstream intersection shall follow a normal distribution, $N(e_i, \sigma_i^2)$. Note that the time interval during which the bus passes both intersections are measured by their differences from the center of the bands. Then, the probability that the departing bus from a stop to stay in the departing band shall equal the probability that the actual arrival time to the downstream intersection is within the departing band of the bus stop, as shown in the shaded area in Figure 5.10. Such a probability can be expressed as follows:

$$P(-0.5b_{i+1} \le e_{i+1} \le 0.5b_{i+1}) = \Phi(\frac{0.5b_{i+1} - E(e_{i+1})}{\sigma_i}) - \Phi(\frac{-0.5b_{i+1} - E(e_{i+1})}{\sigma_i})$$

$$= \Phi(\frac{0.5b_{i+1} - e_i}{\sigma_i}) - \Phi(\frac{-0.5b_{i+1} - e_i}{\sigma_i}) \quad (5.36)$$

where $E(e_{i+1})$ denotes the expectation of actual arrival time, which equals e_i. Note that the value of e_i shall lie between $-0.5b_i$ and $0.5b_i$. The effective bandwidth at intersection i can be obtained by integrating the probability with e_i as follows:

$$b_i^e = \int_{-0.5b_i}^{0.5b_i} P(-0.5b_{i+1} \le e_{i+1} \le 0.5b_{i+1}) de_i = \int_{-0.5b_i}^{0.5b_i} \Phi(\frac{0.5b_{i+1} - e_i}{\sigma_i}) - \Phi(\frac{-0.5b_{i+1} - e_i}{\sigma_i}) de_i \quad (5.37\text{ a})$$

where b_i^e denotes the effective bandwidth at intersection i. By the same token, the inbound effective bandwidth can be expressed as follows:

$$\bar{b}_{i+1}^e = \int_{-0.5\bar{b}_{i+1}}^{0.5\bar{b}_{i+1}} \Phi(\frac{0.5\bar{b}_i - \bar{e}_{i+1}}{\bar{\sigma}_i}) - \Phi(\frac{-0.5\bar{b}_i - \bar{e}_{i+1}}{\bar{\sigma}_i}) d\bar{e}_{i+1} \quad (5.37\text{ b})$$

In summary, for those links without a bus stop, the effective bandwidth can be directly obtained with Eq. (5.35). In contrast, for other links with a bus stop, one shall take into account the impact caused by bus dwell time uncertainty and apply Eq. (5.37) to estimate the effective bandwidth. Conceivably, a larger effective bandwidth can guarantee a higher number of transit vehicles to receive the progression at two consecutive intersections. Hence, the total effective bandwidth for each pair of intersections along the arterial can serve as an indicator for evaluating the effectiveness of a signal plan. However, Eqs. (5.37 a) and (5.37 b) are highly non-linear in nature due to the presence of integral and normal distributions. To improve the computing efficiency, one can employ the linearization steps introduced in Appendix to yield the optimal solution.

In brief, the final enhanced model, BUSBAND, incorporating the stochastic dwell times in computing bus progression bands, can be summarized as follows:

$$\boldsymbol{Max} \sum_i \varphi_i b_i^e + \sum_i \bar{\varphi}_i \bar{b}_i^e$$

s.t. Eqs (5.2)-(5.5), (5.10), (5.14)-(5.19), (5.23)-(5.32), (5.35), (5.37)

$b^e_i, \bar{b}^e_i, w_i, \bar{w}_i, \tau_i, \bar{\tau}_i, \varsigma_i, \bar{\varsigma}_i, a_i, \bar{a}_i, S_i, \bar{S}_i, H_{i.k} \geq 0$ for i=1,..,N

n_i, $\bar{n}_i$, $c_{1,i}$, $\bar{c}_{1,i}$, $c_{2,i}$, $\bar{c}_{2,i}$ are integer variables for i=1,…,N

s_i, $\bar{s}_i$ are binary variables, for i=1,…,N

$x_{j,i}$, $\bar{x}_{j,i}$, are binary variables, for j=1,2,3 and i=1,…,N

$y_{j,i}$, $\bar{y}_{j,i}$, are binary variables, for j=1,2 and i=1,…,N.

$T_{j,i}, \bar{T}_{j,i} \geq 0$ for j=1,…,4 and i=1,…,N

$I_{i,k}, \bar{I}_{i,k}, I'_{i,k}, \bar{I}'_{i,k}, y^z_{i,k}, \bar{y}^z_{i,k}, y'^z_{i,k}, \bar{y}'^z_{i,k}$ are binary variables, for $j = 1, 2, 3,$ and $i = 1, \ldots, N$

5.4 Numerical Analysis

The experimental analysis is first conducted to evaluate the quality of bus progression produced by the proposed models in terms of the percentage of buses which can experience the progression along the target arterial. The overall network performance under such models is included in the evaluation. The results are compared with the progression plan, generated by MULTIBAND, the state-of-art model in the literature for signal progression. More specifically, signal progression plans for numerical analysis are produced from the following two models:

- BUSBAND: A two-way progression model designed for bus operations considering bus dwell times, bus stop constraints, and intersection traffic queues as well as bus stop locations
- MULTIBAND: a two-way progression model designed for passenger cars

In this section, all mixed-integer-linear-programming formulations are solved within CPLEX ILOG, operated on a desktop with 8GB RAM and Intel i7 processor.

5.4.1. Experimental Design

To evaluate the potential of the proposed models for real-world applications, this study has selected an arterial segment on MD586 in the state of Maryland for case study. The simulation network consists of five intersections with two roadside bus stops in each direction. The simulation network consists of six intersections. The key features of each segment, such as bus stop locations, distance between intersections, and travel times, are as summarized in Figure 5.11.

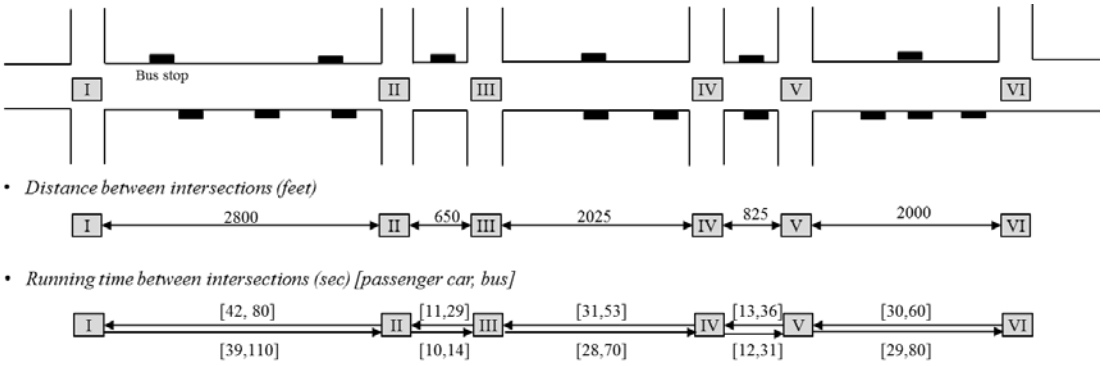

Figure 5.11 General information of the study site

In order to test the performance under different traffic demands, this study has adopted two traffic volume scenarios, Demand 1 (Q1) and Demand 2 (Q2), as shown in Figure 5.12. The signal timings are calculated with the traffic volumes, as shown in Figure 5.13. Note that all intersections have a common cycle length, a 3-second yellow interval, and a 2-second all-red interval in each phase.

Demand	Intersection	I			II			III			IV			V			VI		
	Movement	L	T	R	L	T	L	T	R	R	L	T	R	L	T	R	L	T	R
1	EB	5	720	25	26	810	32	112	679	34	71	676	36	67	589	77	69	687	
	WB	4	543	16	7	565	5	151	490	52	70	650	40	68	571	60		684	75
	NB	1	1	1	39	3	8		147	105	25	4	26	133	411	57			
	SB	132	4	18	15	7	1		548	87	18	6	22	107	417	57	12		9
2	EB	6	716	25	26	851	34	113	721	37	78	715	35	65	616	79	78	757	
	WB	5	588	23	10	640	6	181	553		86	735	50	85	660	73		823	92
	NB	1	1	1	70	10	9		149	103	25	4	26	157	493	71			
	SB	162	6	21	17	5	1		729	103	18	6	22	140	491	60	12		9

Figure 5.12 Traffic volume (vehicle per hour)

Intersection	I		II		III		IV		V		VI	
Demand	Q1	Q2	Q1	Q2	Q1	Q2	Q1	Q2	Q1	Q2	Q1	Q2
PHASE 1	64	83	60	83	49	63	60	82	44	60	79	108
PHASE 2	10	10	10	17	30	42	13	15	14	14	11	12
PHASE 3	16	27	10	10	11	15	17	23	18	32		
PHASE 4			10	10					14	14		

Figure 5.13 Signal plan and timings (seconds)

Bus dwell times at bus stops in each direction are assumed to follow normal distributions with mean and standard deviation (seconds), and the dwell times at each intersection are independent. The average dwell times are set to be 20 seconds and 25 seconds at each bus stop for Demand 1 and Demand 2, respectively. To test the performance under different dwell time variances, three dwell time standard deviations of zero (constant dwell time), 5 and 10 seconds are evaluated under the same average for all dwell times.

To evaluate the network's performance under different optimization models, this study adopts VISSIM, microscopic multi-modal traffic flow simulation software, as a simulation platform. The signal plan, produced from each model for comparison, has been simulated with different traffic volumes and dwell time variances. The standard exercise of fifteen minute warm-up period and one hour simulation times are adopted in the simulation experiments. Due to the stochastic nature of the employed microscopic traffic simulation program, each scenario has been simulated with five replications with different random seeds.

Model Evaluation I: Bus operations performance

To assess the performance of BUSBAND, this study has adopted the number of intersections that each bus can progress over the target arterial under different traffic demands and dwell times as the MOE. All buses are simulated to pass the first intersection during the green phase. That is, 40 buses per hour and 30 buses per hour in each direction for Demand 1 (CL=90seconds) and Demand 2 (CL=120 seconds) were scheduled.

Figure 5.14 illustrates the level of progression experienced by those buses under simulated environments. The proposed model, BUSBAND, provided a good progression for buses under a dwell time deviation of zero (seconds). Under Demand-1 scenario, 42 percent of buses could pass the arterial without stops, and 90 percent experiencing stops less than two intersections. Similarly, under Demand-2 scenario, 53 percent of buses enjoyed full progression, and 93 percent of buses experienced only one intersection to stop along the arterial. On the other hands, given the signal plan with MULTIBAND, no buses could pass the arterial without stops. Under Demand-1, all buses had to stop at more than one intersection and 52 percent of buses experienced more than two intersection stops. As the cycle length increases under Demand-2, some buses (i.e., 11 percent of buses) could pass the arterial with one stop, yet most buses still experienced two or more stops along the arterial.

Despite a slight increase in a dwell time deviation (i.e., dwell time deviation of five second), the BUSBAND remains effective. For instance, under Demand-1 scenario, 32 percent of buses enjoyed full progression over the arterial, and 60 percent of them proceeded over the arterial with one or two stops. As the cycle length increases from 90 seconds to 120 seconds under Demand-2, buses, progressed over the arterial with less than two intersection stops, increased from 49 percent under Demand 1 to 71 percent. On the other hands, given the signal plan with MULTIBAND, only a few buses could pass the arterial without stops (i.e., 1 percent and 4 percent for Demand 1 and Demand 2). Note that under Demand 1, all buses had to stop at least two stops, and 48 percent of them stopped at more than two intersections along the arterial. As the cycle length increases under Demand 2, 30

percent of buses could pass the arterial with one stop. However, most buses still experienced two or three intersection stops along the arterial.

With a large dwell time deviation of 10 (seconds), 23 percent of buses under Demand-1 could progress through all intersections without stop; 37 percent of buses experienced one intersection stop; and 95% of buses can proceed over the arterial with less than three stops. However, under Demand-2, 13 percent of those buses enjoyed the full progression; 45 percent stopped at one or two intersections; and another 40 percent of buses stopped at three intersections. However, it seems difficult to offer effective bus progression bands under the scenarios of high bus volume and high dwell time variance even with the proposed BUSBAND due to the congested traffic conditions and dwell time uncertainty.

To sum up, the proposed model, BUSBAND, indeed performs well under low/medium dwell time deviation conditions. As dwell time uncertainty increases, inevitably, more buses may deviate from the designed bus bands, encounter some interference from non-transit flows, and experience more stops at intersections.

	Demand-1	Demand-2
DW1 (zero)		
DW2 (5 sec)		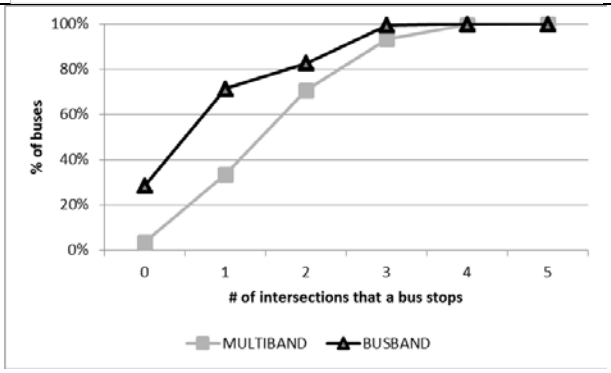
DW3 (10 sec)		

Figure 5.14 Percentages of buses that stop at an intersection along the arterial

Model Evaluation II: Network Performance

To evaluate the network's overall performance under different bus progression plans, this study has taken the following measures of effectiveness: average stopped delay per passenger car, average stopped delay per bus, the average number of stops per passenger car, and the average number of stops per bus. A total of 60 buses per hour in each direction were scheduled and to simulate the stochastic bus entry time to the arterial, a dummy stop is located at the upstream of the first intersection in each direction with a high dwell time deviation of 20 seconds.

Table 5.6 shows the comparison results with respect to those performance measures. Overall, the bus-based progression model could offer the expected operational benefits to buses under Demands 1 to 2. For example, under Demand-1 and zero dwell time deviation, BUSBAND can decrease the average bus stopped delay by 45.22 percent from 39.57 seconds to 21.67 seconds, compared to the results with MULTIBAND. The average number of stops also decreased by 6.51 percent from 11.38 to 10.67. Note that these numbers include stops at the bus stops. Due to the trade-off nature, BUSBAND may cause an increase in the average delay per passenger car. However, compared to MULTIBAND, the proposed model could improve the performance of transit vehicles, but not cause a significant increase in the average delay per passenger car. For example, under the condition of no dwell time deviation, BUSBAND can increase the average stopped delay for passenger car by 0.24 % (from 27.23 to 27.30) and 2.93% (from 38.47 to 39.60) for Demands 1 and 2, respectively, compared to those under MULTIBAND.

Note that any increase in the dwell time variability will inevitably deteriorate the performance of the proposed BUSBAND model. However, BUSBAND can still outperform MULTIBAND under most scenarios. For example, under Demand -2 and dwell time deviation of 10 seconds, the results from BUSBAND clearly contribute to decrease in the average stopped delay per bus by 20.03 percent from 62.96 seconds to 50.35%. The average number of stops per bus also decreases by 1.21% from 12.42 to 12.29.

Table 5.6 (a) Network performance comparison between MULTIBAND and BUSBAND under no dwell time deviation

	Demand-1			Demand-2		
	MUILTI-BAND	BUS-BAND	Changes in %	MUILTI-BAND	BUS-BAND	Changes
Average Stop Delay (s), Auto	27.23	27.30	0.24%	38.47	39.60	2.93%
Average Stop Delay (s), Bus	39.57	21.67	- 45.22%	57.70	42.31	-26.67%
Average # of stops, Auto	1.47	1.62	9.74%	1.73	1.87	8.15%
Average # of stops, Bus	11.38	10.64	-6.51%	12.28	12.22	-0.48%

Table 5.6 (b) Network performance comparisons between MULTIBAND and BUSBAND under dwell time deviation of ten seconds

	Demand-1			Demand-2		
	MUILTI-BAND	BUS-BAND	Changes in %	MUILTI-BAND	BUS-BAND	Changes in %
Average Stop Delay (s), Auto	27.23	26.87	-1.32%	38.8	39.14	0.88%
Average Stop Delay (s), Bus	40.41	29.74	-26.39%	62.96	50.35	-20.03%
Average # of stops, Auto	1.49	1.60	7.57%	1.80	1.90	5.52%
Average # of stops, Bus	11.58	10.96	-5.35%	12.42	12.29	-1.21%

5.5 Closure

Existing TSP control strategies may not be applicable to arterials experiencing heavy bus flows due to both excessive activations and negative impacts on the network. Under such circumstances, a passive control strategy, directly using the bus volume in design of signal offsets, can be a viable option to facilitate bus flows and to increase bus ridership. This chapter has presented a signal progression model to optimize the offsets for an urban arterial that needs to accommodate high volume of transit flows. The developed model for bus-based progression considers average bus dwell time, the relatively slow bus speed, and the physical constraints of bus stops. In addition, to ensure that the bus progression will not be interrupted by the intersection traffic queues, the proposed model formulations have reflected the queue formation/discharging process and its relations with the bus stop location and the uncertainty of bus dwell times.

The results of extensive numerical investigations have confirmed that the proposed models can indeed provide a quality progression to buses under different traffic conditions and dwell time certainties. It is also clear that BUSBAND can outperform MULTIBAND with respect to stopped delays, and the number of stops at signals, also yielding acceptable impacts on delays for passenger cars.

This pre-timed plan with the proposed model can serve as a base plan for the arterial with heavy bus flows. By cooperating other real-time transit strategies such as active TSP control, one can further improve the efficiency and stability of transit operations by capturing the stochastic nature of the dwell times, bus travel time, and general traffic demands.

Hence, a real-time TSP, grounded with pre-timed BUSBAND, will be a viable operation despite the effectiveness of BUSBAND, it is inadequate to contend with the scenarios of high volume and high dwell time uncertainty.

Chapter 6: An Integrated Transit Signal Priority Control System for Real-time Operations

6.1 Introduction

In view of the complex interactions between all critical variables contributing to the design of bus progression bands, it is expected that the total band width of such a system and its effectiveness generally decrease with the number of intersections included in the control boundaries. This is due to one or several intersections that are likely to become bottlenecks or constraints in maximizing the progression bandwidth along the entire arterial.

For example, the bus progression bands designed for six intersections in the arterial shown in Figure 6.1 (a) are clearly constrained by intersection III where its available green duration for progression is the minimum among all coordinated intersections. As bus progression bands are for both directions, intersection VI also becomes the bottleneck to limit the expansion of the progression bandwidth. It is also notable that the resulting bands at intersection II become narrower in the expanded system shown in Figure 6.1(b).

Conceivably, one may mitigate the impacts of such bottleneck intersections on the bus progression band by offering a more flexible function for their signal controls such as a timely green extension or red truncation to facilitate the bus progression and bus band expansion. Hence, one may expect the arterial to yield higher benefits for bus operations if its passive TSP (such as the proposed BUSBAND) is integrated optimally with an active TSP in real time at some critical intersections.

However, since an active TSP often benefits the bus movements at the cost of vehicles on the cross street, excessive deployment of the active TSP at non-critical intersections may result in undesirable impacts on non-priority movements of traffic flows, and not to achieve the expected benefits for bus flows with respect to bus progression bandwidth. For instance, if the buses granted with a green extension need to stop at the downstream intersections, then the deployment of an active TSP at the intersection may not yield the expected benefits from the perspective of bus operations over the entire arterial. Hence, to best the performance of an integrated passive and active TSP controls for an arterial, it is essential to first identify the optimal intersection for active TSP operations, and then select the proper TSP strategies for such intersections.

Grounded on the pre-timed bus progression model (BUSBAND) in the last chapter, this chapter presents an integration of an active TSP control with a pre-timed BUSBAND for real-time operations. Section 6.2 presents an integrated transit signal priority control system, including the logic of an active TSP employed in the integrated real-time operations. Section 6.3 reports the results of extensive simulation evaluations with respect to the effectiveness of the proposed integrated system. Section 6.4 presents a model to select an intersection to deploy an active TSP along with a summary of its main contributions in the last section.

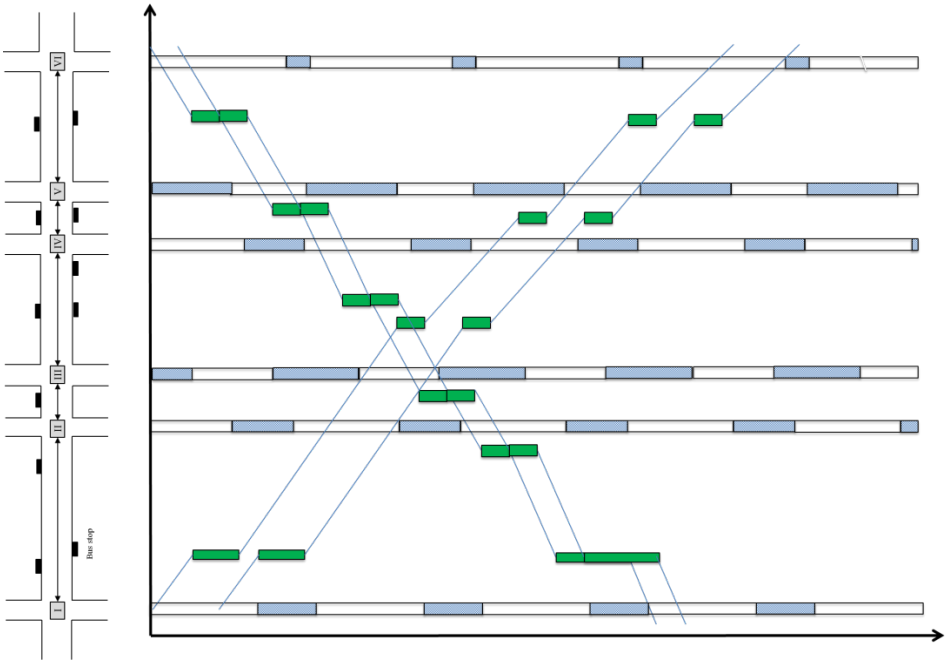

(a) Progression along six intersections

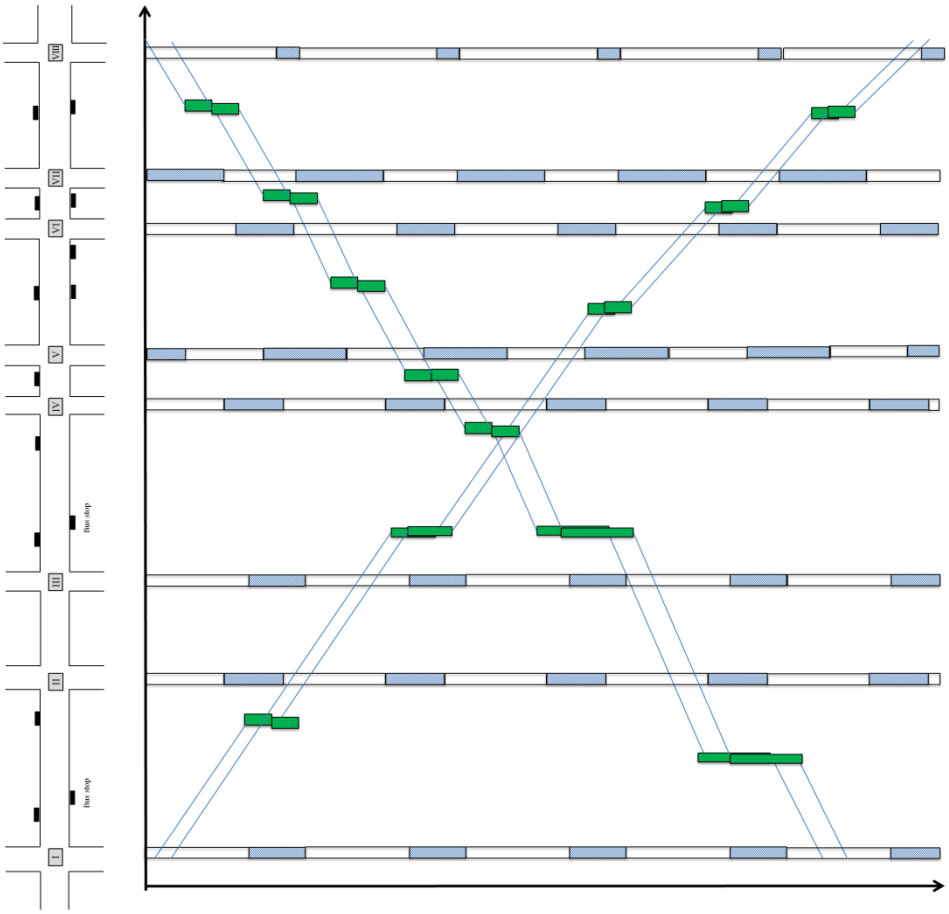

(b) Progression along eight intersections

Figure 6.1 Example of the progression efficiency

6.2 Integrations of an active TSP with a pretimed BUSBAND

6.2.1 Operational flows of the integrated System

Figure 6.2 illustrates the operational flows of the proposed integrated real-time operations for bus progression, including system components and their interrelations.

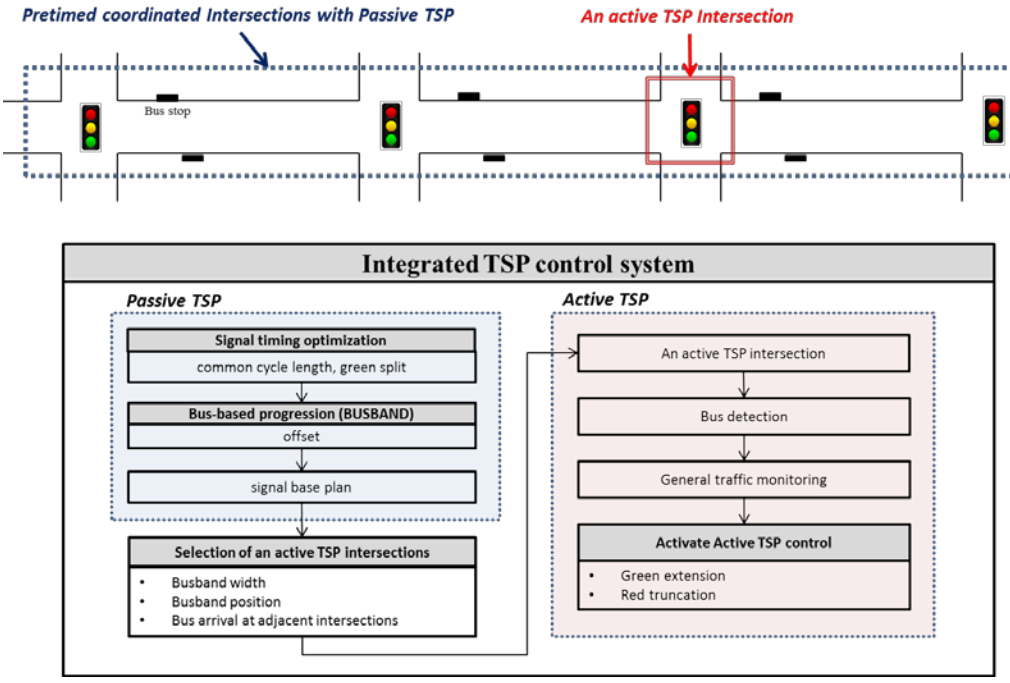

Figure 6.2. The operational flows of the integrated TSP control system

The key function of each principal component is summarized below:

- Passive TSP: provide the base offsets for all coordinated intersections to progress bus over the entire arterial.
- TSP selection module: determine the intersection for deploying an active TSP, based on the passive TSP design to best the benefits of the integrated TSP operations.
- Active TSP activation module: execute the green-extension or a red truncation at the target intersection to maximize the bus progression bands along an arterial with the minimal impacts on those non-priority movements

6.2.2 Key functions of an active TSP

An active TSP system is generally composed of three major components: vehicle detection module that can detect the presence of transit vehicles; traffic signal control module to receive and process the priority calls; and communications module to link vehicle detection with traffic signal control. Such an active TSP is often operated at the intersection level.

Upon receiving the priority requests, most conventional TSP strategies (i.e., green extension or red truncation) will activate the control if a bus is detected by the detectors located at its upstream intersection. As shown in Figure 6.3, if a bus is detected at the end of the pretimed green duration, a green extension will be granted to the current phase. If a bus is detected during the preset red phase, the TSP module will activate the red phase truncation to end the current red phase early for incoming buses to experience less stop delay. Note that the detection and extension intervals are determined with the distance between the detector location and the intersection's stop line.

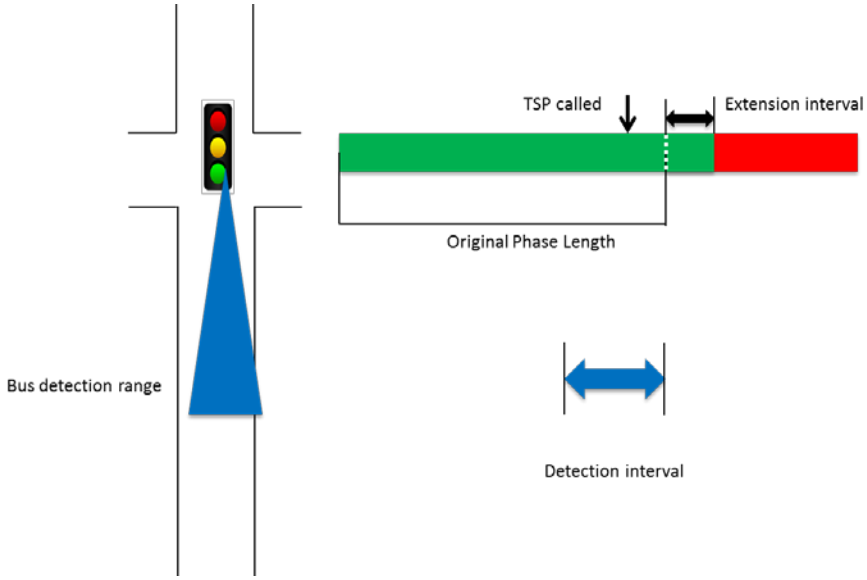

(a) Green extension

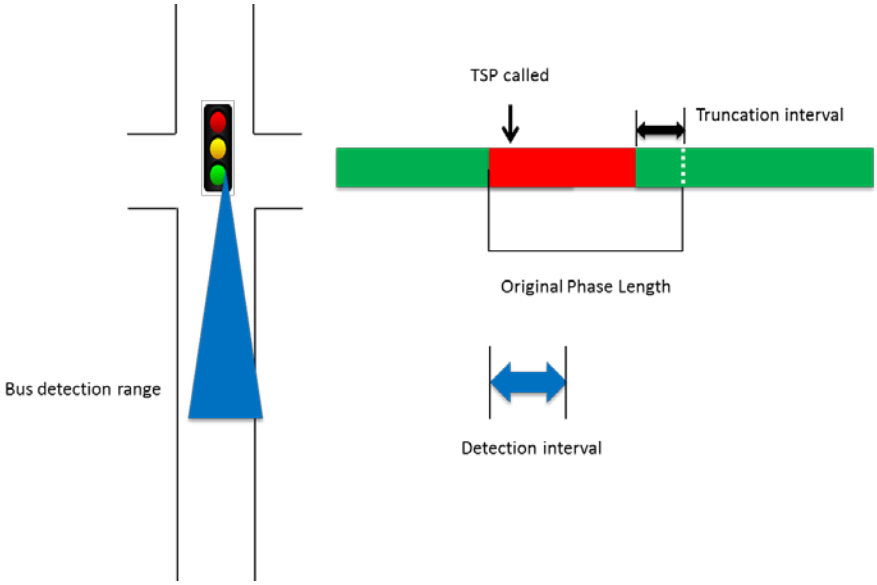

(b) Red truncation

Figure 6.3 Detection and extension intervals for a green extension and a red truncation

Most active TSP modules for green extensions and early green recalls employ a rule-based strategy. The TSP strategies presented hereafter, to facilitate the pre-timed bus progression operations and to minimize its impacts on non-priority movements, are operated with the following rules:

- Approaching buses are detected at a user-specified distance upstream of the signal stop line.
- If two or more TSP-control requests are concurrently received from conflicting approaches, no changes shall be made to the signal timings, due to the difficulty in prioritizing these priority requests.
- No activation shall be made to change the cycle length so as to preserve the coordination with its adjacent intersections.
- No phase skipping is allowed while transitioning to-and-from a priority phase.

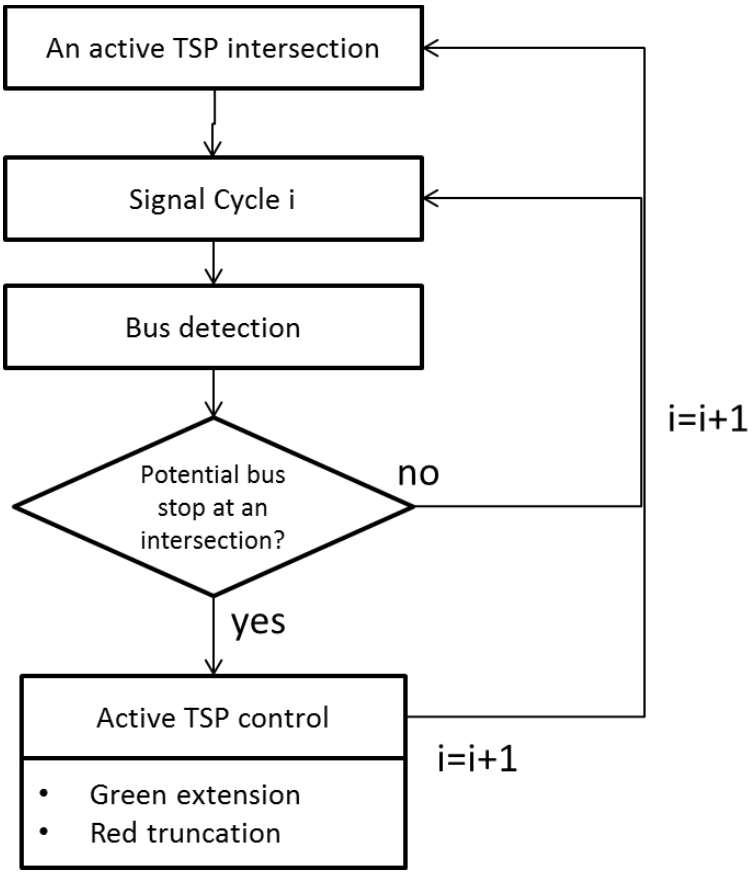

Figure 6.4 The logic of an active TSP activation process

6.3 Numerical Analysis

The experimental analysis is used to investigate the integrated real-time TSP control with respect to the number of buses to encounter a red phase, the total delay for buses, and the average delay for autos. The bus-based progression plan without real-time TSP control will also be adopted as the basis for comparing the effectiveness of the proposed integrated control strategy. All cases for performance comparison are set to operate with one of the following models:

- BUSBAND: The passive TSP generated with the bus-based progression model (Chapter 5) without active TSP;
- BUSBAND with TSP: The proposed real-time TSP on top of the BUSBAND signal plan; and

Since the key evaluation is the progression effectiveness resulted from the computed offsets, all signal control parameters such as cycle length, phase sequence, and signal timings are set to be unchanged for all experimental scenarios. Note that all computations for solving the mixed-integer-linear-programming formulations are solved with CPLEX ILOG on a desktop with 8GB RAM and Intel i7 processor.

6.3.1. Experimental Design

Based on the evaluation results given in the last chapter, one can observe an increase in bus travel times and the number of intersection stops along the arterial with the pre-timed BUSBAND due to the fluctuation of general traffic flows and bus dwell time uncertainty. Hence, to evaluate the effectiveness and necessity of the proposed real-time control module, this study has again used the selected field site, shown in Figure 5.11, for numerical evaluation. In order to test the performance under

highly uncertain travel time condition, this study has adopted a high traffic volume, such as Demand 1(Q1) in Figure 5.12 for experimental analysis. Also, bus dwell times at bus stops in each direction are assumed to follow normal distributions with mean of 25 seconds and standard deviation of 10 seconds, and the dwell times at each intersection are viewed to independent.

All experimental scenarios for analysis are set with the following common features:

- The bus detection range is up to 200ft upstream from the stop line.
- Detection interval for green extension is within the last 5 seconds of the green phase and the durations of green extension are set to 5 seconds.
- This study has adopted VISSIM as an unbiased traffic simulation tool, and the active TSP is implemented with COM interface and Visual Basic code.
- The simulation duration is set to one and a half hours, and the averages of five simulation runs are adopted for minimizing the random variation due to the embedded stochastic nature in traffic simulation.
- A total of 60 buses per hour in each direction were scheduled and to simulate the stochastic bus entry time to the arterial, a dummy bus stop is located at the upstream of the first intersection in each direction with a high dwell time deviation of 20 seconds.

6.3.2. Model Evaluation

To assess the bus operational performance and the overall network performance under the proposed integrated real-time TSP control, this study has investigated the following measurements of effectiveness: 1) the local intersection deployed with an

active TSP, 2) the downstream intersection of the active TSP intersection, and 3) the bus stop at the downstream link of the intersection with an active TSP. This is due to the fact that traffic conditions and bus performance over those links and stops upstream of the TSP intersection will not be impacted by the real-time operations taking place only at their downstream intersection.

1) At the local intersection with an active TSP

Figure 6.5 illustrates the performance of bus operations and average delays of general traffic at the intersection with an active TSP. The proposed integrated real-time TSP control, BUSBAND with TSP, has reduced the number of buses to encounter a red phase at the intersection with an active TSP (Figure 6.5 (a)). For example, under the scenario of deploying an active TSP at intersection 3, the number of buses encountering a red phase decreases from 53.44 to 37.58 by 29.68%, compared to pre-timed BUSBAND only. Under the scenario of having an active TSP at intersection 4, those numbers also decrease from 17.32 to 13.18 by 23.94%.

The total delay of buses per hour also decreases with the proposed integrated real-time TSP control (Figure 6.5 (b)). For instance, under the scenario of implementing an active TSP at intersection 3, the total bus delay at the intersection drops from 1,964.20 seconds to 1,520.128 seconds by 22.61%, compared to pre-timed BUSBAND only. By deploying an active TSP at intersection 2, the total bus delay at the intersection also decreases from 2,008.12 seconds to 1,510.36 seconds by 24.79%.

Despite the considerable improvement in bus performance (i.e., number of buses to encounter a red phase and delay), the impacts of the proposed control on the general traffic at the TSP intersection are insignificant. For instance, under the

scenario of having active TSP at intersection 3, the average delay of non-priority movements, which experience a shorten green time due to the TSP activation, increases from 42.92 seconds to 52.74 seconds by 22.88%, compared to pre-timed BUSBAND only. However, by considering general traffic from all approach at the active TSP intersection, the increase in the average delay of general traffic is less (i.e., from 27.57 seconds to 32.57 seconds by 18.12%). By employing the active TSP at intersection 4, the average delay of non-priority movements increases only by 6.86% (i.e., 23.92 seconds to 25.56 seconds) compared to pre-timed BUSBAND only. Following the same trend, the average delay for general traffic from all approaches to the TSP intersection increases only by 2.21 % (i.e., 6.91 seconds to 7.06 seconds). Note that under scenarios of an active TSP at intersection 3 or 5, the impacts of an active TSP on non-priority movements are higher than under other scenarios since the crossing streets of those two intersections are a major arterial. However, it seems that offering additional green to buses with TSP also benefits the general traffic in the same movements thus its negative impacts of an active TSP on the total delay of the entire intersection performance.

To sum up, the integrated real-time TSP control, BUSBAND with an active TSP, indeed performs well under the conditions of high traffic volume and high dwell time uncertainties, especially with respect to reducing the number of stops and delay of buses at the intersection. Although, the average delay for non-priority movement inevitably increases, but within the acceptable range, especially after taking into account the benefits to those vehicles which follow the bus flows to pass the intersection during the period of green extension

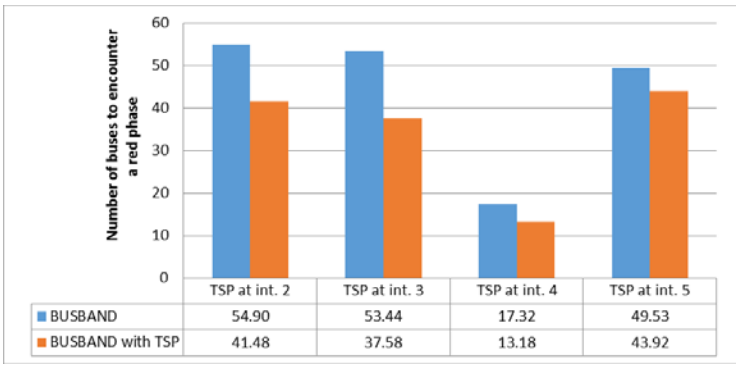

	TSP at int. 2	TSP at int. 3	TSP at int. 4	TSP at int. 5
BUSBAND	54.90	53.44	17.32	49.53
BUSBAND with TSP	41.48	37.58	13.18	43.92

(a) Number of buses encountering a red phase at the local intersection

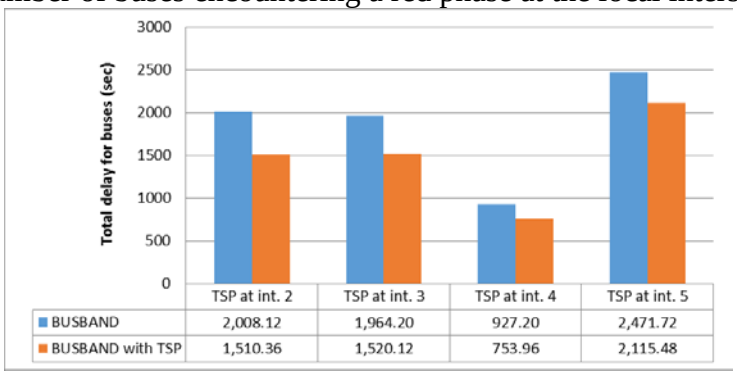

	TSP at int. 2	TSP at int. 3	TSP at int. 4	TSP at int. 5
BUSBAND	2,008.12	1,964.20	927.20	2,471.72
BUSBAND with TSP	1,510.36	1,520.12	753.96	2,115.48

(b) Total bus delay per hour at the local intersection

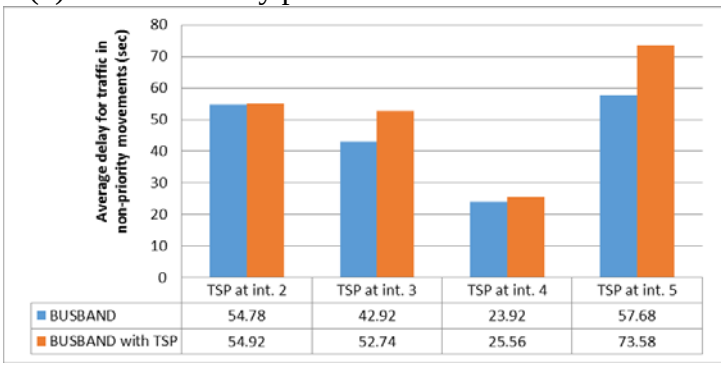

	TSP at int. 2	TSP at int. 3	TSP at int. 4	TSP at int. 5
BUSBAND	54.78	42.92	23.92	57.68
BUSBAND with TSP	54.92	52.74	25.56	73.58

(c) Average delay for traffic in non-priority movements at the local intersection

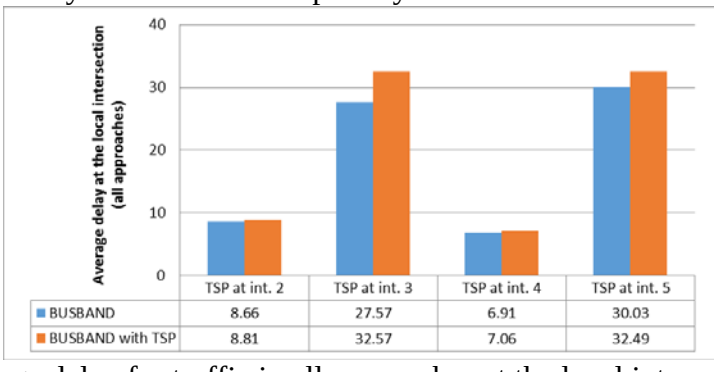

	TSP at int. 2	TSP at int. 3	TSP at int. 4	TSP at int. 5
BUSBAND	8.66	27.57	6.91	30.03
BUSBAND with TSP	8.81	32.57	7.06	32.49

(d) Average delay for traffic in all approaches at the local intersection

Figure 6.5 the performance of bus operations and average delays of general traffic at the intersection with an active TSP

2) At the downstream intersection of the one deployed with an active TSP

Figure 6.6 illustrates the performance of bus operations at the downstream intersection of the one deployed with an active TSP. Under the proposed integrated real-time TSP control, BUSBAND with TSP, the benefits of an active TSP (i.e., reductions in the number of buses to encounter a red phase and bus delay) can also be sustained at its downstream intersection. For example, under a scenario of an active TSP at intersection 3 the number of buses to encounter a red phase reduces from 47.70 to 44.14 by 7.46% at its downstream intersection, compared to pre-timed BUSBAND only. The bus delay also drops from 1,875.14 seconds to 1,682.06 seconds by 10.30%.

However, deploying an active TSP at intersection 2 does not seem to benefit its downstream intersections. The number of buses stopping at the intersection increases from 25.74 to 29.52 by 14.69% and the total bus delay also increases from 1,002.84 seconds to 1,100.44 seconds by 9.73%. In this case, the benefits from an active TSP diminish at the downstream intersection and more buses experiencing more stops and delays.

To sum up, the benefits from the integrated real-time TSP control, BUSBAND with an active TSP, are likely to extend over to its downstream intersection but the resulting benefits vary with the location of the TSP intersection within the entire arterial.

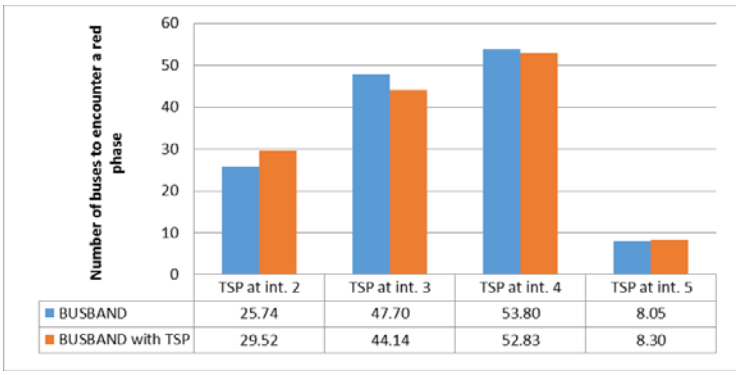

(a) Number of buses encountering a red phase

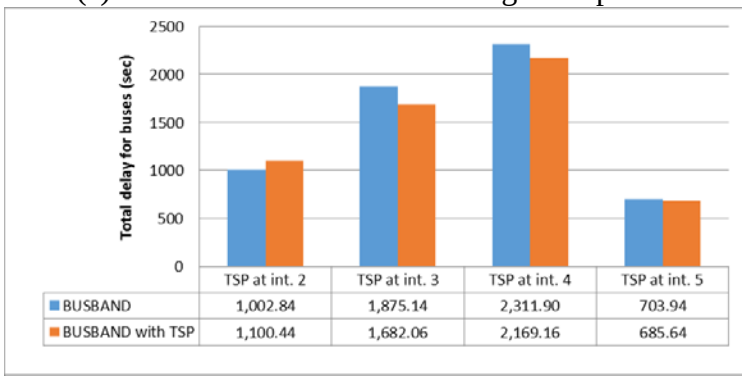

(b) Total delay for buses

Figure 6.6 the performance of bus operations at the downstream intersection of one with an active TSP

3) At the downstream bus stop of the intersection deployed an active TSP

Figure 6.7 shows that the proposed integrated real-time TSP control, BUSBAND with TSP, can reduce the standard deviation of headways at the downstream bus stop of the intersection deployed with an active TSP. For instance, under a scenario of an active TSP at intersection 3 the standard deviation of headways reduces from 43.67 seconds to 41.92 seconds by 4.002% at the downstream bus stop, compared to pre-timed BUSBAND only. Under the scenario of having active TSP at intersection 5 it also reduces from 43.68 seconds to 40.74 seconds by 6.72% at the downstream bus stop. On the other hand, when the active TSP is deployed at intersection 4, the standard deviation of headways increases from 35.48 seconds to 37.47 seconds by

5.59 %. This indicates that when an active TSP is deployed at a proper location, it can produce more stable bus schedule at the downstream bus stop.

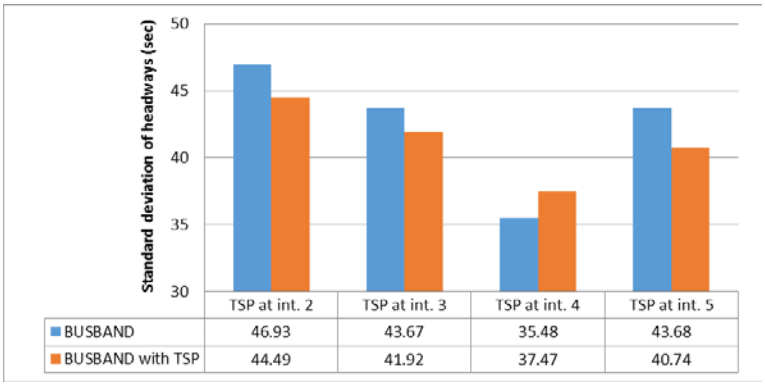

Figure 6.7 the performance of bus operations at the downstream intersection of one with an active TSP

To sum up, integrating an active TSP with the pre-timed BUSBAND can indeed increase the performance of bus operations with minimal impacts on non-priority movements at the TSP intersection in terms of fewer numbers of buses to encounter a red phase, and less bus delay. Such a system can also result in less number of buses to encounter a red phase at the downstream intersection of the TSP deployed intersection, and a smaller standard deviation of headways at the downstream bus stop.

Since the benefits of such an active TSP when integrating with pretimed busband model may vary with the location of the selected intersection, it seems essential to have an algorithm to select an optimal intersection for deploying active TSP so that the overall benefits can be maximized.

6.4 Selection of Critical Intersections for real-time TSP

6.4.1. Critical issues associated with selecting an active TSP intersection

In design of bus progression bands along an arterial, one may view an intersection as a bottleneck, if the boundaries of bus bands are at the start or end of its green phase (i.e., interference constraints in BUSBNAD model (Eqs. 5.3 (a) and 5.3 (b)) are bounded). Taking Figure 6.8 as an example, the bus bands for inbound and outbound flows are constrained at intersection *i* and i+2, respectively, as follows:

- *At intersection i:*

  $w_i - 0.5b_i = 0$ *(Outbound)* **and** $0.5\bar{b}_i - \bar{w}_i = 0$ *(Inbound)*

- *At Intersection i*+2:

  $w_{i+2} + 0.5b_{i+2} = g_{i+2}$ *(Outbound)* **and** $0.5\bar{b}_{i+2} + \bar{w}_{i+2} = \bar{g}_{i+2}$ *(Inbound)*

With a properly deployed active TSP (i.e., green extension and red truncation), one could expand these bus bands by allocating additional green time to the target synchronized phases. However, the impacts of each TSP strategies (i.e., green extension and red truncation) on the resulting bus bands may vary with the progression direction and most importantly where the bands are allocated within the green phase. For example, at intersection *i*, a green extension would widen the inbound bus band but not for the outbound; a red truncation can expand the outbound bus band but not for the inbound. On contrast, a green extension at intersection *i*+2 can widen the outbound busband but not for inbound flows; the red truncation may be expected to expand the inbound busband, but not for the outbound.

Notably, both the distribution of different busband widths on those arterial links and where they are located within their green times play key roles in identifying the critical intersections for deploying an active TSP.

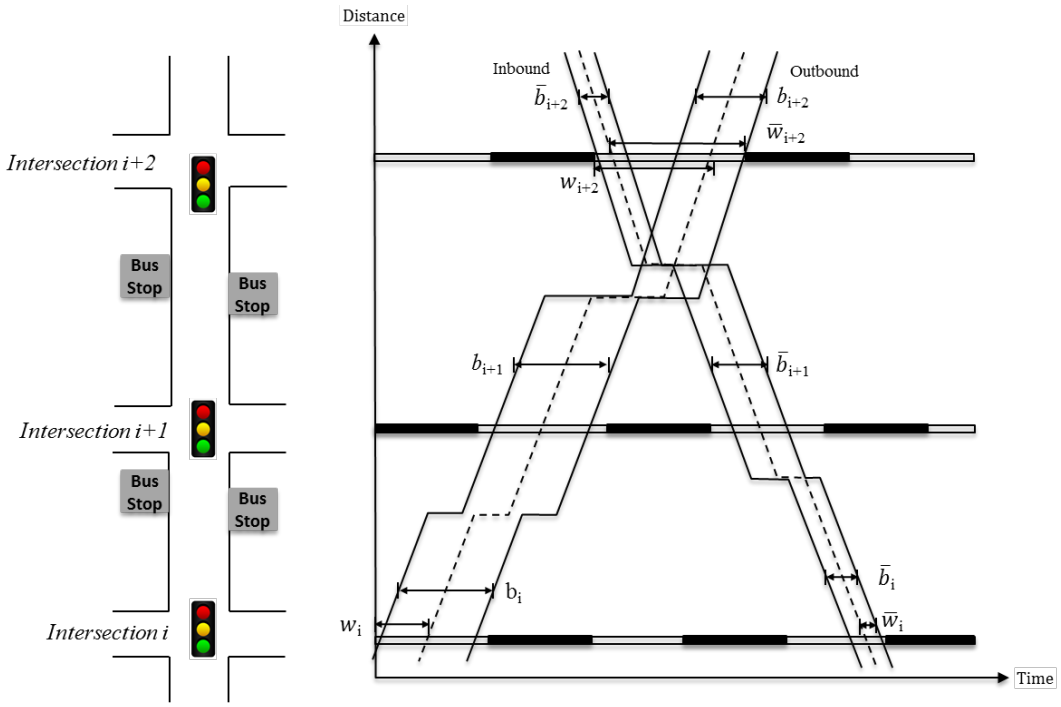

Figure 6.8 Critical Intersections to the bus bands

Also note that one shall evaluate the effectiveness of an active TSP (i.e., green extension and red truncation) at a candidate intersection based on the stop delays of those TSP granted buses at its downstream intersection, and the number of buses benefiting from such real-time activations.

Taking a green extension in Figure 6.9 as an example, if those buses being granted with TSP are most likely to stop at the downstream intersections (Figure 6.9 (a)), then the execution of the active TSP may not show its effectiveness. Because even though the bus delays have been reduced at the target TSP intersection, causing the buses to encounter the red phase at its downstream intersection may offset the

benefits from those reduced delays. Thus, to have an effective active TSP for bus progression along the arterial, the green extension granted by the TSP intersection shall be able to facilitate those buses to reach the downstream intersection during its green phase (see Figure 6.9(b)).

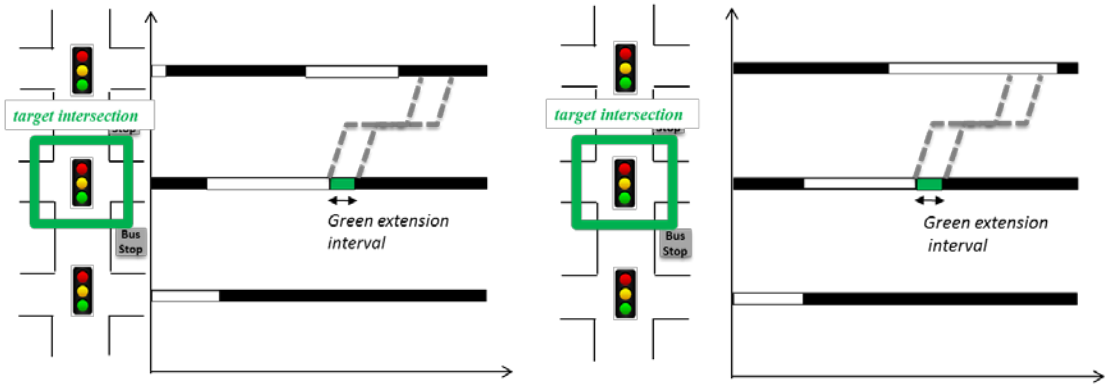

(a) stop at the downstream intersection

(b) pass through the downstream intersection

Figure 6.9 Effects of TSP related to the downstream intersection

Conceivably, if the busbands are generated from the coordination between the TSP‘s green extension and the red-phase at its upstream intersection, such TSP activation may not be effective because it can only benefit very few buses (See Figure 6.10 (a)). On contrast, more buses are likely to benefit from the TSP activation if the interrelations of the TSP activation and its upstream green phase are similar to that illustrated in Figure 6.10(b).

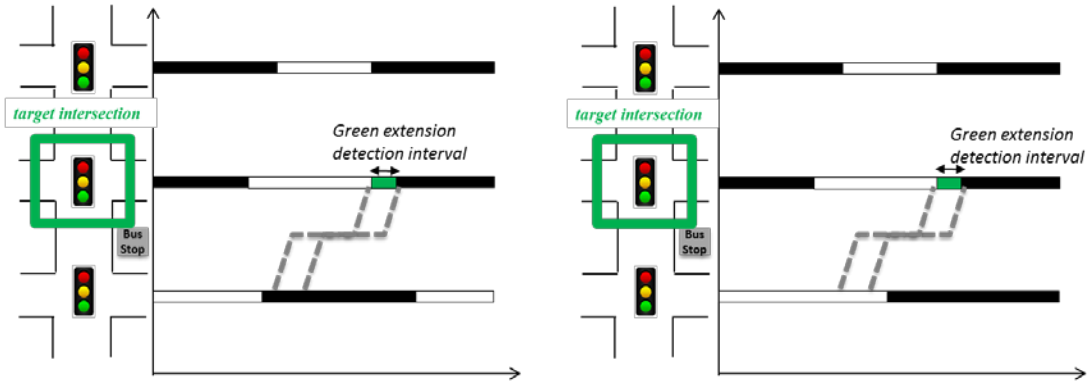

(a) (b)

Figure 6.10 Effects of TSP related to the upstream intersection

In brief, a model to select an active TSP intersection, grounded on the logic of BUSBAND, needs to explicitly address the following critical issues: 1) preventing the bus progression bands computed offline from being constrained at some intersections; 2) activating a proper TSP strategy at the optimally selected intersection so as to maximize the sum of all weighted bus bandwidths, and 3) minimizing the undesirable impacts on non-priority movements.

6.4.2. Model Formulation

This section presents a set of formulations for selecting an active TSP intersection that can best facilitate the bus progression operations. Table 6.1 shows the notations of those key variables in such a model.

Table 6.1 Key notations

Notation	Description
Parameters	
N	Total number of intersections
B	Total number of active TSP intersections
C	Cycle length (seconds)
$g_i(\bar{g}_i)$	The outbound(inbound) green interval at intersection i (seconds)
$\phi_{i,k}(\bar{\phi}_{i,k})$	Weighting factor of extra bus bands due to TSP (green extension (k=g) and red truncation (k=r)) at intersection i
$t_{b,i}$ ($\bar{t}_{b,i}$)	Average outbound (inbound) travel time for buses from intersection i (i+1) to intersection i+1 (i), which is sum of bus running time and bus dwell time (seconds)
$\tilde{\theta}_i$	Relative offset at intersection i (seconds)
u	Green extension interval and red truncation interval (seconds)
α	Weighting factor for upstream additional band
β	Volume-to-capacity ratio threshold for the non-priority movement
v_i/c	Volume-to-capacity ratio of the non-priority movement at intersection i
M	Large number
Variables	
b_i^k ($\bar{b}_i^k$)	Extra band due to TSP (green extension (k=g) and red truncation (k=r)) in outbound (inbound) at intersection i for buses (seconds)
$b_{j,i}^k$ ($\bar{b}_{j,i}^k$)	Upstream(j=1) and downstream(j=2) bandwidth of extra band due to TSP (green extension (k=g) and red truncation (k=r)) in outbound (inbound) at intersection i for buses (seconds)
e_i	Binary variable indicates if an intersection i is selected to implement active TSP, 1; otherwise 0
$h_{j,i}^k$ ($\bar{h}_{j,i}^k$)	Binary variable indicating if the extra bus band due to TSP (green extension (k=g) and red truncation (k=r)) to the upstream(j=1) and downstream(j=2) intersection i-1 (i+1) exists, 1; otherwise 0.

Given the signal plan and phase sequence at each intersection, the core notion of such a model is to maximize the effectiveness of the selected TSP intersection, represented

with its resulting bandwidths. The proposed model to do so can be summarized as follows:

$$Max \sum \phi_{i,k} b_i^k + \sum \bar{\phi}_{i,k} \bar{b}_i^k \tag{6.1}$$

s.t.

$$\sum e_i \leq B \tag{6.2}$$

$$e_i \leq 1 + \beta - \frac{v_i}{c} \tag{6.3}$$

$$b_{1,i}^g \leq (\tilde{\theta}_{i-1} + g_i + e_i\mu) - (g_{i-1} + e_{i-1}\mu + t_{i-1}) + h_{1,i}^g M \tag{6.4}$$

$$b_{2,i}^g \leq (\tilde{\theta}_i + g_{i+1} + e_{i+1}\mu) - (g_i + t_i) + h_{2,i}^g M \tag{6.5}$$

$$\bar{b}_{1,i}^g \leq (-\tilde{\theta}_i + g_i) - (g_{i+1} + e_{i+1}\mu + \bar{t}_i) + \bar{h}_{1,i}^g M \tag{6.6}$$

$$\bar{b}_{2,i}^g \leq (-\tilde{\theta}_{i-1} + g_{i-1} + e_{i-1}\mu) - (g_i + \bar{t}_{i-1}) + \bar{h}_{2,i}^g M \tag{6.7}$$

$$b_{1,i}^r \leq (\tilde{\theta}_{i-1}) - (-e_{i-1}\mu + t_{i-1}) + h_{1,i}^r M \tag{6.8}$$

$$b_{2,i}^r \leq (\tilde{\theta}_i - e_{i+1}\mu) - (-e_i\mu + t_i) + h_{2,i}^r M \tag{6.9}$$

$$\bar{b}_{1,i}^r \leq (-e_i\mu) - (\tilde{\theta}_i - e_{i+1}\mu + \bar{t}_i) + \bar{h}_{1,i}^r M \tag{6.10}$$

$$\bar{b}_{2,i}^r \leq (-e_{i-1}\mu) - (\tilde{\theta}_{i-1} - e_i\mu + \bar{t}_{i-1}) + \bar{h}_{2,i}^r M \tag{6.11}$$

$$b_{j,i}^k \leq (1 - h_{j,i}^k) C \tag{6.12}$$

$$\bar{b}_{j,i}^k \leq (1 - \bar{h}_{j,i}^k) C \tag{6.13}$$

$$b_i^k \leq (1 - \alpha) b_{1,i}^k + \alpha b_{2,i}^k \tag{6.14}$$

$$\bar{b}_i^k \leq (1 - \alpha) b_{1,i}^k + \alpha b_{2,i}^k \tag{6.15}$$

$$b_{j,i}^k \leq e_i C \tag{6.16}$$

$$\bar{b}_{j,i}^k \leq e_i C \tag{6.17}$$

$b_{j,i}^k, \bar{b}_{j,i}^k, b_i^k, \bar{b}_i^k \geq 0$ *and integer for j=1 and 2, k=g and r, i=1,…,N*

e_i is binary variable for i=1,…,N

In the above optimization model, the control objective (Eq. (6.1)) is to maximize the weighted extra bandwidths of bus bands due to an active TSP. By considering the bandwidth of the original bus bands and where they are located, the weighting factor, $\phi_{i,k}(\bar{\phi}_{i,k})$, can be specified as follows:

$$\phi_{i,r} = 1/(g_i - (w_i - 0.5b_i) + 1) \tag{6.18}$$

$$\phi_{i,g} = 1/(g_i - (w_i + 0.5b_i) + 1) \tag{6.19}$$

$$\bar{\phi}_{i,r} = 1/(g_i - (\bar{w}_i + 0.5\bar{b}_i) + 1) \tag{6.20}$$

$$\bar{\phi}_{i,k} = 1/(g_i - (\bar{w}_i - 0.5\bar{b}_i) + 1) \tag{6.21}$$

Note that Eq. (6.2) is to ensure that the total number of selected active intersections does not exceed the number of candidate intersections. Eq. (6.3) constrains the volume-to-capacity ratio of the non-priority movement at intersection i to be less than the user-defined level of saturation (e.g., 0.9). Eqs. (6.4)-(6.7) and (6.8)-(6.11) are for calculating the upstream and downstream extra bandwidths under the green extension and red truncation at intersection *I*, given the signal plans and bus travel times. Eqs. (6.12) and (6.13) indicate that there are no upstream or downstream bands under the active TSP at intersection *i* if $h_{j,i}^k(\bar{h}_{j,i}^k)$ is 1. Eqs. (6.14) and (6.15) show that the extra bands by an active TSP at intersection i is the weighted sum of its upstream and downstream extra bands. Eqs. (6.16) and (6.17) are to ensure that the inbound and outbound bus bands exist only if there is an active TSP at intersection i (i.e., $e_i = 1$).

6.5 Closure

The pre-timed BUSBAND may not be effective under the high uncertainty of traffic volume and dwell times. Under such circumstances, a real-time TSP, grounded with pre-timed BUSBAND, can be a viable operation to contend with the stochastic nature of the dwell times, bus travel time, and general traffic demands.

This chapter has presented an integration of an active TSP control with a pre-timed BUSBAND for real-time operations. The results of extensive numerical investigations have confirmed that the proposed integrated system can indeed improve the performance of bus operations at the local intersection as well as at the downstream intersection and/or bus stop. It is also clear that BUSBAND with TSP can outperform BUSBAND-only with respect to the number of buses to stop and bus delays at the local intersection, yielding acceptable impacts on non-priority movements at the local intersection.

This chapter also has presented a model to select an intersection to deploy an active TSP to maximize the benefits of an active TSP. The developed model for selecting a critical intersection considers the position and width of bus progression bands computed offline in a green interval, impacts on non-priority movements, and the extended bus bandwidths at neighboring intersections.

Chapter 7: Conclusions

7.1 Research Summary and Contributions

To enhance the performance of bus operations along an arterial with heavy bus flows, this dissertation has proposed an integrated system for transit signal priority control that consists of three main modules of pseudo-detection system, pre-timed signal optimization, and real-time transit signal priority control. The pseudo-detection module is designed to decompose the network into sub-links and view each as one pseudo detector, in which a bus in a sub-link is to function as a moving pseudo sensor so as to provide time-varying speed data. Taking advantage of rich traffic information for both bus and general traffic from the pseudo-detection system, the proposed integrated system employs a bus-based progression model for design of pre-timed signal plans along an arterial. The final stage of the integrated system's control actions is to execute its embedded real-time control function (i.e., green extension and red truncation) at a critical intersection to provide signal priority control to bus flows when they are detected to encounter a red phase.

In summary, this dissertation has made the following contributions to enhancing the quality of bus operations and in turn promoting transit ridership in urban arterial:

- ***Development of an effective operational structure for integrated traffic control for arterials plagued by heavy bus flows***: With an embedded traffic monitoring function and a two-stage signal control function, the proposed integrated system is designed to estimate traffic condition for both bus and general traffic flows along the arterial, and produce pre-timed signal plans using bus-based progression to facilitate heavy bus flows. The system can further contend with traffic fluctuations by dynamically adjusting the signal plan (i.e., green extension and red truncation) at a critical intersection with its real-time control module.
- ***Development of a bus-GPS-based pseudo detection system for estimating traffic conditions***: The core logic of a pseudo detection system is to convert the real-time bus GPS data into geographic-based sensors that can estimate both bus and general traffic conditions in urban networks beyond its original function of monitoring each buses speed and location. Taking advantage of heavy bus flows, the proposed pseudo detection module provides more extensive information (such as link and movement-specific speeds) than conventional point-measurement detectors. The system potentially provides the spatial and temporal variation of general traffic conditions by converting the time-varying bus speed in each sub link, viewed as a pseudo sensor. The results of a case study with field data have demonstrated that the proposed pseudo detection system can indeed provide time-varying and movement-specific speeds.

- ***Development of bus-based progression models along the arterial, accounting for bus operational characteristics and its relations with general traffic***: The base proposed model, grounded on MAXBAND, accounts for bus operational characteristics, such as dwell times at bus stops, bus stop storage capacity, and traffic queues at intersections and their relationship with bus stop location, to yield bus progression band in both directions under a predetermined phasing plan. The enhanced model (BUSBAND) further takes into account the uncertainty of dwell times at bus stops in maximizing the progression band with offsets for the entire arterial. The results of extensive numerical experiments have demonstrated that the proposed models can clearly outperform the conventional design methods (e.g., MULTIBAND) under different traffic demands and different bus dwell time variances.
- ***Integration of an active Transit Signal Priority (TSP) with a pre-timed BUSBAND to enhance the performance of bus operations throughout the arterial:*** The proposed real-time system includes TSP selection module and an active TSP activation module. The first is to select an optimal intersection to deploy an active TSP so as to release the impacts of bottleneck intersections on the bus progression band and best benefits from the pre-timed BUSBAND in activating an active TSP. By offering a flexible function for signal controls such as a green extension or a red truncation at such critical intersections, it is achieved to expand bus bands and facilitate the bus progression under traffic fluctuations. The results of extensive numerical experiments have demonstrated that an active TSP module can supplement the pre-timed bus-

based signal plans in terms of less intersection stops and less delays for bus flows with minimized negative impacts on non-priority movements.

7.2 Future Research

Despite the effectiveness of the integrated transit signal priority control system developed in this dissertation, some critical issues remain to be solved. Future research directions along this study are listed below:

Development of an optimal traffic control model to concurrently account for general traffic and bus flows progression along an arterial

The system proposed in this dissertation has focused on the optimal signal control with a priority to heavy bus flows along an arterial. As a pre-timed control, signals are coordinated to facilitate the bus flows. In real-time operations, when a bus is predicted to stop at a downstream intersection, a green extension or red truncation will be provided at critical intersections. Such control logic has demonstrated its effectiveness in enhancing the performance of bus operations in terms of less intersection stops and delays. However, depending on the general traffic demands and the uncertainty of bus travel times along the arterial, traffic congestion at critical intersections and degradation in bus-based progression may be inevitable. As such, the objective of signal control shall consider the network's overall performance for both the general traffic and bus flows.

Hence, it is essential to develop the following models for potential real-world applications: 1) total travel delay model to compute those traveling delays for both general traffic and buses; and 2) optimization model that determines the control

objective among auto-based, bus-based, and concurrent progression models under a certain condition so as to minimize the total travel delay over the entire network.

Integration of both traffic signal control and transit fleet operations for transit operations and traffic management along an arterial.

This research has mainly focused on traffic signal controls at intersections along the arterial experiencing heavy bus flows to enhance the bus operations. However, unreliable bus operations on the arterial may be caused by a variety of factors. For instance, aside from the unpredicted delays at an intersection, a change in passenger demands at bus stops may also result in unstable bus services along the arterial. Moreover, when the distance between a bus stop and stop bar of its downstream intersection is relatively short, intersection vehicle queues under traffic fluctuations may cause significant reduction of bus progression. In addition, under congested and fluctuating traffic conditions, an active TSP may cause non-negligible negative impacts on non-priority movements.

Hence, to effectively deal with other issues contributing to unreliable bus operations in urban networks, one shall further extend this study to transit fleet management; and such a system shall be capable of effectively coordinating bus holding, speed control, and queue-jump control strategies.

Appendices

Step 1: Discretizing the arriving band

First, the arriving band at the upstream intersection is divided into several small intervals. For each small interval in the band, the effective bandwidth is calculated based on its associated interval in the distribution. To define the boundaries of those intervals, one can introduce the following linear constraints for the outbound bands:

$$u_{ik} = \frac{0.5b_{i+1} - \left(-0.5b_i + k \times \alpha\right)}{\sigma_i} - MI_{ik} \tag{A1}$$

$$u'_{ik} = \frac{-0.5b_{i+1} - \left(-0.5b_i + k \times \alpha\right)}{\sigma_i} - MI_{ik} \tag{A2}$$

where $u_{ik}(u'_{ik})$ represents the variate of the standard normal distribution in Eq. (5.37) for interval k, whose length is α of the cycle length; I_{ik} is a binary variable, indicating whether or not interval k is within the green band. These two equations show the expression of those two terms at the right-hand side of Eq. (5.37) for buses departing from the upstream band at different times.

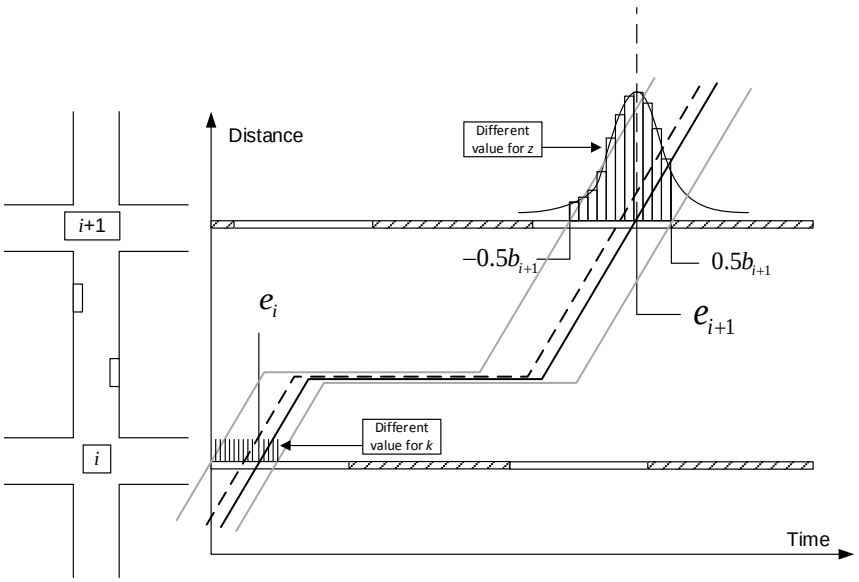

Figure A-1 Linearization method of the enhanced model

By applying (A1)-(A2), buses passing the upstream intersection during interval k are considered to pass at the beginning of that period, as shown in Figure A-1. Since only the buses from the upstream band are considered, (A1)-(A2) should be invalid when the considered time point is out of the upstream band. This is accomplished by introducing the following binary variables, I_{ik}, which indicates whether the corresponding value of k is within the reasonable range.

$$I_{ik} < \frac{k \times \alpha - b_i}{M} + 1 \tag{A 3}$$

$$I_{ik} \geq \frac{k \times \alpha - b_i}{M} \tag{A 4}$$

Through (A 3) and (A 4), when the total length of k intervals is greater than the bandwidth, u_{ik} and u'_{ik} are set to be small enough not to contribute to the calculation of effective bandwidth and then, the lower and upper limit of integration in Eq. (5.37) can be determined.

Step 2: Estimating the probability of vehicles staying in the departing band

Given the results of step 1, the value of $u_{ik}(u'_{ik})$ is used to determine the probability with Eq. (5.36). To estimate the probability that a vehicle from an interval remains in the band when reaching its downstream intersection, one can formulate this process as shown below:

$$y_{ik}^{z} < \frac{u_{ik} - \left(-\beta + z \times \gamma\right)}{M} + 1 \tag{A 5}$$

$$y_{ik}^{z} \geq \frac{u_{ik} - \left(-\beta + z \times \gamma\right)}{M} \tag{A 6}$$

$$y'^{z}_{ik} < \frac{u'_{ik} - \left(-\beta + z \times \gamma\right)}{M} + 1 \tag{A 7}$$

$$y'^{z}_{ik} \geq \frac{u'_{ik} - \left(-\beta + z \times \gamma\right)}{M} \tag{A 8}$$

$$H_{ik} = \sum_{z=1}^{Z} n_z \left(y_{ik}^{z} - y'^{z}_{ik}\right) \tag{A 9}$$

where,

- n_z is the cumulative density of the z-th interval of the standard normal distribution, $n_z = \Phi(-\beta + \gamma \times (z+1)) - \Phi(-\beta + \gamma \times z)$.
- $y^{z}{}_{ik}(y'^{z}{}_{ik})$ is a binary variable, indicating whether or not the resulting variate is greater than a certain value, which will determine the interval where $u_{ik}(u'_{ik})$ exists.
- γ is the length of intervals, shown as the width of rectangular at the top right part of Fig.B1.

- H_{ik} is the approximate probability that a bus from interval k will stay in the band when passing the downstream intersection, which is expressed as Eq. (35).

By defining the value for series of binary variables, $y^z_{ik}(y'^z_{ik})$, Eq. (5.37) and (A1)-(A2) will determine which rectangular under the cumulative density function should be included in calculation of the probability. Eq. (A9) sums up the corresponding area of the rectangles to obtain the total probability (approximation of the exact probability) which is expressed as the rectangular area in Figure A-1.

Step 3: finding the effective bandwidth

By multiplying the length of each small interval and its corresponding probability, one can obtain the equivalent effective portion of the interval, and then use Eq. (A10) to sum up the resulting effective portion to obtain the total effective bandwidth as follows:

$$b_i^e = \sum_{k=1}^{K} \alpha H_{ik} \tag{A10}$$

Given the linearized effective bandwidths, the size of k, which should be sufficiently large to keep the approximation reasonable, is set to equal 20. The range of z, denoting the number of intervals within the arriving band, and the value of β and γ, shall be so determined to ensure that $\Phi(-\beta+\gamma)$ is sufficiently small and $\Phi(-\beta+Z\times\gamma)$ is close to 1. For example, this study assumes $\beta=-2.8$, $\gamma=0.4$, and $Z=13$, then the segment (-2.4, 2.4) on x axis is divided into 12 intervals, each having a value for n_z, the cumulative density. The constraints for inbound directions

are specified in the similar structure. The effective bandwidths for inbound direction can be calculated with the same logic.

Bibliography

Alsabaan, M., Naik, K., and Khalifa, T. (2013). Optimization of Fuel Cost and Emissions Using V2V Communications. In IEEE Transactions on Intelligent Transportation Systems, Vol, 14(3), 1449-1461.

Altun, S.Z., and Furth, P.G. (2009). Scheduling Buses to Take Advantage of Transit Signal Priority. Transportation Research Record: Journal of the Transportation Research Board, No. 2111, 50-59.

Asadi, B. and Vahidi, A. (2011). Predictive Cruise Control: Utilizing Upcoming Traffic Signal Information for Improving Fuel Economy and Reducing Trip Time, IEEE Transactions on Control Systems Technology, Vol. 19 (3).

Barnett, A. (1974). On controlling randomness in transit operations. Transportation Science, 8(2), 101–116.

Bertini, R. L., and Tantiyanugulchai , S. (2004). Transit Buses as Traffic Probes: Use of Geolocation Data for Empirical Evaluation. In Transportation Research Record: Journal of the Transportation Research Board, No. 1870, Transportation Research Board of the National Academies, Washington, D.C., 2004, 35–45.

Bodenheimer, R., Brauer, A., Eckhoff, D. and German, R. (2014), Enabling GLOSA for Adaptive Traffic Lights. In 6th IEEE Vehicular Networking Conference (VNC 2014). Paderborn, Germany: IEEE. 103–110.

Bodenheimer, R., Eckhoff. D. and German, R. (2015). GLOSA for Adaptive Traffic Lights: Methods and Evaluation. 2015 7th International Workshop on Reliable Networks Design and Modeling (RNDM).

Cathey, F. W., and Dailey, D. J. (2002). Transit Vehicles as Traffic Probe Sensors. In Transportation Research Record: Journal of the Transportation Research Board, No. 1804, Transportation Research Board of the National Academies, Washington, D.C., 23–30.

Cathey, F. W., and Dailey, D. J. (2003). Estimating Corridor Travel Time by Using Transit Vehicles as Probes. In Transportation Research Record: Journal of the Transportation Research Board, No. 1855, Transportation Research Board of the National Academies, Washington, D.C., 60–65.

Chakroborty, P., and Kikuchi, S. (2004). Using Bus Travel Time Data to Estimate Travel Times on Urban Corridors. In Transportation Research Record: Journal of the Transportation Research Board, No. 1870, Transportation Research Board of the National Academies, Washington, D.C., 2004, 18–25.

Chang, E. C., Cohen, S. L., Liu, C., Chaudhary, N. A., and Messer, C. (1988). MAXBAND-86: Program for optimizing left-turn phase sequence in multiarterial closed networks , Transportation Research Record, 1181, 61-67.

Chaudhary, N.A., V.G. Kovvali, C.-L. Chu, J. Kim, and Alam, S.M. (2002). Software for Timing Signalized Arterials. Report FHWA/TX-03/4020-1, Texas Transportation Institute, the Texas A&M University System, College Station, Texas.

Chen, C., Kwon,J., Rice, J., Skabardonis, A. and Varaiya, P. (2003). Detecting Errors and Imputing Missing Data For Single Loop Surveillance Systems. Transportation Research Record: Journal of the Transportation Research Board, No. 3507, 160-167

Chiou, J., Zhang, Y., Chen, W and Chang, C. (2014). A functional data approach to missing value imputation and outlier detection for traffic flow data. Transportmetrica B: Transport Dynamics Vol 05, 2014, 2(2)

Christofa, E., and Skabardonis, A. (2011). Traffic Signal Optimization with Application of Transit Signal Priority to an Isolated Intersection. In Transportation Research Record: Journal of the Transportation Research Board, No. 2259, Transportation Research Board of the National Academies, Washington, D.C., pp. 192–201.

Christofa, E., K. Ampountolas, and A. Skabardonis (2016). Arterial traffic signal optimization: A person-based approach. Transportation Research Part C: Emerging Technologies, 66, 27-47.

Coifman, B., and Kim, S. (2006). Using Transit Vehicles to Measure Freeway Traffic Conditions. Proc., 9th International Conference on Applications of Advanced Technology in Transportation, Chicago, Ill., Aug. 13–16, ASCE, Reston, Va.

Delgado, F., Muñoz, J. C., Giesen, R. and Cipriano, A. (2009). Real-Time Control of Buses in a Transit Corridor Based on Vehicle Holding and Boarding Limits. In Transportation Research Record: Journal of the Transportation Research Board, No. 2090, TRB, Washington, D.C., pp. 59–67.

Delgado, F., Muñoz, J. C. and Giesen, R.(2012). How Much Can Holding and Limiting Boarding Improve Transit Performance? Transportation Research Part B, Vol. 46, 1202–1217.

Delgado, F., Muñoz, J. C., Giesen, R. and Wilson, N.H.M. (2015). Integrated Real-Time Transit Signal Priority Control for High-Frequency Segregated Transit

Services, Transportation Research Record: Journal of the Transportation Research Board, No. 2533, Transportation Research Board of the National Academies, Washington, D.C., 28–38.

Dion, F. and Rakha, H. (2005). Integration Transit Signal Priority with Adaptive Traffic Signal Control Systems, presented at 84th Annual Meeting of the Transportation Research Board, Washington, D.C.

Eberlein, X.J., Wilson, N.H.M., and Bernstein, D. (2001). The holding problem with real-time information available. Transportation Science 35 (1), 1–18.

Fu, L. and Yang, X. (2002). Design and implementation of bus-holding control strategies with real-time information. Transportation Research Record 1791, 6–12.

Fuchs, H., Kedem, Z.M., Naylor, B.F. (1980). On visible surface generation by a priori tree structures. In Proceeding SIGGRAPH '80 Proceedings of the 7th annual conference on Computer graphics and interactive techniques, 124–133.

Furth, P. G. and Muller, T. H. J. (2000). Conditional Bus Priority at Signalized Intersections Better Service with Less Traffic Disruption. Transportation Research Record: Journal of the Transportation Research Board, No. 1731, Transportation Research Board of the National Academies, Washington, D.C., 23-30.

Furth, P.G., Cesme, B., and Rima, T. (2010). Signal priority near major bus terminal. In Transportation Research Record: Journal of the Transportation Research Board, No. 2192, Transportation Research Board of the National Academies, Washington, DC, 89–96.

Gartner, N.H., Assman, S.F., Lasaga, F., and Hou D.L. (1991). A multi-band approach to arterial traffic signal optimization. Transportation Research Part B, 25(1), 55-74.

Gartner, N. H., and Stamatiadis, C. (2002). Arterial-based control of traffic flow in urban grid networks. Mathematical and computer modelling, 35(5), 657-671.

Gartner, N. H., and Stamatiadis, C. (2004). Progression optimization featuring arterial-and route-based priority signal networks. Journal of Intelligent Transportation Systems, 8(2), 77-86.

Greenfeld, J. S. (2002). Matching GPS observations to locations on a digital map. In Proceedings of the 81th annual meeting of the transportation research board. Washington D.C.

Hashemi, M. and Karimi, H. A. (2014). A critical review of real-time map-matching algorithms: Current issues and future directions. Computers, Environment and Urban Systems 48, 153–165

He, Q., Head, K.L. and Ding, J.. (2011). Heuristic Algorithm for Priority Traffic Signal Control. Transportation Research Record: Journal of the Transportation Research Board, No. 2259, pp.1-7.

Hickman, M. (2001). An analytic stochastic model for the transit vehicle holding problem. Transportation Science 35 (3), 215–237.

Hounsell, N.B., F.N. McLeod, K. Gardner, J.R. Head, and D. Cook. (2000). Headway-based bus priority in London using AVL: first results. Tenth International Conference of Road Transport Information and Control, 218-222.

Hounsell, N.B. and Shrestha, B.P. (2012). A New Approach for Co-operative Bus Priority at Traffic Signals. IEEE Transactions on Intelligent Transportation Systems, pp. 6-14, Vol. 13, No. 1.

Hu, J., B. B. Park, and Y.-J. Lee (2015). Coordinated Transit Signal Priority Supporting Transit Progression under Connected Vehicle Technology. Transportation Research Part C: Emerging Technologies, Vol. 55, pp. 393-408.

Hu, J., Park, B. B., and Lee, Y. J. (2016). Transit signal priority accommodating conflicting requests under Connected Vehicles technology. Transportation Research Part C: Emerging Technologies, 69, 173-192.

Katsaros, K., Kernchen, R., Dianati, M. and Rieck, D. (2011). Performance study of a green light optimized speed advisory (GLOSA) application using an integrated cooperative its simulation platform. In 7th International Wireless Communications and Mobile Computing Conference (IWCMC), 918–923.

Kim, W., Jee, G., Lee, J. (2000). Efficient use of digital road map in various positioning for ITS. In: IEEE Symposium on Position Location and Navigation, SanDeigo, CA.

Janos, M. and Furth, P. G. (2002). Bus Prioirty with Highly Interruptible Traffic Signals Simulation of San Juan's Avenida Ponce de Leon, Transportation Research Record: Journal of the Transportation Research Board, No. 1811, 157-65.

Li, L., Quddus, M., and Zhao, L. (2013). High accuracy tightly-coupled integrity monitoring algorithm for map-matching. Transportation Research Part C, 36, 13–26.

Lin, Y., X. Yang, N. Zou, L. Jia, and Shu. (2013a). A New Passive Transit Signal Priority Control at Urban Arterials. Journal of Northeastern University: Natural Science (In Chinese), 2013, Vol. 34, No. 9

Lin, Y., X. Yang, G.L. Chang, and N. Zou. (2013b). Transit Priority Strategies for Multiple Routes Under Headway-Based Operations. In Transportation Research Record: Journal of the Transportation Research Board, No. 2356, Transportation Research Board of the National Academies, Washington, D.C., 2013, 34-43.

Lin, Y.J., Yang, X.F., Zou, N, and Jia L. (2013c). Real Time Bus Arrival Prediction: A Case Study of Jinan China, Journal of Transportation Engineering ASCE, 139(11):1134-1140.

Ling, K. and Shalaby, A. (2004). Automated transit headway control via adaptive signal priority. Journal of Advanced Transportation, Vol. 38, No. 1, pp 45-67.

Little J.D.C. (1966). The synchronization of traffic signals by mixed-integer linear programming. Operation Research, 14(4), 568-594.

Little J.D.C., Kelson, M.D., and Gartner, N.H. (1981). MAXBAND: A program for setting signals on arteries and triangular networks. Transportation Research Record, 795, 40-46.

Ma, W., and Bai,Y. (2007). Serve Sequence Optimization Approach for Multiple Bus Priority Requests Based on Decision Tree. Proceedings of the Seventh International Conference of Chinese Transportation Professionals Congress.

Ma, W., Yang, X. and Liu, Y. (2010). Development and Evaluation of a Coordinated and Conditional Bus Priority Approach. In Transportation Research Record: Journal of the Transportation Research Board, No. 2145, TRB, Washington, D.C., 49–58.

Mesbah, M., Sarvi, M., Ouveysi, I., and Currie, G. (2011). Optimization of transit priority in the transportation network using a decomposition methodology. Transp. Res. Part C: Emerg. Technol. 19 (2), 363–373.

Morgan, J.T. and Little J.D.C. (1964). Synchronizing traffic signals for maximal bandwidth. Operation Research, 12(6), 896-912.

Muthuswamy, S., McShane, W.R., and Daniel, J.R. (2007). Evaluation of transit signal priority and optimal signal timing plans on transit and traffic operations. In Transportation Research Record: Journal of the Transportation Research Board, No. 2034, TRB, Washington, DC, 92–102.

Najjar, M.E., Bonnifait, P. (2003). A roadmap matching method for precise vehicle Localization using belief theory and Kalman filtering. In: The 11th International Conference in Advanced Robotics, Coimbra, Portugal, June 30–July 3.

Ni, D. (2005). Multiple imputation scheme for overcoming the missing values and variability issues in ITS data. Journal of transportation engineering, ASCE, December 2005, 931-938

Pu, W. and Lin, J., and Long, L. (2009). Real-Time Estimation of Urban Street Segment Travel Time Using Buses as Speed Probes. Transportation Research Record: Journal of the Transportation Research Board, No. 2129, Transportation Research Board of the National Academies, Washington, D.C., 2009, 81–89.

Pyo, J., Shin, D., Sung, T. (2001). Development of a map matching method using the multiple hypothesis technique. In IEEE Proceedings on Intelligent Transportation Systems, 23–27.

Quddus, M. A., Ochieng, W. Y., Zhao, L., and Noland, R. B. (2003). A general map matching algorithm for transport telematics applications. GPS Solutions, 7(3), 157–167.

Quddus, M.A., Ochieng, W.Y., Noland, R.B. (2006). A high accuracy fuzzy logic-based map matching algorithm for road transport. Journal of Intelligent Transportation System Technology Planning Operation. 10 (3), 103–115.

Quddus, M. A., Ochieng, W. Y., Noland, R. B. (2007). Current map-matching algorithms for transport applications: State-of-the art and future research directions, Transportation Research Part C, 15, 312–328

Quddus, M. and Washington, S. (2015). Shortest path and vehicle trajectory aided map-matching for low frequency GPS data. Transportation Research Part C, 55, 328–339

Sáez, D., Cortés ,C.E., Milla, F., Núñez, A., Tirachini, A. and Riquelme, M. (2012) Hybrid predictive control strategy for a public transport system with uncertain demand. Transportmetrica, Vol 8(1), 61-86

Satiennam, T., Fukuda,A., Muroi, T., and Jansuwan, S.(2005). An Enhanced Public Transportation Priority System for Two-lane Arterials with Nearside Bus Stops. Proceedings of the Eastern Asia Society for Transportation Studies, Vol. 5, 1309-1321.

Seredynski, M., Mazurczyk, W., and Khadraoui, D. (2013). Multi-Segment Green Light Optimal Speed Advisory. In 2013 IEEE 27th International Symposium on Parallel & Distributed Processing Workshops and PhD Forum. 459-465

Skabardonis, A. Control Strategies for Transit Priority. In Transportation Research Record: Journal of the Transportation Research Board, No. 1727, TRB, National Research Council, Washington, D.C., 2000, pp. 20–26.

Smith, B. L. and Conklin, J. H. (2002) Use of Local Lane Distribution Patterns to Estimate Missing Data Values from Traffic Monitoring Systems. Transportation Research Record: Journal of the Transportation Research Board, No. 2965

Smith, B. L., Scherer, W. T. and Conklin, J. H.(2003). Exploring Imputation Techniques for Missing Data in Transportation Management Systems. Transportation Research Record: Journal of the Transportation Research Board, No. 2894, 132-142

Srinivasan, D., Cheu, R. L., and Tan, C. W. (2003). Development of an improved ERP system using GPS and AI techniques. In Proceedings of Intelligent Transportation Systems Conference (Vol. 1), 554–559, IEEE.

Stamatiadis, C., and Gartner, N. H. (1996). MULTIBAND-96: a program for variable-bandwidth progression optimization of multiarterial traffic networks. Transportation Research Record, 1554(1), 9-17.

Stevanovic, J., Stevanovic, A., Martin, P.T., and Bauer, T. (2008). Stochastic optimization of traffic control and transit priority settings in VISSIM. Transp. Res. C: Emerg. Technol. 16, 332–349.

Stevanovic, A., Stevanovic, J. and Kergaye, C. (2013). Green Light Optimized Speed Advisory Systems Impact of Signal Phasing Information Accuracy. Transportation Research Record: Journal of the Transportation Research Board, No. 2390, TRB, Washington, D.C., 2013, pp. 53–59.

Sun A., Hickman M. (2008). The Holding Problem at Multiple Holding Stations. In Computer-aided Systems in Public Transport, 339-359

Syed, S., Cannon, M.E. (2004). Fuzzy logic-based map matching algorithm for vehicle navigation system in urban canyons. In Proceedings of the Institute of Navigation (ION) National Technical Meeting, 26–28 January, California, USA.

Taylor, G., Blewitt, G., Steup, D., Corbett, S., and Car, A. (2001). Road reduction filtering for GPS-GIS Navigation. Transactions in GIS, 5(3), 193–207.

Tian, Z., and Urbanik, T. (2007). System partition technique to improve signal coordination and traffic progression. Journal of transportation engineering, 133(2), 119-128.

Turnquist, M. and Blume, S. (1980). Evaluating potential effectiveness of headway control strategies for transit systems. Transportation Research Record, 746, 25–29.

Urbanik, I. I (1977). Priority treatment of buses at traffic signals. Transportation Engineering, 1977, pp. 31-33.

Velaga, N. R., Quddus, M. A., and Bristow, A. L. (2009). Developing an enhanced weight-based topological map-matching algorithm for intelligent transport systems. Transportation Research Part C: Emerging Technologies, 17(6), 672–683.

Vincent, R.A., Cooper, B.R., Wood, K. (1978). Bus-Actuated Signal Control at Isolated Intersections–Simulation Studies of Bus Priority, REPORT 814, Crowthorne, Berkshire in England, Transport and Road Research Laboratory.

Washington State Transportation Center (2005), AVL-Equipped Vehicles as Speed Probes, Report No. WA-RD 617.1

White, C. E., Bernstein, D., and Kornhauser, A. L. (2000). Some map matching algorithms for personal navigation assistants. Transportation Research Part C: Emerging Technologies, 8(1), 91–108.

Wilbur Smith and Associates (1968), Study of Evolutionary Urban Transportation, Volumes I, II and III. Westinghouse Airbrake Co., and Institute of Public Administration. U.S. Department of Housing and Urban Development.

Xu, B., Zhang, F., Wang, J., and Li, K., (2015). B&B Algorithm-Based Green Light Optimal Speed Advisory Applied to Contiguous Intersections. 15th COTA

International Conference of Transportation, 2015 American Society of Civil Engineers.

Xu, M., Ye, Z., Sun, H., & Wang, W. (2016). Optimization model for transit signal priority under conflicting priority requests. Transportation Research Record: Journal of the Transportation Research Board, (2539), 140-148.

Yagar, S., and Han, B. (1994). A Procedure for Real-Time Signal Control That Considers Transit Interference and Priority. Transportation Research Part B, Vol. 28, No. 4, 315–331.

Yang, X., Chang, G., and Rahwanji, S. (2014). Development of a Signal Optimization Model for Diverging Diamond Interchange. Journal of Transportation Engineering, 140(5)

Yang, X., Cheng,Y., Chang, G. (2015). A multi-path progression model for synchronization of arterial traffic signals, Transp. Res. C, vol. 53, 93-111.

Ye, Z., and Xu, M. (2017). Decision Model for Resolving Conflicting Transit Signal Priority Requests. IEEE Transactions on Intelligent Transportation Systems, 18(1), 59-68.

Yu, B and Yang, Z. (2009). A dynamic holding strategy in public transit systems with real-time information. Applied Intelligence, Vol 31 (1), 69–80

Yu, Z., V. V. Gayah, and E. Christofa. (2017). Person-Based Optimization of Signal Timing: Accounting for Flexible Cycle Lengths and Uncertain Transit Vehicle Arrival Times. Transportation Research Record: Journal of the Transportation Research Board, (2620), 31-42.

Zeng, X., Sun, X., Zhang, Y., and Quadrifoglio, L. (2015). Person-Based Adaptive Priority Signal Control with Connected-Vehicle Information. Transportation Research Record: Journal of the Transportation Research Board, (2487), 78-87.

Zhou G. and Gan A. (2006). Design of Transit Signal Priority at Signalized Intersections with Queue Jumper Lanes. In Journal of Public Transportation, Vol. 12, No. 4, 2009, pp.117-132.

Zhao, J., Bukkapatnam, S., and Dessouky, M. (2003). Distributed architecture for real-time coordination of bus holding in transit networks. IEEE Transactions on Intelligent Transportation Systems 4 (1), 43–51.

Zhong, M., Lingras, P. and Sharma, S. (2004). Estimation of missing traffic counts using factor, generic, neural, and regression techniques. Transportation Research Part C 12, 2004, pp 139-166

Zhou, G., Gan, A., Shen, L.D. (2007). Optimization of adaptive transit signal priority using parallel genetic algorithm. Tsinghua Sci. Technol. 12 (2), 131–140.

Zolfaghari, S., Azizi, N., and Jaber, M. (2004). A model for holding strategy in public transit systems with real time information. International Journal of Transport Management 2 (2), 99–110.